

# An Investigation of Time-Dependent Behavior of Medium Density Polyethylene Pipes

by

© Suprio Das

A thesis submitted to the

School of Graduate Studies

in partial fulfillment of the requirement for the degree of

Master of Engineering

Faculty of Engineering & Applied Science

Memorial University of Newfoundland

**May 2021**

St. John's, Newfoundland, Canada

## **ABSTRACT**

Medium density polyethylene (MDPE) pipes are extensively used for gas distribution system in Canada and worldwide. MDPE pipe material possesses time-dependent mechanical properties that governs the performance of the pipes in service. In this research, laboratory investigation is carried out to investigate the time-dependent behavior of a MDPE pipe material. Uniaxial tensile tests were conducted with samples (coupons) cut from the wall of a 60-mm diameter MDPE pipe. A tensile test with a sample of full cross-section of the pipe is also conducted to investigate the influence of sample type on the test results. The test program includes uniaxial testings at various strain rates to capture the effects of loading rates, creep testing and relaxation testing. The experimental results are used to develop a numerical approach for modeling the time-dependent behavior using a commercially available finite element software, Abaqus. The strain-rate dependent material behavior of MDPE is incorporated in Abaqus through development of a user subroutine. The proposed modeling approach is found to successfully simulate the uniaxial test results. Applicability of the proposed modeling framework is demonstrated through investigating the time-dependent behavior of conventional buried MDPE pipe subjected to surface load and a pipeline subjected to rate-dependent lateral ground movement.

## **ACKNOWLEDGEMENTS**

First of all, I would like to take the opportunity to acknowledge the help and support of several individuals who have contributed in many different ways to this work. I would like to express my sincere and heartfelt gratitude to Dr. Ashutosh Sutra Dhar for his proper guidance and valuable suggestions, sincere supervision, and co-operation throughout the research work. I have been very fortunate that Dr. Ashutosh Sutra Dhar is my supervisor, and I have learnt many lessons in working under his guidance that I will remember for the rest of my life. Thank you very much for being my guide, mentor and role model.

I would also like to thank Dr. Kshama Roy, Mr. Abu Hena Muntakim, Mr. Suborno Debnath, Mr. Ripon Karmaker and Mr. Anan Morshed for their invaluable suggestions, insightful guidance and continuous encouragement throughout the program.

I would also like to thank the staff and technicians, especially Mr. Steve Steele who have helped me during the laboratory tests. Furthermore, I highly appreciate the support given by the research and administration staff of the Faculty of Engineering and Applied Science, Memorial University of Newfoundland who helped me in different ways.

I would not have been able to undertake this work without the financial support of the Natural Sciences and Engineering Research Council of Canada (NSERC), FortisBC Energy Inc., InnovateNL of the province of Newfoundland and Labrador, the Faculty of Engineering and Applied Science, and the School of Graduate Studies.

I cannot express with words my gratitude towards my parents, brother, and friends, for encouraging and supporting me throughout this journey.

# Table of Contents

ABSTRACT .....	II
ACKNOWLEDGEMENTS.....	III
List of Figures.....	VII
List of Tables .....	IX
CHAPTER 1	
Introduction	
1.1 Background and Motivation .....	1
1.2 Objectives and Scopes .....	3
1.3 Outline of the Thesis .....	4
CHAPTER 2	
Literature Review	
2.1 Introduction.....	6
2.2 Polyethylene Pipe .....	6
2.2.1 Structure and Properties of Polyethylene.....	7
2.2.2 Mechanical Behavior of MDPE .....	8
2.2.3 Time Dependent Behavior of MDPE.....	10
2.3 Theoretical Method of Linear Viscoelastic Analysis .....	12
2.3.1 Integral and Differential Formulations.....	12
2.3.2 Mechanical Models .....	13
2.3.2.1 Maxwell Model .....	14
2.3.2.2 Kelvin-Voigt Model.....	15
2.3.2.3 Standard Linear Solid Model.....	16
2.4 Application of MDPE Pipe .....	17

2.4.1 Manufacturing and Use of MDPE Pipe .....	17
2.4.2 Performance Limit.....	19
2.5 Research on Polyethylene Pipe Performance .....	20
2.5.1 Experimental Study to Determine Polyethylene Pipe Performance.....	20
2.5.2 Analytical Models Used to Determine Polyethylene Pipe Performance .....	21
2.5.2.1 Power Law Model .....	22
2.5.2.2 Hyperbolic Constitutive Model .....	23
2.5.3 Numerical Study to Determine Polyethylene Pipe Performance .....	24
2.4 Summary .....	26
 CHAPTER 3	
Nonlinear Time-Dependent Mechanical Behavior of a Medium Density Polyethylene Pipe Material	
3.1 Introduction.....	27
3.2 Test Methods .....	31
3.3 Test Results.....	36
3.3.1 Constant Strain Rate Tests.....	36
3.3.2 Relaxation and Creep Tests .....	41
3.4 Modeling Time-dependent Behavior.....	44
3.4.1 Prony Series .....	44
3.4.2 Creep Law .....	48
3.5 Proposed Modeling Framework .....	51
3.6 Nonlinear Strain-Rate Dependent Stress–Strain Relations .....	52
3.7 Implementation In Abaqus .....	55
3.7.1 Validation of the Modeling Approach .....	56
3.7.2 Simulation of Uniaxial Tension Tests.....	57

3.7.3 Simulation of Creep and Relaxation Tests .....	60
3.8 Conclusions .....	64
CHAPTER 4	
Modeling Time-Dependent Behavior of Medium Density Polyethylene Pipes	
4.1 Introduction .....	69
4.2 Time-Dependent Model .....	71
4.3 Deflection of Buried Pipes .....	73
4.3.1 Finite Element Model.....	75
4.3.2 Time-Dependent Responses .....	77
4.3.3 Short-Term Deflections.....	80
4.3.4 Time-Dependent Deflections.....	81
4.3.5 The Proposed Method of Deflection Calculation.....	84
4.3.6 Evaluation with Simplified Design Equation .....	84
4.4 Pipeline Subjected to Lateral Ground Movement .....	85
4.4.1 Pipe-Soil Interaction Element.....	86
4.4.2 FE Modeling .....	88
4.4.3 Time-Dependent Responses .....	90
4.5 Conclusions .....	93
CHAPTER 5	
Conclusions and Recommendations for Future Research	
5.1 Conclusions .....	100
5.1.1 Experimental Investigation Under Uniaxial Tension Test.....	100
5.1.2 Development of Rate Dependent Constitutive Relations .....	101
5.1.3 Development of FE Modeling Technique.....	102
5.1.4 A Conventional Buried Pipe Subjected to Ground and Surface Load.....	102

5.1.5 A Conventional Buried Pipe Subjected to Lateral Ground Movement .....	103
5.2 Recommendations for Future Study .....	103
References .....	105
APPENDIX A.....	110

## List of Figures

Figure 2.1. Microstructure of, (a) Amorphous; (b) Crystalline; (c) Semi-crystalline.....	8
Figure 2.2. Stress–strain behavior for polyethylene .....	9
Figure 2.3. Creep behavior of polyethylene .....	10
Figure 2.4. Typical relaxation behavior of polyethylene .....	11
Figure 2.5. Maxwell model .....	14
Figure 2.6. Kelvin-Voigt model.....	15
Figure 2.7. Standard linear model.....	16
Figure 3.1. Prony series model .....	29
Figure 3.2. Test set up and loading apparatus for full pipe test: (a) UTM machine; (b) Mechanism of grips.....	32
Figure 3.3. Test set up and loading apparatus for coupon tests: (a) Schematic of coupon specimen; (b) Tensile testing machine .....	33
Figure 3.4. Experimental results for constant strain rate tests.....	37
Figure 3.5. Rate dependent stress–strain responses test (mean values).....	38
Figure 3.6. Experimental results for strain-rate-change test.....	40
Figure 3.7. Experimental results for loading-unloading-reloading test .....	40

Figure 3.8. Experimental results for relaxation tests (a, b, c are mean values) .....	42
Figure 3.9. Stress–strain responses of mean relaxation tests.....	42
Figure 3.10. Experimental results of creep tests (a, b, c are mean values) .....	43
Figure 3.11. Variation of normalized relaxation modulus $g_t$ with time from relaxation tests.....	46
Figure 3.12. Variation of normalized compliance, $C_t$ with time from creep tests.....	47
Figure 3.13. Creep law parameter ‘n’ from creep test data.....	50
Figure 3.14. Creep law parameter ‘n’ from relaxation test data.....	51
Figure 3.15. Comparison of mean test results with hyperbolic model .....	54
Figure 3.16. FE model.....	57
Figure 3.17. Finite element simulations of uniaxial tension tests: a) Proposed model; b) Prony series.....	58
Figure 3.18. Simulation of strain-rate-change test.....	59
Figure 3.19. Simulation of loading-unloading-reloading test.....	60
Figure 3.20. Simulation for creep tests: a) Proposed model; b) Prony series .....	61
Figure 3.21. Simulation for relaxation tests: a) Proposed model; b) Prony series .....	63
Figure 4.1. FE model of buried pipe .....	75
Figure 4.2. Time-dependent deflections of buried MDPE pipe: a) Vertical deflection; b) Horizontal deflection.....	78
Figure 4.3. Von Mises stresses in the pipes with time: a) Crown stresses; b) Springline stresses .....	79
Figure 4.4. Normalized time-dependent elastic moduli .....	83
Figure 4.5. Comparison of deflections from FE analysis and simplified design equation .....	85
Figure 4.6. Pipe-soil interaction model: (a) 4 noded PSI element; (b) 6 noded PSI element .....	87

Figure 4.7. Pipeline perpendicular to ground movement .....	88
Figure 4.8. Finite element mesh for the analysis of ground movement (schematic) .....	89
Figure 4.9. Maximum stress at different rates of ground movement.....	91
Figure 4.10. Maximum strain at different rates of ground movement.....	92
Figure 4.11. Time-dependent responses of the deflected pipe .....	93

### **List of Tables**

Table 2.1. Relaxation power law exponent for MDPE .....	22
Table 2.2. Parameters for hyperbolic model of HDPE pipe.....	24
Table 3.1. Test Program .....	35
Table 3.2. Initial modulus of MDPE at various strain rates .....	39
Table 3.3: Prony series parameter obtained from relaxation test .....	47
Table 3.4. Prony series parameters obtained from creep tests.....	48
Table 3.5. Creep law parameters for creep tests.....	49
Table 3.6. Creep law parameters for relaxation tests.....	50
Table 3.7. Parameters for hyperbolic model.....	54
Table 4.1. Parameters for the hyperbolic model (Das and Dhar 2020).....	72
Table 4.2. Creep law parameters for creep tests (Das and Dhar 2020).....	76
Table 4.3. Comparison of Initial deflections .....	81
Table 4.4. Comparison of time dependent deflections.....	83
Table 4.5. Parameters considered for the analysis of pipe subjected to ground movement.....	90

# CHAPTER 1

## Introduction

### 1.1 Background and Motivation

Pipelines are the most efficient and common means of transporting gas, water, sewage, other fluids from one point to another. Cast iron, ductile iron, steel, and polymers are the common types of pipe materials used for liquid and gas transportation and distribution systems. In the last few decades, polyethylene pipe uses are increasing due to its several advantages over metallic pipes, the most relevant being the cost. In addition, the lightweight and flexibility offered by plastic pipes are likely to reduce the cost relating to pipe installation. According to PIPA (2001), plastic pipes require less maintenance during their lifetime operation if the pipes are properly designed and installed. Another key advantage is its virtual freedom from the chemical attack of soils, and ambient water and moisture. Being a non-conductor of electricity, polyethylene is immune to the electrochemical based corrosion process induced by electrolytes such as salts, acids, and bases. Under external loading, plastic pipes offer greater deformation tolerance and stress relaxation. Due to these advantages, plastics pipes can be used in a sturdy region, in the presence of aggressive chemicals and extreme climates.

In North America, the usage of plastic pipes in the natural gas distribution system is more than 90%, of which 99% are plastic pipes (PIPA 2001). According to Stewart et al. (1999), due to the higher flexibility and long-term strength of medium density polyethylene (MDPE) compared to high-density polyethylene (HDPE), more than 60% of pipes used in the natural gas distribution industry are MDPE materials. These gas pipes are manufactured in a different size in diameter ranging from 12.5 mm to 600 mm and are available in a wide range of wall thicknesses. Usually,

large-diameter steel pipes are used to design high-capacity transmission lines that transmit natural gas from source to refineries, and small diameter plastic pipes are used in distribution locations.

However, the long-term performance of buried polyethylene pipes is not well-known, due to the lack of data available for an understanding of the time-dependent pipe-soil interaction. As polymer material possesses time, temperature, and strain-rate dependent behavior, analysis of buried pipe accounting for the time, temperature, and strain-dependent behavior requires complex algorithms. There is a common practice to use simple secant modulus in the analysis of polymer pipes to capture the time-dependent effects (Katona 1990, Moser 1997, Suleiman et al. 2003). Existing design codes (i.e., AASHTO 2010) recommend using short-term and long-term values of the modulus of elasticity of pipe material for calculating the short-term and long-term responses, respectively. However, the approach does not account for the non-linear rate-dependent stress-strain behavior of the material.

Several linear viscoelastic material models have been used in finite element analysis to investigate the mechanical response of HDPE pipes (Chua, 1986; Chua and Lytton, 1989; Hashash, 1991; Moore, 1994;). Although most of the above-mentioned models can successfully simulate the stress-strain behavior at lower strain (less than 1%), these models were unsuccessful at higher strains. Linear viscoelasticity can be applied to polyethylene pipes when the stresses are about 60% of the yield stress (Moore 1994). A nonlinear viscoelastic and viscoplastic modeling approach was then employed to reasonably simulate the stress-strain behavior under various loading conditions (Zhang and Moore,1997). Several other constitutive models were also developed for polymer materials to simulate the time-dependent behavior (Chehab and Moore 2006, Suleiman and Coree 2004, Siddiquee and Dhar 2015). However, very limited information is currently available on the study of MDPE pipe materials. Few authors expressed the modulus of elasticity

for MDPE pipe using the power-law relation of time (Husted and Thompson, 1985; Janson, 1985; Keeney, 1999). According to Bilgin et al. (2007), these models are only applicable at lower strains (less than 1%).

## **1.2 Objectives and Scopes**

The primary objectives of the dissertation are

1. To develop a time-dependent constitutive model for MDPE pipe material; and
2. To develop a feasible method to account for the time-dependent effect in the soil-pipe interaction analysis.

The following methods were employed to achieve the objectives:

1. Conduct an experimental investigation to identify the strain-rate dependent stress-strain behavior, relaxation behavior, and creep behavior of MDPE pipe material;
2. Develop rate-dependent constitutive relations through the interpretation of test results;
3. Develop a FE modeling technique to simulate the nonlinear time-dependent behavior;
4. Demonstrate the developed techniques through application to conventional soil-pipe interaction problems.

### 1.3 Outline of the Thesis

This thesis is prepared in the manuscript format. The outcome of the study is presented in five Chapters and one appendix (Appendix A). The outline is as follows:

- Chapter 1 highlights the backgrounds, motivation, and objectives of the research work.
- Chapter 2 presents a brief review. However, as the thesis is prepared in manuscript format, the problem-specific literature reviews are provided in Chapters 3 and 4.
- Chapter 3 presents an extensive experimental and numerical investigation of MDPE pipe material behavior under uniaxial loading to characterize the nonlinear and time-dependent mechanical response under a wide range of loading histories. The numerical modeling framework developed to simulate the time-dependent responses is discussed in this chapter. The chapter has been accepted for publication in the ASCE Journal of Materials in Civil Engineering. A part of the research has also been published in the CSCE Annual Conference 2019, Greater Montreal, Laval, Canada, June 12–15, 2019 (attached in Appendix A).
- Chapter 4 presents the application of developed time-dependent modeling framework to investigate a conventional buried pipe subjected to ground and surface load, and a pipeline subjected to rate-dependent lateral ground movement. This research work has been submitted for submission to the ASCE Journal of Pipeline Systems – Engineering and Practice.
- Chapter 5 summarizes the outcomes of the research and recommendations for future studies.

As the thesis is prepared in manuscript format, the references cited in Chapters 3 and 4 are listed at the end of each chapter. The references cited in Chapters 1 and 2 are listed in the 'Reference' section at the end of the thesis.

**Co-Authorship:** The research presented in this thesis has been performed by the author of this thesis, Mr. Suprio Das, under the supervision of Dr. Ashutosh Sutra Dhar. He also prepared the draft manuscript.

## **CHAPTER 2**

### **Literature Review**

#### **2.1 Introduction**

As the thesis has been written in manuscript format, a problem-specific literature review is presented in Chapters 3 and 4. This chapter provides a brief overview of the mechanical properties of polyethylene pipe, the theoretical background for the development of the constitutive models, and the relevant literature on both theoretical and experimental investigations.

#### **2.2 Polyethylene Pipe**

Plastics contain one or more polymeric substances which can be shaped by flow. The basic ingredients of plastics are polymers, which compose a broad class of materials like colorants, stabilizers, antioxidants, or other ingredients required to protect or enhance properties. Polyethylene (PE) was first invented by the Imperial Chemical Company (ICI) in 1933 in England (PPI 1993). In early days, high-pressure (14,000 to 44,000 psi) autoclave reactors and temperatures of 2000 to 6000 F were used for the polymerization processes, which was dangerous and expensive. Polyethylene produced at low pressure was first introduced in the 1950s, which is used for the manufacturing of pipes (PPI 1993).

Plastics are mainly divided into two basic groups, thermosets, and thermoplastics. Thermosets include the composition of PE, polypropylene, and polyvinyl chloride in which polymer chains are chemically bonded to each other by new cross-links. Through cross-linking, thermoset resin forms a permanent and infusible shape. Thus, these cannot be re-melted after curing. Thermoplastics are similar to thermoset except for curing. In the case of thermoplastics, physical forces are applied to immobilize polymer chains, which prevent them from slipping each

other. Upon the application of heat, these forces weaken and allow the material to soften or melt. Thermoplastics are allowed to assume a new form or shape after melted, without significant alterations on its properties.

Polyethylene is one of the most widely used thermoplastics in the world because of its good properties like excellent chemical inertness, toughness, ease of processing, and low electrical conductivity. The mostly used polyethylene are high-density polyethylene (HDPE), medium-density polyethylene (MDPE), and low-density polyethylene (LDPE). HDPE consists of a long molecular chain without major branching, which helps the molecules to form closely packed together and causes high crystallinity. Due to high crystallinity, HDPE exhibits high tensile and compressive strength compared to MDPE and LDPE. On the other hand, LDPE consists of many long branches of the main molecular chain, which prevents the molecule from forming close packing together and causes low crystallinity. MDPE has less branching than LDPE and more branching than HDPE. It has a good impact and drops resistance, less notch sensitivity, and better cracking resistance than HDPE (AZOM 2001).

### **2.2.1 Structure and Properties of Polyethylene**

Polyethylene is produced by the polymerization of ethylene molecules. In the microstructure of polyethylene, there exist two phases: crystalline and amorphous. In the amorphous region, there is no definite molecular arrangement. On the other hand, the polymer chain in the crystalline region aligns themselves in closely packed. Because of their close packing, crystalline regions are denser than amorphous regions. As polyethylene contains both regions, it is called semi-crystalline material. Fig. 2.1 shows the microstructure of amorphous, crystalline, and semi-crystalline structure. Both regions play an important role in determining the material's microscopic response. At room temperature, the amorphous component behaves like rubbery, which allows the

crystalline part to move and change shape without cleaving. The molecular chains are not broken in this type of deformation. It is often termed as plastic, which is often largely recoverable.

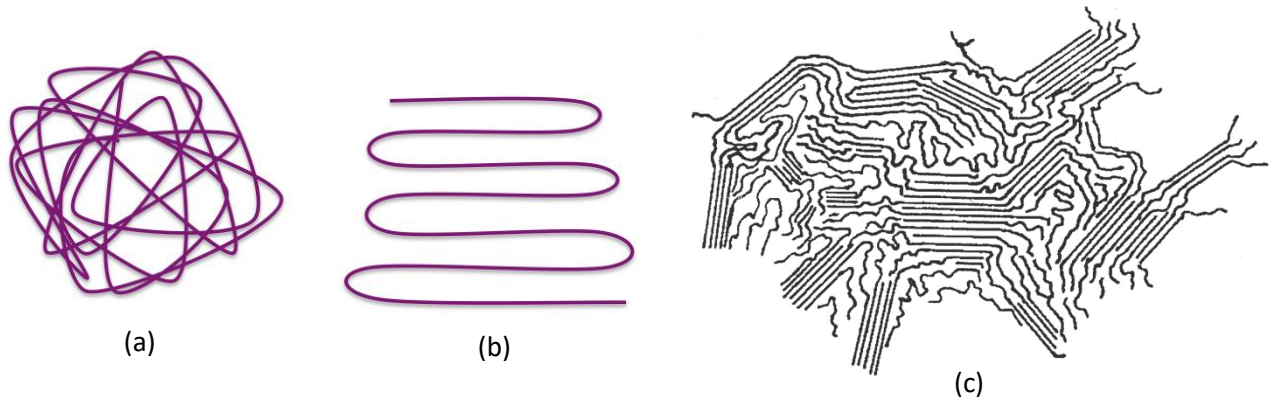


**Fig. 2.1.** Microstructure of, (a) Amorphous; (b) Crystalline; (c) Semi-crystalline (PPI 1993).

In semi-crystalline material, polymer leads to high toughness due to this type of deformation. High-density polyethylene can consist of up to 90% crystalline region compared to 40% for low-density polyethylene.

### **2.2.2 Mechanical Behavior**

To explain the mechanical response of polymeric materials, it is important to understand the molecular structure of polymers. As stated earlier, polyethylene has two different molecular formations: Amorphous and Crystalline. Long-chain molecular formation of crystalline form the backbone of the structure. The crystallinity of molecular structure is mainly responsible for the elastic-like behavior of polyethylene. On the other hand, the amorphous short branches extending from these molecules form the cross-links with the adjoining crystalline molecules (Powel 1983). The amorphous structure is mainly responsible for the viscous behavior of polyethylene. The response of amorphous and crystalline structures under loading determine short-term and long-

term mechanical response of polyethylene. The different properties of the high, medium and low-density polyethylene can be explained from their respective molecular structure.

Fig. 2.2 shows the schematic diagram of the typical stress-strain response of polyethylene. From Fig. 2.2, we can see that the stress-strain behavior of polyethylene can be categorized into three regions. The first region can be termed as an elastic region. In this region, polyethylene behaves like elastic material in which strain can be recovered instantaneously. The second region is termed the viscoelastic region. Both the viscous and elastic property of polyethylene are active in this region. The strain that occurs in this region is partly recovered due to the existence of elastic property. The third region is termed the viscoplastic region. Only the viscous property of polyethylene exists in this region. As there is no elastic property in this region, the strains remain irrecoverable. However, it is not possible to separate these regions during the straining process of polyethylene. In reality, the elastic region is too small that viscoelastic response can be observed at small strain levels.

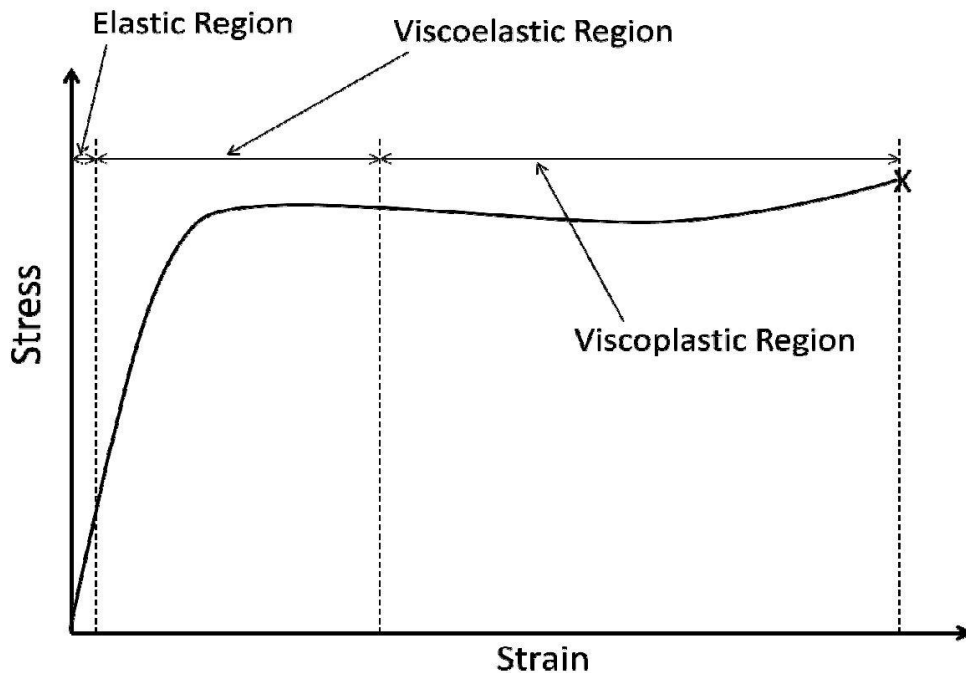


**Fig. 2.2.** Stress–strain behavior for polyethylene (Weerasekara, 2011).

### 2.2.3 Time-Dependent Behavior of MDPE

Like other polymer material, MDPE shows significant time-dependent behavior. Creep, stress relaxation, and strain rate dependence are the main characteristics of time-dependent behavior. Creep tests and relaxation tests are mostly used to determine the viscous properties of a material.

The creep is the change in deformation with time when the material is held at constant load. Creep behavior can be subdivided into three categories: primary, steady-state creep, and tertiary. Fig. 2.3 shows a schematic diagram of the creep responses. For a material that exhibits creep behavior, creep compliance can be calculated from the creep curve. The compliance can be defined as  $\varepsilon(t)/\sigma$ , where  $\varepsilon(t)$  is the time-dependent strain and  $\sigma$  is the stress. For linear material, creep compliance is independent of the stress of the material. Single compliance can describe all creep behavior for that material. For nonlinear material, creep compliance is a function of stresses applied. Except at low stresses, the compliance of polyethylene is found to be significantly nonlinear (Ebbott, 1987).

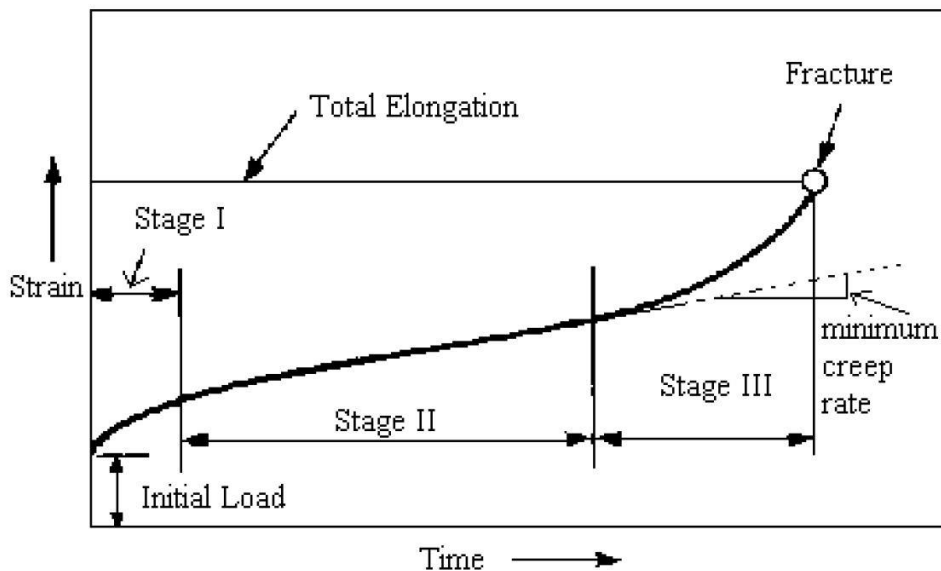


**Fig. 2.3.** Creep behavior of polyethylene (MC, 1999).

Stress relaxation is a decrease in stress with time when the material is held at constant strain. Fig. 2.4 shows a schematic diagram of the relaxation response. Similar to the creep compliance, a relaxation modulus can be calculated for the material, which shows relaxation behavior. It can be defined as a ratio of time-dependent stress to the applied strain. For linear viscoelastic material, a single relaxation modulus can be used to describe all relaxation responses. However, the relaxation modulus is strain-dependent for non-linear material. Bilgin et al. (2007) investigated the non-linear behavior of MDPE using a relaxation test. It was found that the relaxation modulus is significantly strain-dependent.

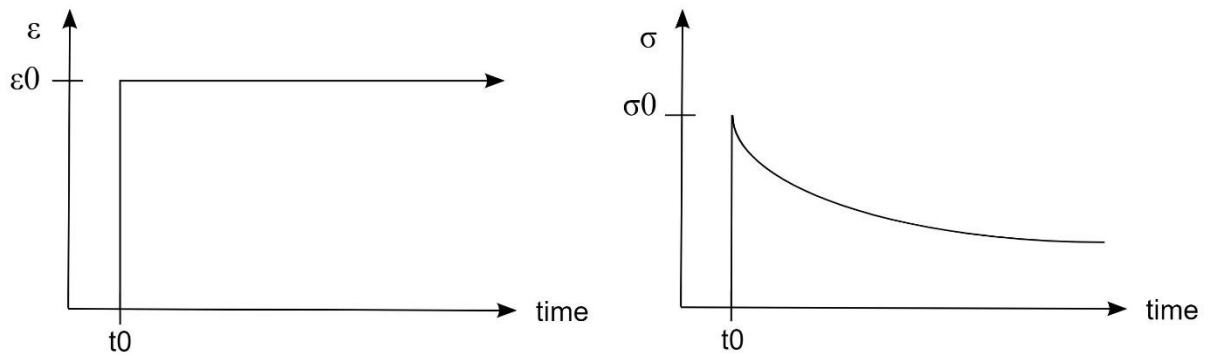


**Fig. 2.4.** Typical relaxation behavior of polyethylene.

## 2.3 Theoretical Methods of Linear Viscoelastic Analysis

### 2.3.1 Integral and Differential Formulations

The mathematical theory of viscoelasticity is well developed for linear material. This theory is based on the Boltzman Superposition Principle: 1) the creep in a specimen is a function of the entire loading history, and 2) each loading step can be obtained by the simple addition to the final deformation. According to this principle, the total creep at time  $t$  can be obtained by the simple addition of each incremental stresses and is given by

$$\varepsilon^c(t) = \Delta\sigma_1 \psi(t - \tau_1) + \Delta\sigma_2 \psi(t - \tau_2) + \Delta\sigma_3 \psi(t - \tau_3) + \Delta\sigma_4 \psi(t - \tau_4) \dots \quad (2.1)$$

where,  $\psi(t - \tau_1)$  is the creep compliance function. The general form of equation (2.1) can be written as,

$$\varepsilon^c(t) = \int_{-\infty}^t \psi(t - \tau) \dot{\sigma}(\tau) d\tau \quad (2.2)$$

Similarly, for the relaxation test, the stress at time  $t$  can be written as

$$\sigma(t) = \int_{-\infty}^t \phi(t - \tau) \dot{\varepsilon}(\tau) d\tau \quad (2.3)$$

where,  $\phi(t - \tau)$  is the stress relaxation modulus. As the current strain or stress is determined by integration with time, the effects of the entire loading history are incorporated. Though this approach can describe creep and relaxation accurately for linear viscoelastic material, it becomes complicated and untraceable when the nonlinear effects are incorporated.

### 2.3.2 Mechanical Models

The constitutive equation for an ideal viscoelastic material is defined as Hooke's law, and the equation is as,

$$\sigma = E\varepsilon \quad (2.4)$$

where,  $E$  is the constant modulus of elasticity. The constitutive equation for an ideal viscous material is defined by Newton's law of viscosity, and the equation is,

$$\sigma = \eta\dot{\varepsilon} \quad (2.5)$$

where,  $\eta$  is the coefficient of viscosity. The viscoelastic material has both of these properties. It responds to stress as if it were a combination of elastic solids and viscous liquid. The behavior of viscoelastic material can be represented as a linear combination of elastic spring, which obeys Hooke's law and viscous dashpot, which obeys Newton's law of viscosity. Maxwell model, Kelvin or Voigt model and Standard linear model are the simplest models used to predict the viscoelastic material response under different loading conditions. These models consist of spring and dashpot either in series or parallel, which also can be equivalently modeled as electrical circuits where stress is represented by voltage and strain rate by the current. And the viscosity of a dashpot is analogous to a circuit's resistance and the elastic modulus of a spring to a circuit's capacitance.

### 2.3.2.1 Maxwell Model

The Maxwell model can be presented by a purely elastic spring and a purely viscous damper connected in series, as shown in Fig. 2.5.

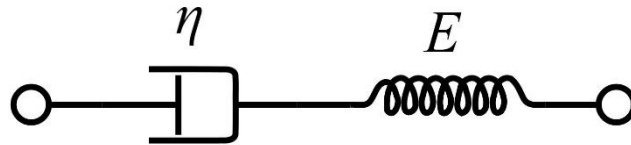


**Fig 2.5.** Maxwell model.

The conservation equation developed for the model is,

$$\sigma + \frac{\eta}{E} \dot{\sigma} = \eta \dot{\epsilon} \quad (2.6)$$

In this model, if the material is put under constant strain, the stresses gradually relax. At constant strain, the stress has two components: elastic component and viscous component. For the elastic component, the corresponding spring relaxes immediately upon the release of strain. For the viscous component, the corresponding dashpot relaxes with time as long as the strain is applied. The stress decays exponentially with time, which is accurate for most polymers. Though this model can give a reliable prediction for relaxation behavior, it can not predict creep behavior accurately.

### 2.3.2.2 Kelvin-Voigt Model

The Maxwell model can be presented by a purely elastic spring and a purely viscous damper connected in parallel, as shown in Fig. 2.6.

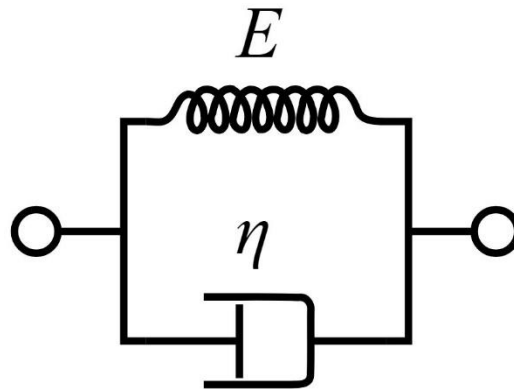


**Fig. 2.6.** Kelvin-Voigt model.

The conservation equation developed for the model is,

$$\sigma = E\varepsilon + \eta\dot{\varepsilon} \quad (2.7)$$

This model is used to describe creep behavior for a viscoelastic material. At constant stress, this model deforms at a decreasing rate and predicts strain to tend to  $\sigma/E$  as times continue to infinity. Though this model can give a reliable prediction for creep behavior, it can not predict relaxation behavior accurately.

### 2.3.2.3 Standard Linear Solid Model

The standard linear model is the combination of a spring and a Kelvin model in series, as shown in Fig. 2.7. It is the simplest model that describes both the creep and relaxation behavior of viscoelastic material accurately.

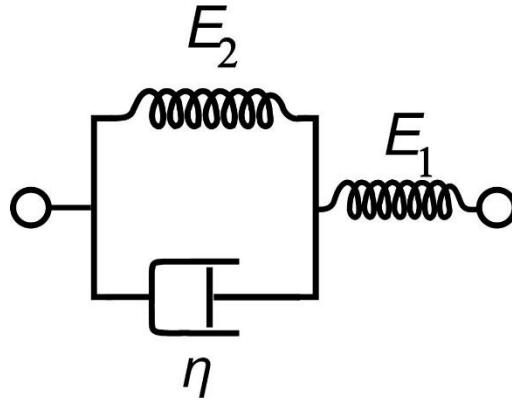


**Fig. 2.7.** Standard linear model.

The governing constitutive relation for this model is,

$$\sigma + \frac{\eta}{E_1 + E_2} \dot{\sigma} = \frac{E_1 E_2}{E_1 + E_2} \varepsilon + \frac{E_1 \eta}{E_1 + E_2} \dot{\varepsilon} \quad (2.8)$$

This model is more accurate than the Maxwell model and the Kelvin-Voigt model.

## **2.4 Application of MDPE Pipe**

### **2.4.1 Manufacturing and Use of MDPE Pipe**

Nowadays, polyethylene pipes are becoming more popular than cast iron, ductile iron, and steel pipe due to their corrosion-resistant, fatigue resistant, leak-free joints, adaptability, and other advantageous properties. In recent years, MDPE is more widely used due to its higher flexibility and long-term strength than HDPE. However, there is a lack of knowledge and experience in using this material in piping, unlike traditional materials like concrete and steel.

As a semi-crystalline polymer, the material property of MDPE is dependent not only on the chemical components but also on the crystallinity and morphology. Since the crystallinity and morphology are temperature dependent, the manufacturing process affects the properties of the final products. The factors related to the manufacturing process that may affect the properties of pipe materials are briefly discussed below.

- i) As a thermoplastic material, the MDPE pipe is manufactured by the extrusion process. If the cooling temperature and the cooling rate are not uniform from the outer surface to the inner, variance in crystallinity and morphology may be developed on the pipe wall's cross-section. Thus, significant variation in the mechanical properties might be developed across the pipe wall.
- ii) The mechanical properties might be affected by the orientation of the microstructure. During the MDPE extrusion, there is a velocity gradient with the minimum velocity at the pipe wall, which results in the extension orientation of the molecule. The degree of molecular orientation also depends on the cooling rate and extrusion temperature. If the extrusion temperature is high, the oriented molecules can relax more rapidly towards the random state. Pipe size and thickness also affect the degree

of molecular orientation. As the larger and thicker pipes are extruded and cooled more slowly, they tend to have a less uniform molecular orientation.

- iii) The mechanical properties of polyethylene are also affected by the residual stresses developed during solidification processes. Many workers investigated the residual stress effect on the mechanical performance of the pipe (e.g., Broutman, 1976; Williams et al., 1981; Bhatnager and Broutman, 1985; Beech et al., 1988; Doshi, 1989). During the extrusion process of thermoplastic material, the outer surface freezes quickly to the required dimension, while the inner surface continues to cool and solidify gradually. As a result, the molten state's inner material tends to shrink away from the external layer upon solidification, which induces stresses in both the outer solidified layer and the inner layer upon solidification. As the outer frozen layer is being 'pulled in' by the inner undergoing solidification layer, the developed stresses in the outer layer act as compression. In the case of the inner layer, these stresses act as tension as they are 'constrained from shrinkage inward' by the outer solidified layer.

The manufacturing technology and the geometry of pipe products control the effect of these factors. Those parameters must be analyzed individually, in order to verify their effects on pipe performance.

## 2.4.2 Performance Limit

Limit state design provides a safe and cost-effective method for buried pipelines and it requires a clear understanding of the performance limits. Moore (1994) suggested three performance limits for the design of buried gravity flow polyethylene pipes: pipe deflection, stress, strain, and buckling.

- i) Pipe deflection: The pipe deflection limit is considered as the primary design criterion for flexible pipes. To ensure integrity and avoid leakage, the deflected shape of the MDPE pipe must be kept in allowable limits. Installation procedure and the properties of the surrounding soil largely control the deflection of pipes. According to Canadian, the US, and European practice, the allowable change in diameter for polyethylene pipe is 7.5% (Zhang, 1996).
- ii) Limiting stress and strain: Stresses can be generated in the pipe wall due to inside pressure and the pressure from earth load on the outside surface of a pipe. Design can be performed by keeping the developed tensile stress below the tensile yield strength and compressive stress below the compressive yield strength. Similarly, the strain in the pipe wall can be kept below the tensile and compressive yield strains. If significant stresses and strains are developed in the pipe wall, slow crack growth may become a major concern.
- iii) Wall buckling: The wall buckling limit requires that the compressive hoop stress in the pipe wall be kept within the allowable limit as this may lead to the buckling failure.

## 2.5 Research on Polyethylene Pipe Performance

### 2.5.1 Experimental Study to Determine Polyethylene Pipe Performance

Laboratory tests were performed in the past to investigate the long-term performance of polyethylene pipes. Loven and Janson (1972) performed a relaxation test on pipe rings where the pipe ring was subjected to constant diametrical compression by point loads. The authors got 1000 hours of relaxation behavior of pipe from this test. To characterize the long-term creep behavior of PE, Findley started a long-term creep test in 1957, and the test was continued to provide data (Findley and Tracy, 1974; Findley 1987). The authors used the Boltzmann superposition principle to predict the short-term and long-term behavior of polyethylene pipe. It was reported from the research that long term creeps term behavior (230,000 h) can be well predicted than short term creep behavior (1900 h). Janson (1985) performed a stress relaxation test on smooth wall HDPE pipe rings for 10000 hours, where the ring was deflected to 4.6% and 13.7%, respectively. To account for the reduction of stiffness with time, he expressed the modulus of HDPE, at a particular strain level, as a power-law relation.

Hashash (1991) performed a test on 24-inch diameter corrugated HDPE pipes under the condition of a constant rate of deformation and stress relaxation. He proposed the following time-dependent secant modulus,

$$E(t) = 329 t^{0.0859} \quad (2.9)$$

Di Francesco (1993) conducted a series of laboratory ring bending tests under a constant rate of deflection and load-relaxation with periodic short-term deflection increments. He found that the short-term tangent modulus of the pipe was independent of the previous loading. Under the additional deflection, the pipe behavior was like that it was never loaded.

Zhang and Moore (1997) performed extensive experimental work on samples cut from the thick-walled HDPE pipe to investigate its nonlinear time-dependent behavior. They conducted tests under constant strain rate, creep, stress relaxation, constant loading rate, abrupt change of strain rate, creep recovery, cyclic strain rate, and various combinations of these loading conditions and developed nonlinear viscoelastic and viscoplastic theoretical models. A nonlinear viscoelastic (NVE) model was found to predict well for constant rate conditions and relaxation behavior at the lower strains. A viscoplastic (VP) model performed better at the larger strains.

Limited research information is currently available in the literature to describe the nonlinear time-dependent behavior of the MDPE pipe. Bilgin et al. (2007) performed an extensive laboratory test to investigate the time-dependent stress relaxation behavior under mechanical and thermal conditions for the MDPE pipe. They investigated the pipes for a temperature range between -6.7 and 49°C to represent the full range of temperatures expected in the field. It was reported that the pipes behave in a manner consistent with linear viscoelastic theory within the expected range of temperature. Simple power-law relaxation formula could be used to determine the pipe stresses.

### **2.5.2 Analytical Models Used to Determine Polyethylene Pipe Performance**

Few analytical models have been developed by the authors to determine the viscoelastic response of polyethylene pipes. Among them, mostly used models are the Power law model and the Hyperbolic constitutive model.

### 2.5.2.1 Power Law Model

Ignoring the temperature dependency, the stress-strain relationship for the viscoelastic material can be expressed in the following form,

$$\sigma = f(\varepsilon, t) \quad (2.10)$$

At lower strain, equation (2.9) can be written as,

$$\sigma = \varepsilon f(t) \quad (2.11)$$

This is termed as “linear” viscoelasticity. Based on this assumption, the relaxation modulus of the pipe at a given time can be written as,

$$E(t) = \frac{\sigma(t)}{\varepsilon_0} = E_0 t^{-n} \quad (2.12)$$

Here,  $E_0$  and  $\varepsilon_0$  indicates the modulus and the corresponding strain at time, 1 minute and  $n$  indicates the rate of stress relaxation. Table 2.1 shows different  $n$  values obtained for MDPE pipe.

**Table 2.1.** Relaxation power-law exponent for MDPE.

	Nominal Temperature	Power Law Exponent, $n$
Husted and Thompson (1985)	70 °F	0.105
Janson (1985)	70 °F	0.081
Keeney (1999)	20 to 120 °F	0.085 ± 0.01

### 2.5.2.2 Hyperbolic Constitutive Model

The hyperbolic model is one of the simplest approaches to model nonlinearity. Kondner (1963) and Duncan and Chang (1970) introduced a simplified hyperbolic model to characterize the time-dependent nonlinear response of the soil. The general equation of the hyperbolic model is given as,

$$\sigma = \frac{\varepsilon}{m+n\varepsilon} \quad (2.13)$$

Here, ‘m’ and ‘n’ are the constants to be estimated through nonlinear regression analysis with test results.

Considering the strain rate dependent behavior of polymer materials, Suleiman and Coree (2004) proposed a modification to the hyperbolic model. This model can be presented in the following format,

$$\sigma = E_{ini} \left( \frac{\varepsilon}{1+\eta\varepsilon} \right) \quad (2.14)$$

Where  $E_{ini}$  and  $\eta$  are hyperbolic constants. These constants are strain-rate dependent and can be obtained using the following equations,

$$E_{ini} = a(\dot{\varepsilon})^b \quad (2.15)$$

$$\eta = E_{ini} \left( \frac{a(\dot{\varepsilon})^b}{c+d\ln(\dot{\varepsilon})} \right) \quad (2.16)$$

Where  $\dot{\varepsilon}$  is the strain rate, and a, b, c, d are constants that can be determined by fitting with the stress–strain responses obtained from uniaxial tension or compression tests.

The hyperbolic constants obtained for HDPE pipe material are listed in Table 2.2 (Zhang and Moore, 1997)

**Table 2.2.** Parameters for the hyperbolic model of the HDPE pipe.

Hyperbolic parameters	Values
a	2000
b	0.137
c	27.5
d	1.29

Though this model can provide a simple framework for accurate modeling of stress–strain behavioral patterns for viscoelastic material, it is not capable of modeling plastic (permanent) deformations and unloading responses. However, it is more efficient with a smaller number of input parameters than polynomial functions.

### **2.5.3 Numerical Study to Determine Polyethylene Pipe Performance**

Many factors can affect pipe behavior like pipe material, surrounding soil material, installation procedure, loading conditions, time, and many others. Laboratory or field tests are limited to conducting exhaustive parametric studies to investigate failure modes as they are both time-consuming and costly. In this case, a numerical simulation may be a useful alternative as it requires much less time and cost.

However, numerical analysis of soil-pipe interaction for polyethylene pipes is complex as the behavior of polymer material is time, temperature, and strain rate dependent. The behavior of polymer material consists of an instantaneous elastic response following by viscoelastic (recoverable) and viscoplastic (irrecoverable) deformations. As the viscoelastic behavior initiates at a low-stress level, it is difficult to identify a well-defined yielding point beyond which permanent

strains develop. Several studies were conducted to investigate the performance of buried HDPE pipe using two-dimensional finite element analysis (Katona, 1988; Hjelmquist and Storakers, 1987; Chua, 1986; Chua and Lytton, 1989). Then, Moore (1994) developed a three-dimensional finite element model to investigate the response of corrugated polyethylene pipe under parallel plate loading. In both two dimensional and three-dimensional analyses, linear viscoelastic constitutive relations were applicable for HDPE at small deflections (Moore, 1994). The limit of applicability of linear viscoelasticity for HDPE were found to be about 0.008 strains (Zhang, 1996). Zhang and Moore (1997) developed a nonlinear viscoelastic and viscoplastic model for large deflection problems. This model could effectively predict the HDPE response under monotonic loading conditions. Pipe responses associated with unloading, strain reversal, and cyclic loading were poorly predicted using the model. To overcome these limitations, few other constitutive models were developed for polymer materials (Chehab and Moore, 2006; Suleiman and Coree, 2004; Siddiquee and Dhar, 2015). However, none of these models used widely as they are not implemented in commercially available finite element software. Muntakim et al. (2018) have developed a model using commercially available finite element software, Abaqus (Dassault systems 2015) which can reasonably predict the rate-dependent and time-dependent behavior of HDPE.

Very limited information is currently available on modeling the time-dependent behavior of MDPE pipe materials. To model the time dependent response of MDPE, Bilgin (2014) used the built-in feature for the Prony series available in a commercially available FE software, Abaqus. He successfully simulated the relaxation behavior of MDPE at very low strain levels (strain < 0.008). This model cannot capture the nonlinearity of pipe material at higher strains. Therefore, a

non-linear material model is required to be developed that can capture the rate-dependent and time dependent effect of MDPE pipe material.

## **2.6 Summary**

An overview of polyethylene pipe material and theoretical and experimental methods used for predicting pipe behavior have been reviewed in this chapter. Although many studies are available on the characterization of HDPE's nonlinear behavior, very limited information is currently available on the MDPE pipe materials. Several studies focused on analyzing the viscous behavior of pipes. Some of them are only suitable for lower strain levels and are complex for application in engineering design. This study aims to develop a numerical modeling technique to simulate the nonlinear time-dependent behavior of the MDPE pipe.

## CHAPTER 3

### **Nonlinear Time-Dependent Mechanical Behavior of a Medium Density Polyethylene Pipe Material**

**Co-Authorship:** This chapter has been accepted for publication in the ASCE Journal of Materials in Civil Engineering as: Das, S. and Dhar, A.S. (2012), ‘Nonlinear Time-Dependent Mechanical Behavior of a Medium Density Polyethylene Pipe Material.’ Most of the research presented in this chapter has been conducted by the first author. He also prepared the draft manuscript. The co-author mainly supervised the research and reviewed the manuscript.

#### **3.1 Introduction**

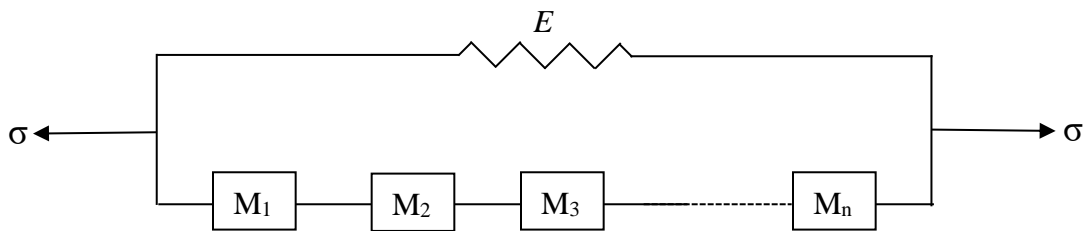
The use of polymer pipes has been increased significantly over the last few decades due to their various advantages over metal pipes, including low cost, lightweights, ease of installation, and corrosion resistance. Water supply, cold water distribution, sewer, gas distribution, and irrigation are the major areas of application of the polymer pipes. Medium-density polyethylene (MDPE) pipes are widely used for water and gas distribution systems. These buried distribution pipes are subjected to loads from the weight of the soil column above the pipe, the surcharge loads including live traffic and dead loads, internal pressure, and loads from ground movement resulting from landslides and seismic activities if any. The behavior of the pipes under these loads is influenced by their interaction with the surrounding soil. Soil-pipe interaction analysis is generally performed to understand the behavior of pipes subjected to various loads. However, modeling of soil-pipe interaction for polyethylene pipes is complex as the behavior of polymer material is time, temperature, and strain rate dependent. Polymer materials exhibit an instantaneous elastic response following by viscoelastic (recoverable) and viscoplastic (irrecoverable) responses. As the

viscoelastic behavior initiates at a low-stress level, it is hard to identify a well-defined yielding point beyond which permanent strains develop.

Studies on understanding the viscoelastic and/or viscoplastic behavior for MDPE pipe material are very limited in the available literature. Hamouda et al. (2007) conducted uniaxial "tension-relaxation" tests using samples cut out from a thick-walled MDPE pipe. Based on the tests conducted at two different strain rates, they revealed that the behavior of MDPE is highly nonlinear and strain-rate dependent. Liu et al. (2008) conducted creep tests with three different High-Density Polyethylene (HDPE) materials and an MDPE pipe material. They revealed that the responses of polyethylene materials could be significantly different under loads due to differences in their molecular structures. Using the creep test results, they determined parameters for a multi-Kelvin type viscoelastic model for these materials. Bilgin et al. (2007) examined the thermal and mechanical properties of an MDPE pipe material through stress relaxation tests and temperature ramp tests with full-scale pipe segments. They proposed constant relaxation modulus, instantaneous modulus, and stress relaxation rates, which are assumed to be independent of the applied strain rate. However, Hamouda et al. (2007) revealed that the relaxation behavior of the material could significantly depend on the applied strain rate. None of these studies extensively investigated the strain-rate dependent stress-strain relations and the relaxation/creep behavior of the MDPE.

Several studies were conducted in the past for modeling the nonlinear time-dependent behavior of polyethylene pipe materials with attention to HDPE. Tobolosky (1960) used convolution integral to simulate the viscoelastic behavior, which relates time-dependent stress with strain by a relaxation modulus. Popelar et al. (1990) expanded this method to include nonlinearity

and temperature effects in stress relaxation behavior. Time-dependent relaxation moduli of HDPE pipe material were also developed as power-law relations with time (Chua and Lytton 1989; Hashash 1991). However, the time-dependent relaxation modulus can only be used to assess the responses at a particular strain level for which the power-law equation is developed. It cannot be used to evaluate the overall strain rate dependent responses of the viscoelastic or viscoplastic material. Few other constitutive models were developed for polymer materials that overcome the limitations (Moore 1994; Zhang and Moore, 1997; Chehab and Moore, 2006; Suleiman and Coree, 2004; Siddiquee and Dhar, 2015; Hamouda et al. 2007). These models were used for finite element (FE) modeling of the time-dependent behavior of the materials. The major challenges with these models include: i) obtaining the model parameters from laboratory tests that would reasonably represent the real behavior, and ii) the complexity of the models for implementation in commercially available FE codes. Viscoelastic models based on Prony series are becoming popular recently due to its ease of implementation in FE codes (Bilgin 2014; Swain and Ghosh 2019). The Prony series is defined as an arrangement of several Maxwell elements in series with a parallel spring element, as shown in Fig. 3.1.



$M_i = i^{\text{th}}$  Maxwell element with  $E_i$  and  $\tau_i$

$n =$  Number of Maxwell elements

$E_i =$  Elastic modulus of  $i^{\text{th}}$  increment

$\tau_i =$  Viscosity of  $i^{\text{th}}$  increment

**Fig. 3.1.** Prony series model.

Bilgin (2014) used the built-in feature for the Prony series available in a commercially available FE software, Abaqus, and successfully simulated the relaxation behavior of an MDPE pipe material at very low strain levels (strain  $< 0.008$ ). At these levels of strain, the stress–strain response of the pipe material is almost linear. However, at higher strains (or stresses), the stress–strain response of the pipe material is nonlinear, which cannot be captured using the conventional Prony series. Bilgin (2014) obtained the model parameters from the relaxation tests data of Bilgin et al. (2007). The creep and the effects of strain rate on the stress–strain responses were not investigated in their study.

The objectives of the current study are to experimentally investigate strain-rate dependent stress–strain behavior, relaxation behavior, and creep behavior of a MDPE pipe material and to develop a numerical method to simulate the nonlinear time-dependent behavior. The motivation of this study is the need to model the MDPE distribution pipes subjected to lateral ground movements at different rates. The pipelines are often subjected to lateral ground movements at various rates causing strains in the axial directions of the pipes. However, test results and a material model are currently not available for modeling of these pipes experiencing various scenarios of the ground movements. This study focuses on extending the database in the body of knowledge for MDPE pipe material, including the development of modeling techniques using commercially available FE software. The study includes 1) an experimental investigation of strain-rate dependent stress-strain behavior, relaxation behavior, and creep behavior using uniaxial tension tests. Tests with a complex loading history were also performed; 2) the development of rate-dependent constitutive relations for use in the FE modeling; 3) the development of a FE modeling technique to simulate the nonlinear time-dependent behavior. In the time-dependent modeling technique, strain-rate dependent stress-strain models are used to simulate loading and unloading behavior,

and a power-law type creep-law model is used to simulate the creep/relaxation behavior. The models developed using the uniaxial tests can be applied for generalized models with multi-axial stress conditions using the von Mises theory (Chehab 2008, Siddiquee and Dhar 2015). The proposed method is validated through comparison with test results and the results from FE analysis using conventional Prony series.

### **3.2 Test Methods**

Tensile tests were performed to investigate the time-dependent behavior (strain rate effect, creep, and relaxation) of an MDPE pipe material commonly used in the Canadian gas distribution system (CSA B 137.4 certified). A test was first conducted on a whole pipe segment. Cholewa et al. (2011) showed for a HDPE pipe that the stress-strain responses from whole pipe segment tests are different from those from coupon tests. The difference is attributed to the presence of residual stresses in the whole pipe resulting from the manufacturing process. However, the residual stress resulting from the manufacturing process is generally unknown, which may be different for pipes with different diameters. As a result, it would be challenging to interpret the results from a whole pipe segment test for the development of a constitutive model of the material. The residual stresses are released when the coupons are cut from the pipe wall. Thus, the coupon tests can be used to investigate the behavior of the pipe material, avoiding the influence of the residual stresses. Coupon tests were therefore used in the present study. The whole pipe test was used to examine the extent of the impact of residual stresses on the pipe considered in this study.

For the whole pipe test, a segment of a 42.2 mm diameter pipe was used with a gauge length of 500 mm. The pipe wall thickness is 4.5 mm. A special arrangement at the ends of the sample was made to apply axial tension using Universal Testing Machine (UTM) (Fig. 3.2a). This arrangement included inserting a threaded metal block of a circular cross-section at each end, well-

fitted inside the pipe (Fig. 3.2b). The metal blocks offer reactions against the gripping forces from the jaws of UTM, allowing the jaws to hold the pipe sample firmly without lateral deflection of the pipe sample. The load was applied to the sample using the vertical movement of the upper crosshead of the machine. The upward movement of the crosshead causes a tensile load, and downward movement causes a compressive load on the specimens.

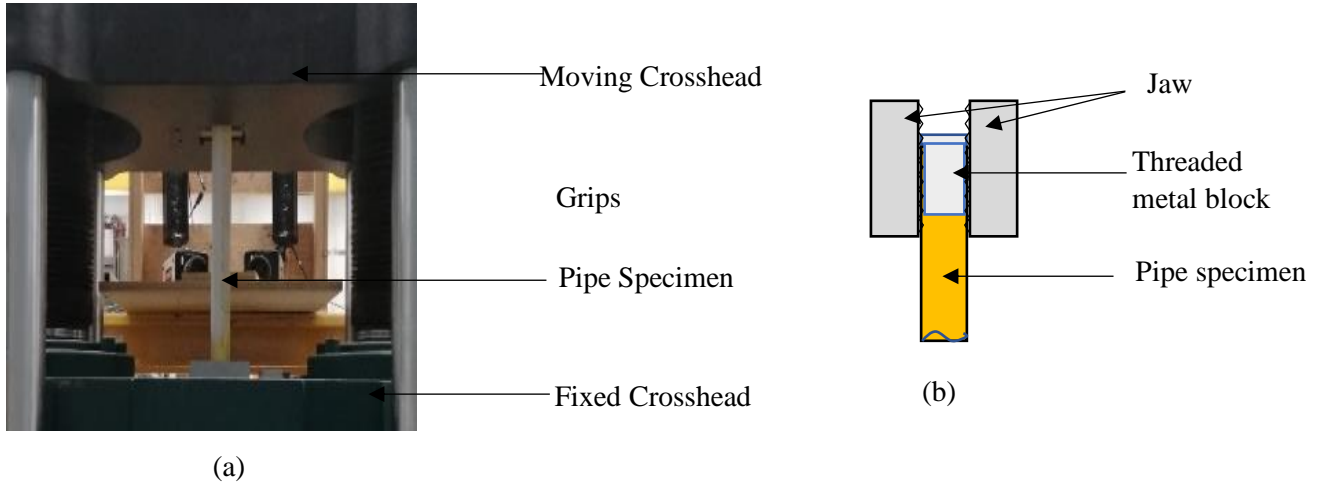
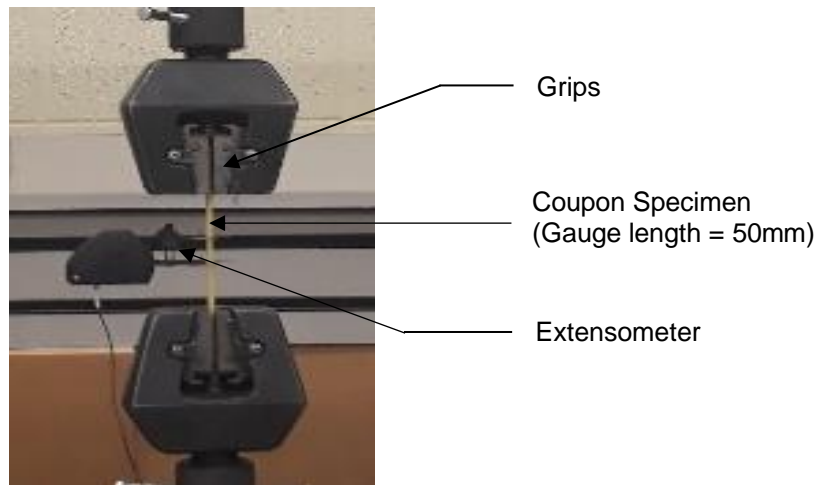
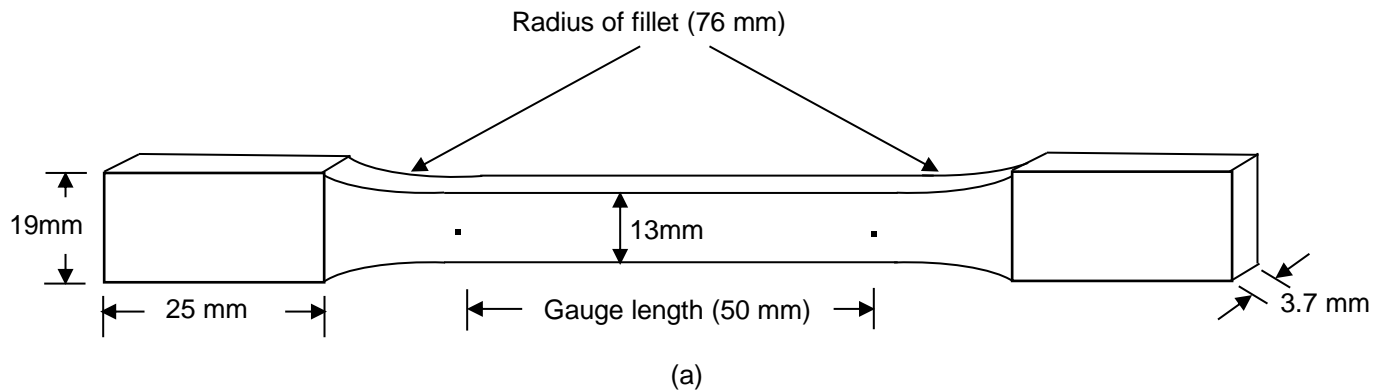


**Fig. 3.2.** Test set up and loading apparatus for full pipe test: (a) UTM machine; (b) Mechanism of grips.

A load transducer, which was mounted in series with the specimen, measures the applied load and converts the load into an electrical signal that an automated control system measures and displays. The change of the height of the specimen was measured by recording the ram position through the displacement transducer of the Instron machine, and the corresponding load was measured by a load cell. A computer-controlled system was used to monitor and record the outputs of the displacement transducer and the load cell.

For the coupon tests, the samples were prepared according to ASTM D638-14 specifications (ASTM 2003). A water jet was used for cutting the pieces from the wall of 60.3 mm diameter MDPE pipes. A surface planer was then used to remove the curvature from the pieces.

The length of the test specimens was parallel to the length of the MDPE pipe. The coupon specimens were tested under uniaxial tension using an INSTRON (5585H) machine equipped with a load transducer (Fig. 3.3). A schematic of the samples is shown in Fig. 3.3a. For measuring strain in coupon specimens, Debnath et al. (2019) used uniaxial strain gauges at the center of the specimens for a cast iron pipe material. However, strain measurement using strain gauges was considered unsuitable for the flexible MDPE coupons since the adhesive for gluing the strain gauges can stiffen the specimen surface, affecting the measured strains (Brachman et al. 2000). Strain within the gauge length was therefore measured using a clip-on extensometer (Fig. 3.3b).



(b)

**Fig. 3.3.** Test set up and loading apparatus for coupon tests: (a) Schematic of coupon specimen; (b) Tensile testing machine.

Tests were conducted under constant strain rates, creep at certain stress levels, and relaxation at certain strain levels. The movements of the crosshead of the machine were used to control the displacement rate during the application of the load. Measured strains (using extensometer) and the corresponding time intervals were then used to interpret the strain rates applied during the tests. The tests were managed, and data was obtained using a computer-controlled system equipped with an Instron proprietary software. All tests were conducted at room temperature ( $22 \pm 1^\circ\text{C}$ ).

The same test was repeated two or three times to examine the repeatability of the test results. Table 3.1 shows a summary of the test program undertaken. As shown in the table, a total of 35 tests were conducted. Tests 1 to 21 are constant strain rate tests conducted at various strain rates, Tests 24 to 29 are relaxation tests, and Tests 30 to 35 are creep tests. Tests 22 and 23 were performed to examine the effect of loading history on stress–strain behavior. In Tests 22, the strain rate was changed during the test, and in Tests 23, a loading-unloading-reloading cycle was applied.

Engineering stresses and strains were calculated based on the measured loads and elongations within the gauge length, respectively, for interpretation of test results. Engineering stresses and strains are conveniently used in practice, which are, however, not significantly different from the corresponding true values at low strain levels typically encountered in buried pipelines (Cholewa et al. 2011).

**Table 3.1.** Test Program.

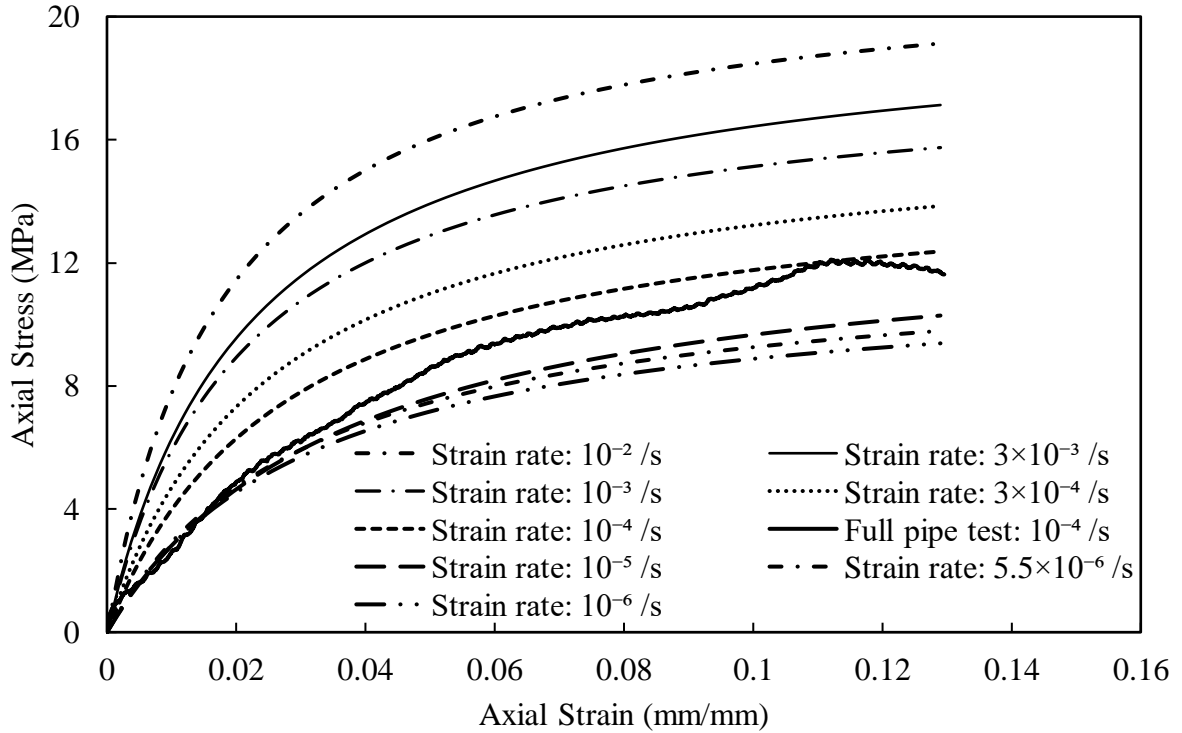
Test Number	Type of Test	Remarks
1,2,3	Uniaxial tension test	Tests were conducted at $10^{-2}$ /s strain rate
4,5,6	Uniaxial tension test	Tests were conducted at $3 \times 10^{-3}$ /s strain rate
7,8,9	Uniaxial tension test	Tests were conducted at $10^{-3}$ /s strain rate
10,11,12	Uniaxial tension test	Tests were conducted at $3 \times 10^{-4}$ /s strain rate
13,14,15	Uniaxial tension test	Tests were conducted at $10^{-4}$ /s strain rate
16,17	Uniaxial tension test	Tests were conducted at $10^{-5}$ /s strain rate
18,19	Uniaxial tension test	Tests were conducted at $5.5 \times 10^{-6}$ /s strain rate
20,21	Uniaxial tension test	Tests were conducted at $10^{-6}$ /s strain rate
22	Strain rate change	Strain rate changed between $10^{-2}$ /s and $10^{-3}$ /s
23	Loading-unloading-reloading test	Loading-unloading-reloading test was conducted at $10^{-3}$ /s strain rate
24,25	Relaxation test	Tests were conducted to 0.014 strain (initial strain rate: $10^{-3}$ /s)
26,27	Relaxation test	Tests were conducted to 0.024 strain (initial strain rate: $10^{-2}$ /s)
28,29	Relaxation test	Tests were conducted to 0.052 strain (initial strain rate: $10^{-2}$ /s)
30,31	Creep test	Tests were conducted to 2 MPa (initial strain rate: $10^{-4}$ /s)
32,33	Creep test	Tests were conducted to 8.5 MPa (initial strain rate: $10^{-3}$ /s)
34,35	Creep test	Tests were conducted to 10 MPa (initial strain rate: $10^{-2}$ /s)

### 3.3 Test Results

#### 3.3.1 Constant Strain Rate Tests

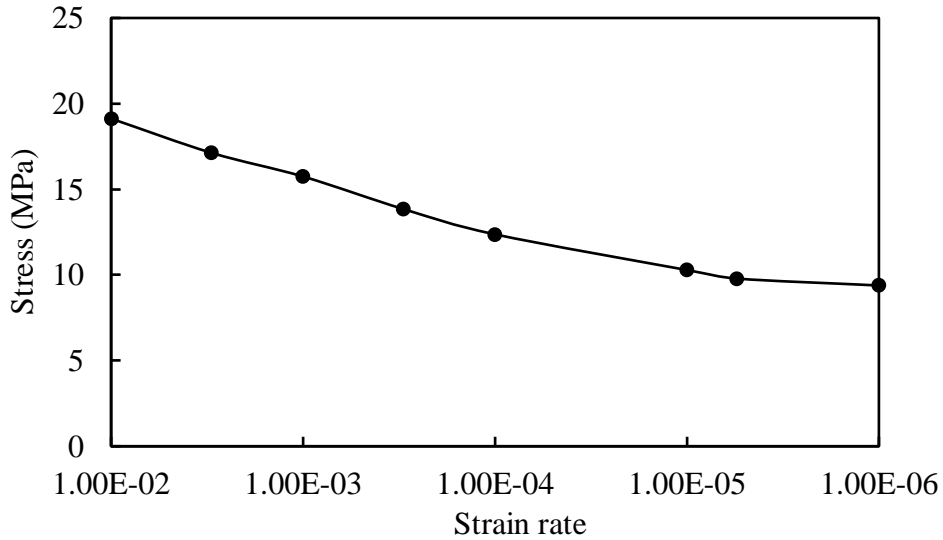
Uniaxial tension tests were performed at constant strain rates ranging from a very small value to  $10^{-2}$  /s. The very low strain rates are selected to identify the lower bound value below which the stress–strain response is independent of the strain rate. The existence of such a lower bound strain rate (termed as 'reference strain rate") is assumed in the development of an isotach based viscoplastic model for HDPE pipe material (Siddiquee and Dhar 2015). However, this phenomenon has not been experimentally validated for MDPE pipe material. The test samples were loaded to strain beyond an "allowable strain limit" according to industry practice in Canada. An allowable strain limit of 8% has been adopted as an industry practice for MDPE pipes (Weerasekara and Rahman 2019). The tests were conducted to a strain of around 13%.

Fig. 3.4 shows the mean stress-strain responses for different strain rates from the constant strain rate tests. The stress-strain responses from multiple tests for each strain-rate (Table 3.1) were found consistent with each other (maximum variation of less than 10% from the corresponding mean values). The mean values presented in Fig. 3.4 are therefore used for comparison and validation of numerical models, discussed later. Fig. 3.4 shows that the stress-strain response of the MDPE material is extensively strain-rate dependent, similar to HDPE pipe material reported in Zhang and Moore (1997). At any particular strain, the stress is higher for the tests conducted at a higher rate of strain. The higher stress at the higher strain-rate is associated with the overstress component of the total stress for the viscous materials. According to the overstress theory (Perzyna 1966), the total stress in the viscous material can be decomposed into an equilibrium stress, and an overstress. The equilibrium component is independent of the strain-rate (i.e., inviscid stress), while the overstress component is strain-rate dependent (i.e., viscous stress).



**Fig. 3.4.** Rate dependent stress–strain responses from the constant strain-rate tests (mean values).

The equilibrium stress-strain relation of materials corresponds to a test conducted at the infinitely slow strain rate. Siddiquee and Dhar (2015) defined a very slow strain rate for HDPE as the “reference strain rate” below which the strain-rate dependence of the stress-strain relation is practically insignificant. The overstresses are then calculated from the total stress-strain response by subtracting the stress-strain response at the reference strain rate. To examine the “reference strain rate” for MDPE, the measured stresses at a particular strain (i.e., 0.13) are plotted against the strain rates in Fig. 3.5. It shows that the stress decreases with the decrease of strain-rate initially. The line is almost horizontal between strain rates of  $5.5 \times 10^{-6}/s$  and  $10^{-6}/s$ , indicating an insignificant influence of strain-rate on the stress. Thus, the strain rate of  $10^{-6}/s$  can be taken as the reference strain rate for the MDPE pipe material.



**Fig. 3.5.** Effect of strain rate on the stresses of MDPE.

Fig. 3.4 shows high nonlinearity in the stress-strain responses for the MDPE pipe material. However, at very small strains (strain < 0.01), the responses are almost linear. Bilgin et al. (2007) also observed close-to linear stress-strain relations at lower strain levels (strains < 0.008) for an MDPE pipe material. They calculated the instantaneous modulus of elasticity (initial tangent modulus) of 958 MPa at room temperature (21°C), which is within the reported values in the literature (Bilgin et al. 2007). Note that the strain rate effect was not accounted for in the initial moduli reported in the literature and in Bilgin et al. (2007). However, as seen in Fig. 3.4, the initial modulus significantly depends on the strain-rates. Initial tangent moduli calculated at various strain rates from the test results are presented in Table 3.2. The table includes the results of two additional preliminary tests conducted at strain rates of  $3 \times 10^{-3}/s$  and  $3 \times 10^{-4}/s$  prior to the execution of the test program. In Table 3.2, the initial modulus is found to range from 325 MPa to over 1000 MPa, depending on the rate of strain. According to the values shown in the table, the initial moduli reported in the literature (i.e., ~ 958 MPa, Bilgin et al. 2007) corresponds to the values at a strain rate of  $10^{-3}/s$  to  $10^{-2}/s$ .

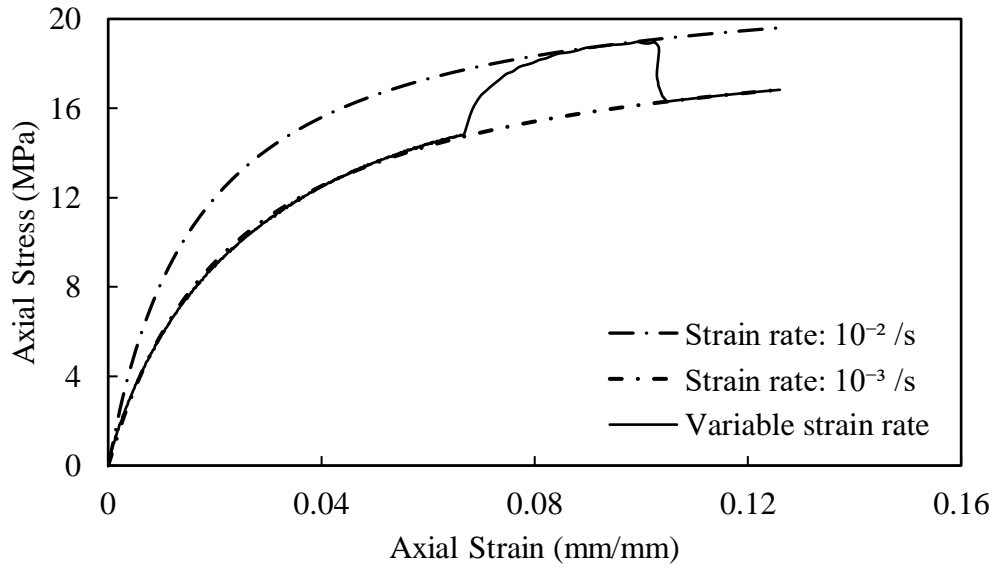
**Table 3.2.** Initial modulus of MDPE at various strain rates.

Strain rate ( /s)	Initial modulus, $E_{ini}$ (MPa)
$10^{-2}$	1,064
$3 \times 10^{-3}$	902
$10^{-3}$	776
$3 \times 10^{-4}$	658
$10^{-4}$	566
$10^{-5}$	413
$5.5 \times 10^{-6}$	337
$10^{-6}$	325

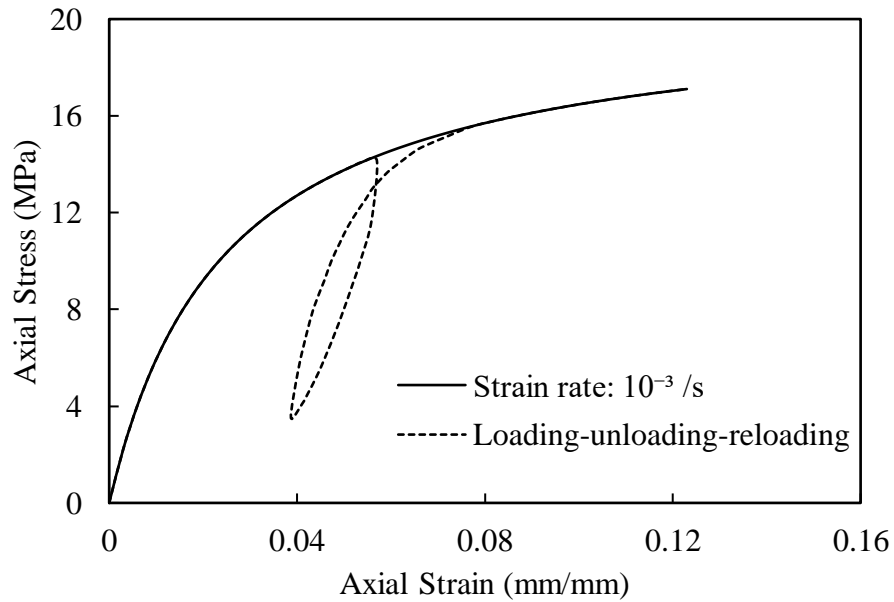
The stress-strain response obtained from the full pipe test is also included in Fig. 3.4. A strain rate of  $10^{-4}$  /s was applied for the test with a full pipe segment. In this test, the stress is initially underestimated, which is due to the slipping of the grips. However, at a higher load, it matches the coupon test results conducted at a similar strain rate ( $10^{-4}$  /s). Thus, the influence of residual stress is insignificant for the pipe, and the coupon test results reasonably represent the mechanical behavior of the pipe material.

In Test 22, a strain rate of  $10^{-3}$ /s was applied up to a strain of 0.065. At 0.065 strain, the rate was changed from  $10^{-3}$ /s to  $10^{-2}$ /s that continued until a strain of 0.11. Then, the strain rate was changed back to  $10^{-3}$ /s. The results are shown in Fig. 3.6, along with the stress–strain responses corresponding to the strain rates of  $10^{-3}$ /s and  $10^{-2}$ /s, respectively. As seen in the figure, for changing the strain rate from  $10^{-3}$ /s to  $10^{-2}$ /s, an increase of stress occurred. The stress–strain curve then matches with the stress–strain response corresponding to the strain rate of  $10^{-2}$ /s. Similarly, when the strain rate was changed back to  $10^{-3}$  /s, the response follows the stress–strain response corresponding to  $10^{-3}$ /s strain rate with a sudden drop. This indicates that the stress–strain

responses of the MDPE material depend predominantly on the strain-rate, which is not affected by the loading history. Similar responses were reported earlier for HDPE in Zhang and Moore (1997).



**Fig. 3.6.** Experimental results for strain-rate-change test.



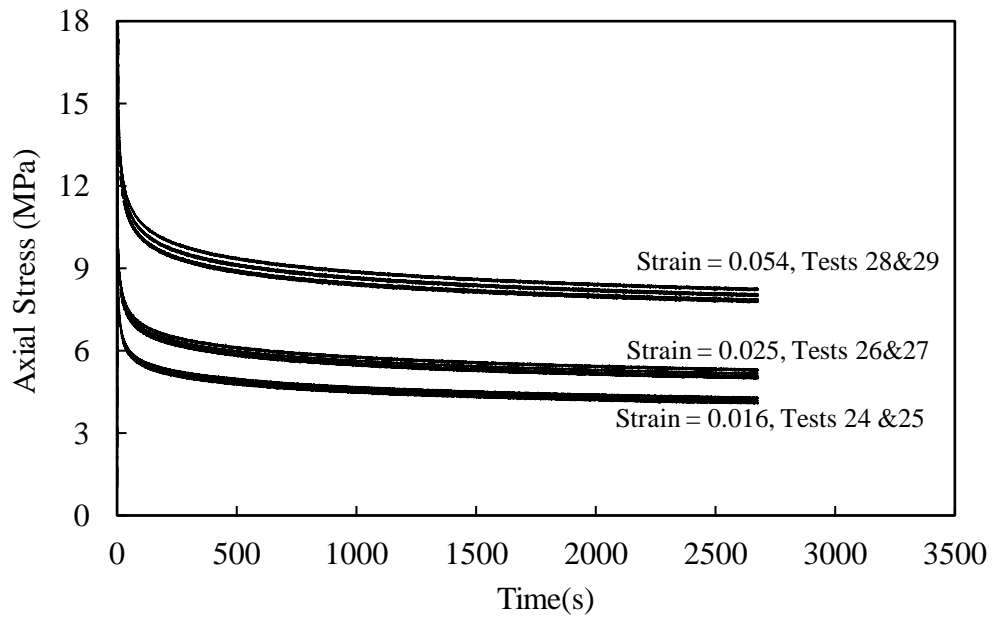
**Fig. 3.7.** Experimental results for loading-unloading-reloading test.

Fig. 3.7 shows the results of the loading-unloading-reloading test. The test was conducted at the same strain rate of  $10^{-3}/s$  during the load-unload-reload cycle. This figure reveals that the unloading and reloading do not affect the strain-rate dependent stress–strain response beyond the previous stress level. As a result, the stress–strain curve for reloading gradually approached the monotonic loading curve corresponding to the strain rate.

### **3.3.2 Relaxation and Creep Tests**

Stress relaxation and creep tests were conducted to examine the viscous behavior of MDPE pipe material. To conduct a relaxation test, a specimen is tensioned at a constant strain rate to a predetermined strain. The strain is then held constant for the rest of the test. Fig. 3.8 shows the results of the stress relaxation tests conducted. Each test was performed twice to examine the repeatability. In Tests 24 and 25, an initial strain rate of  $10^{-3}/s$  was applied up to a strain of  $\sim 0.016$ , and the strain was then held constant. In Tests 26 and 27, an initial strain rate of  $10^{-2}/s$  was applied up to a strain of 0.025. In Tests 28 and 29, an initial strain rate of  $10^{-2}/s$  was applied up to a strain of 0.053 when the strain was held constant. The average maximum stresses at the three sets of tests were 9.2 MPa, 12.8 MPa, and 17.8 MPa, respectively. As seen in Fig. 3.8, each pair of relaxation tests for a particular strain level are consistent with each other, confirming repeatability of the test results. The average responses are therefore used for further interpretations.

Fig. 3.8 shows that the MDPE pipe material exhibits typical relaxation behavior with a high decrease of stress initially that stabilizes after a period of time. The relaxation behavior is expected to stop when the stress reaches the equilibrium (inviscid) stress-strain relation (i.e., reference stress-strain relation), and the overstress becomes zero (Colak and Dusunceli 2006).



**Fig. 3.8.** Experimental results for relaxation tests (in-between lines represent the mean values).

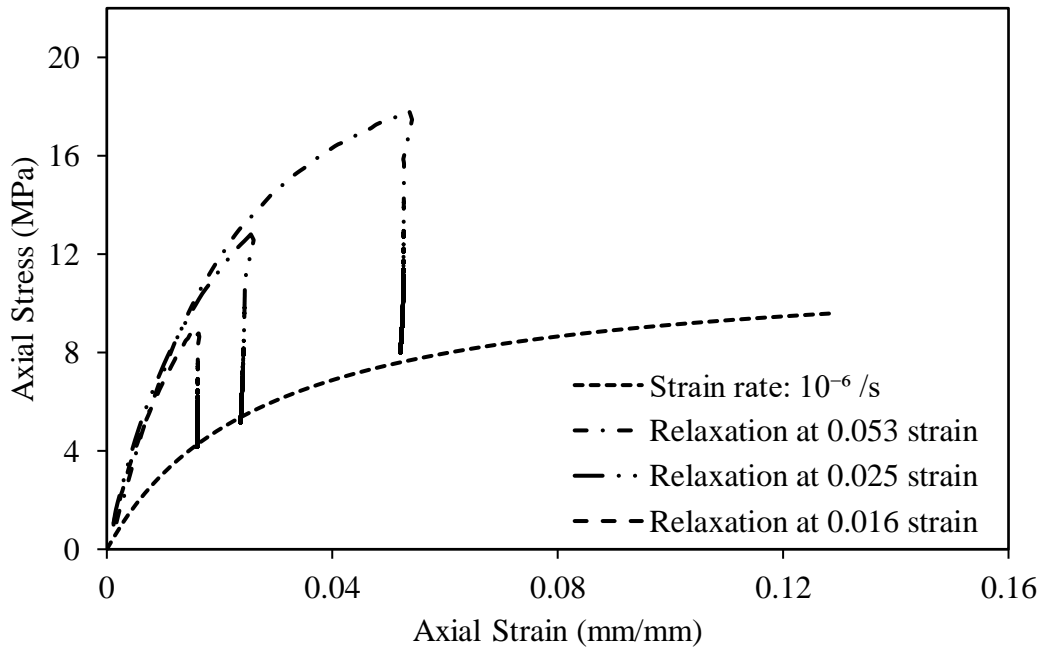


**Fig. 3.9.** Stress–strain responses of the relaxation tests.

The stress–strain responses during the relaxation tests are compared with the reference stress–strain relation (at the strain rate of  $10^{-6}/s$ ) in Fig. 3.9. It reveals that the stress reduces at constant strains during relaxation and finally stop at the minimum values corresponding to the reference (equilibrium) stress–strain relations. This observation confirms the existence of the reference (equilibrium) stress–strain relations. This observation confirms the existence of the reference stress–strain responses at the strain rate of  $10^{-6}/s$  for the MDPE pipe material.

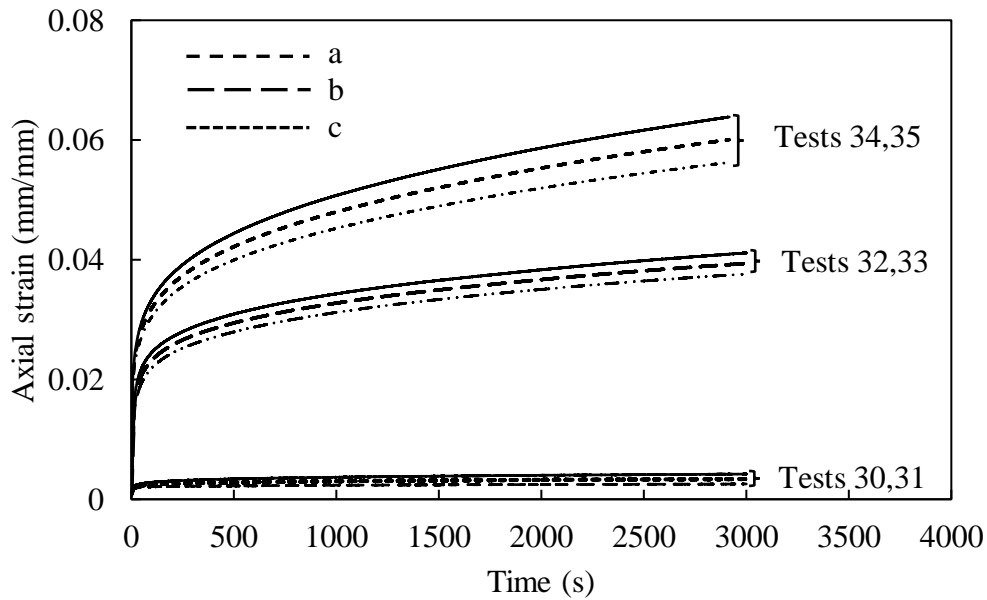


**Fig. 3.10.** Experimental results of creep tests (a, b, c are mean values).

In the creep tests, the specimens were subjected to tension at constant rates and deformed to the predetermined load levels. The load is then kept constant for the rest of the test duration. Fig. 3.10 shows the results of the creep tests conducted. In Tests 30 and 31, an initial strain rate of  $10^{-4}/s$  was applied up to 2 MPa of stress. In Tests 32 and 33, an initial strain rate of  $10^{-3}/s$  was applied up to 8.5 MPa of stress, and in Tests 34 and 35, an initial strain rate of  $10^{-2}/s$  was applied up to 10 MPa of stress. The initial strains corresponding to the applied stress levels are 0.021, 0.025, and 0.052 in the tests conducted with strain rates of  $10^{-4}/s$ ,  $10^{-3}/s$  and  $10^{-2}/s$ , respectively.

Fig. 3.10 shows that only primary creep and secondary creep are there over the test durations. At the primary creep stage, the increase of creep strain is relatively high with time, while at the secondary creep stage, the creep strain rate is almost constant. No tertiary creep was observed within the test duration, even for the highest stress level considered.

### **3.4 Modeling Time-Dependent Behavior**

Different constitutive models were developed in the past to capture the time-dependent behavior of HDPE materials (Chua and Lytton 1989; Zhang and Moore 1997; Chehab and Moore 2006; Suleiman and Coree 2004; Siddiquee and Dhar 2015). However, models for MDPE pipe material are very limited. A constitutive model adaptable to the framework of a widely used finite element (FE) model is required for the assessment of the performance of the pipe structure using FE analysis. A framework for modeling the time-dependent behavior of MDPE pipe material is developed here using the features available in a commercially available FE software, Abaqus (Dassault systemes 2015).

In Abaqus, two features are available for modeling the viscous behavior of material such as: Prony series and Creep law. Both features are employed here to simulate the experimental results.

#### **3.4.1 Prony Series**

The Prony series is a simplistic form of modeling the viscous effect of viscoelastic material (Powel 1983). This model is based on the linear viscoelastic theory, where the elastic and viscous components are modeled as combinations of springs and dashpots. Here, the spring is considered as the linear-elastic component and is represented using following stress ( $\sigma$ )–strain ( $\varepsilon$ ) relation:

$$\sigma = E\varepsilon \quad (3.1)$$

where E is the elastic modulus (spring constant).

The dashpot is considered as the viscous component. Its stress is dependent on the strain rate and is given as:

$$\sigma = \eta \frac{\delta \varepsilon}{\delta t} \quad (3.2)$$

where,  $\eta$  is the viscosity constant. Linear viscoelastic constitutive models are constructed by the superposition of these components. As the response of the dashpot is time-dependent, the behavior of a viscoelastic material that is modeled by parallel and/or series combination of springs and dashpots is also time-dependent.

The most general form of the linear model for viscoelasticity is known as the Generalized Maxwell model. This model is consisted of 'n' spring-dashpot Maxwell elements arranged in series. The Prony series is basically based on the generalized Maxwell model with the addition of a parallel spring element (Fig. 1). Prony series expansion for relaxation modulus ( $G$ ) of material can be expressed as (Dassault systemes, 2013):

$$G(t) = G_0 \left\{ 1 - \sum_{i=1}^N g_i \left( 1 - e^{-t/\tau_i} \right) \right\} \quad (3.3)$$

Where,  $G(t)$  is the modulus of at time  $t$ ,

$G_0$  is the instantaneous modulus (corresponding to the parallel spring element),

$g_i$  is the normalized modulus ( $G_i/G_0$ ) of  $i$ 'th Maxwell element, and

$\tau_i$  is the retardation time constant of the  $i$ 'th element, defined as  $\eta_i/G_0$ .

In Abaqus, several Maxwell elements are used in parallel to a spring element in order to simulate available data. The parameters of the Prony series model in Abaqus, can be defined using one of the three options: (i) direct specification of Prony series parameters, (ii) inclusion of relaxation test data, and (iii) inclusion of creep test data. Prony series parameters, including the number of Maxwell elements, are automatically calculated using the relaxation or creep data in options (ii) and (iii). Relaxation data is provided as normalized relaxation modulus ( $g_t$ ), and creep data is provided as normalized compliance ( $C_t$ ), which are calculated by dividing the corresponding data by its initial value. Since the strain is constant, the normalized values of the relaxation modulus (the ratio of the out stress to the input constant strain) is the same as the ratio of stress,  $\sigma(t)$  to the initial stress. Similarly, the normalized value of compliance (the ratio of output strain to the input constant stress) can be obtained through dividing the strain,  $\varepsilon(t)$  by its initial value. In the current study, both the creep test data and relaxation test data obtained from the laboratory tests are used. The normalized relaxation moduli calculated for each of the three relaxation tests are shown in Fig. 3.11.

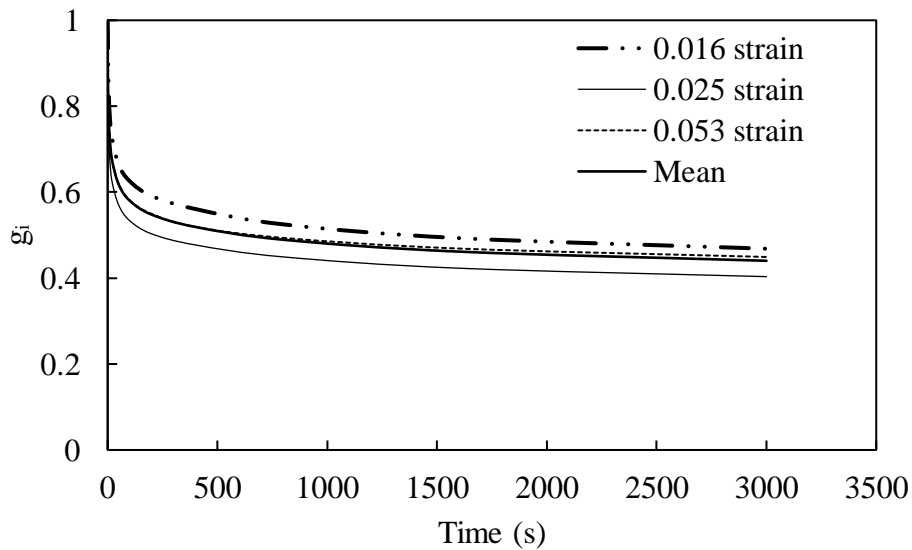


**Fig. 3.11.** Variation of normalized relaxation modulus  $g_t$  with time from relaxation tests.

The average values from these three curves were implemented in Abaqus to calculate the Prony series parameters. Table 3.3 shows the Prony series parameter obtained using the relaxation test data. Normalized modulus and retardation time for four Maxwell elements are obtained from Abaqus (Table 3.3).

**Table 3.3.** Prony series parameter obtained from relaxation test.

$i$	$g_i$	$\tau_i$
1	0.0796	0.14397
2	0.18199	3.9036
3	0.16192	43.873
4	0.13642	789.72

Similarly, the average normalized compliance calculated from creep test results was used in Abaqus to calculate the Prony series parameter. Fig. 3.12 shows the normalized compliance calculated using creep test results.

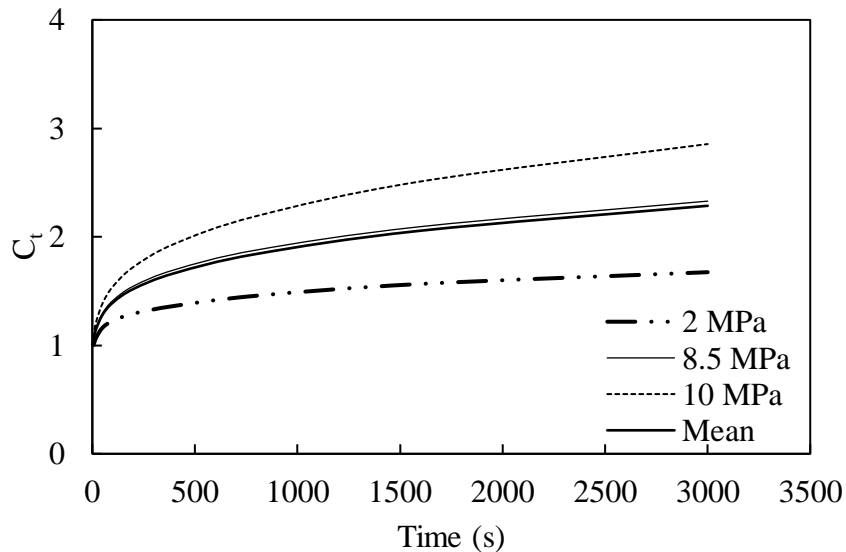


**Fig. 3.12.** Variation of normalized compliance,  $C_t$  with time from creep tests.

Table 3.4 shows the Prony series parameters obtained using the data. Parameters for two Maxwell elements are obtained, as presented in the table. Thus, Prony series parameters from relaxation test data (Table 3.3) are different from those from creep test data (Table 3.4). The effects of these different sets of parameters on the modelling of the time-dependent behavior are examined through simulation of the test results, as discussed later in the paper.

**Table 3.4.** Prony series parameters obtained from creep tests.

$i$	$g_i$	$\tau_i$
1	0.27382	34.754
2	0.28876	634.90

### 3.4.2 Creep Law

Creep law is another feature available in Abaqus for modeling the viscous behavior of viscoelastic material. The main advantage of this model over the Prony series is that this model can consider both the plasticity and viscous behavior simultaneously. In Abaqus, creep behavior can be defined using user subroutine 'creep' or providing some creep laws parameter as input. Two common creep laws are available: the power law and the hyperbolic-sine law. Among them, the power-law creep model is the simplest. However, the power-law model is not applicable for simulation near crack tips where creep strain rates frequently show an exponential dependence on the stress. The power-law creep model is considered in the current study.

There are two versions available for the power-law model, such as Time-hardening version and Strain-hardening version. Time hardening version is applicable when the stress state remains essentially constant, and the later one is applicable when the stress state varies during analysis. In this study, a time-hardening version of the power law creep model has been used to simulate creep

where the stress state is constant. The equation of the time hardening form of the model is given below (Eq. 3.4):

$$\dot{\epsilon}_c = A\tilde{q}^n t^m \quad (3.4)$$

where,

$\dot{\epsilon}_c$  = Creep strain rate,

$\tilde{q}$  = Deviatoric stress,

t = Total time,

A, n, m are the power-law constants. Eq. (3.4) is the rate formulation of Norton-Bailey creep law, which is applicable in primary and secondary creep regimes (May et al., 2013). The constants of the equation can be determined from curve fitting with the creep and relaxation test data. Table 3.5 shows the parameters obtained through the fitting with creep test data.

**Table 3.5.** Creep law parameters for creep tests.

Maximum stress (MPa)	A	n	m
2	$3 \times 10^{-11}$	1.825	-0.7
8.5	$3 \times 10^{-11}$	1.87	-0.7
10	$3 \times 10^{-11}$	1.89	-0.7

Since viscoelasticity and viscoplasticity in polymer generally occur during the deviatoric deformations (Pulungan et al. 2018; Siddiquee and Dhar 2015), the deviatoric component is considered for the determination of parameters. The number of Prony series terms required to match with the test data is automatically obtained from Abaqus. As seen in Table 3.5, 'A' and 'm'

are the same for each stress level, while 'n' increases with the increment of stress level. The variation of 'n' with maximum applied stress are plotted in Fig. 3.13.

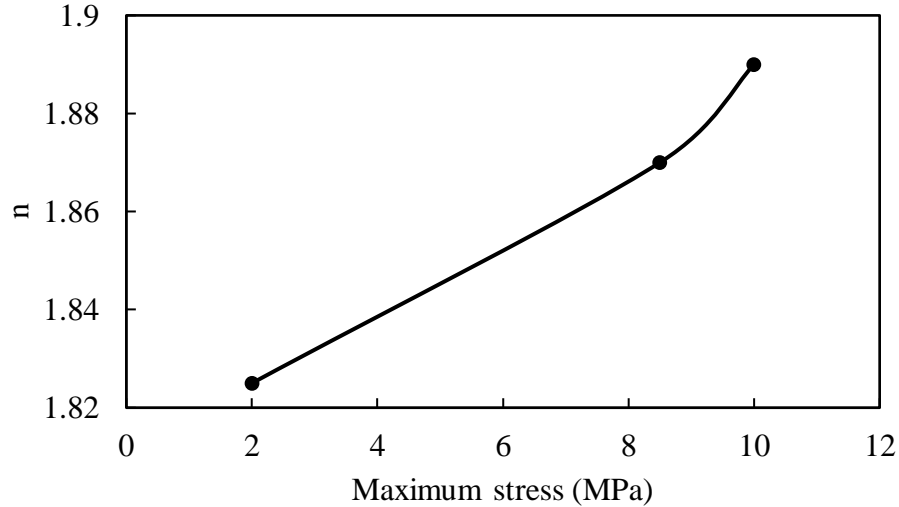


**Fig. 3.13.** Creep law parameter 'n' from creep test data.

Similarly, parameters obtained for relaxation tests are shown in Table 3.6 where 'A' and 'm' are constant. However, 'n' decreases with the increase of strain levels. The variation of 'n' with maximum applied strain is plotted in Fig. 3.14. The change of 'n' with an increase in stress or strain is almost linear for the ranges of stresses and strain observed.

**Table 3.6.** Creep law parameters for relaxation tests.

Maximum strain (mm/mm)	A	n	m
0.014	$3 \times 10^{-11}$	1.915	-0.92
0.024	$3 \times 10^{-11}$	1.875	-0.92
0.052	$3 \times 10^{-11}$	1.815	-0.92

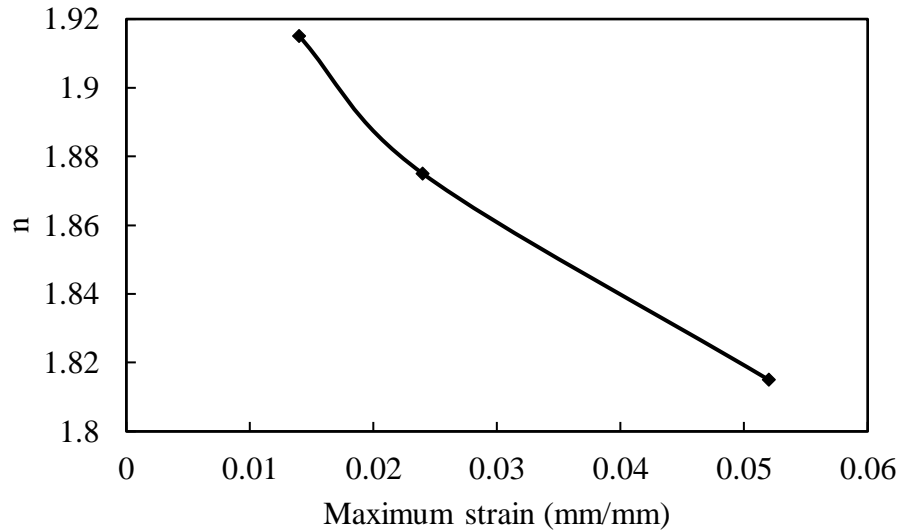


**Fig. 3.14.** Creep law parameter ‘n’ from relaxation test data.

### 3.5 Proposed Modeling Framework

Different approaches were employed in modeling the time-dependent behavior of polymer materials including the empirical models developed through the fitting with experimental data (Suleiman and Coree 2004), rheological models using springs and dashpots (Chehab and Moore 2006, Bilgin 2014) and the overstress theory (Colak and Dusunceli 2006, Siddiquee and Dhar 2015). The models are sometimes too complex for implementation in FE analysis using available software. Among these, the empirical models are relatively simple and can provide practical solutions with only a few fitting parameters. The empirical models are proposed here that can be implemented using the features available in Abaqus.

The tests conducted in this study reveals that the stress–strain behavior of the MDPE pipe material is highly nonlinear and strain-rate dependent. To account for the nonlinear strain-rate dependent stress–strain relation, creep, and relaxation, the following approach is proposed.

1. Nonlinear strain-rate dependent stress–strain relations are developed from experimental data and are provided as input to the FE model. The appropriate constitutive model from the input relations is then used in the analysis based on instantaneous strain rates calculated at a time step (discussed later in more detail).
2. The creep law (Eq. 3.4), which is available in Abaqus, is used to simulate the relaxation and creep. In Abaqus, creep strain rate calculated using Eq. (3.4) is used to calculate the strain increment ( $\Delta\varepsilon$ ) for any time increment ( $\Delta t$ ). This incremental strain is added to the total strain obtained from the previous time step for simulation of creep (when the stress is constant). Since the total strain is constant during relaxation, the elastic component of strain is reduced by  $\Delta\varepsilon$  (the creep strain increment). The stress calculated from the elastic strain is thus reduced.

The proposed modeling approach is implemented in Abaqus using its USDFLD feature.

### **3.6 Nonlinear Strain-Rate Dependent Stress–Strain Relations**

The hyperbolic model is one of the simplest approaches to model nonlinearity. Kondner (1963) and Duncan and Chang (1970) introduced a simplified hyperbolic model to characterize the time-dependent nonlinear response of the soil. The general equation of the hyperbolic model is given as (Eq. 3.5):

$$\sigma = \frac{\varepsilon}{m+n\varepsilon} \quad (3.5)$$

Here, 'm' and 'n' are the constants to be estimated through nonlinear regression analysis with test results.

Considering the strain rate dependent behavior of polymer materials, Suleiman and Coree (2004) proposed a modification to the hyperbolic model for HDPE pipe material as:

$$\sigma = E_{ini} \left( \frac{\varepsilon}{1 + \eta \varepsilon} \right) \quad (3.6)$$

Where  $E_{ini}$  is the initial modulus and  $\eta$  is a hyperbolic constant. The parameters are strain-rate dependent and can be obtained using the following equations (Suleiman and Coree 2004),

$$E_{ini} = a(\dot{\varepsilon})^b \quad (3.7)$$

$$\eta = \frac{a(\dot{\varepsilon})^b}{c + d \ln(\dot{\varepsilon})} \quad (3.8)$$

Where  $\dot{\varepsilon}$  is the strain rate, and a, b, c, d are constants that can be determined by fitting with the stress–strain responses obtained from uniaxial tension or compression tests.

As stated earlier, MDPE pipe material exhibits highly nonlinear and strain-rate dependent material behavior. The model proposed in Suleiman and Coree (2004) is therefore employed here to represent the nonlinear stress–strain relations. Parameters for the models are determined based on the strain-rate dependent stress–strain relations obtained from the uniaxial tensile tests discussed earlier. The parameters calculated from the curve fitting are shown in Table 3.7. Fig. 3.15 compares the test results with the stress–strain relations obtained from the hyperbolic model with the parameters in Table 3.7. This reveals that the developed hyperbolic model reasonably predicts the experimental stress–strain relations. The stress–strain response corresponding to the reference strain rate is independent of strain rate. Therefore, Eq. (3.6) with strain-rate independent initial modulus and hyperbolic constant (corresponding to the test data for strain-rate of  $10^{-6}$ /s) is used to model the stress–strain response at and below the reference strain rate ( $10^{-6}$ /s).

**Table 3.7.** Parameters for hyperbolic model.

Hyperbolic parameters	Values
a	2000
b	0.137
c	27.5
d	1.29

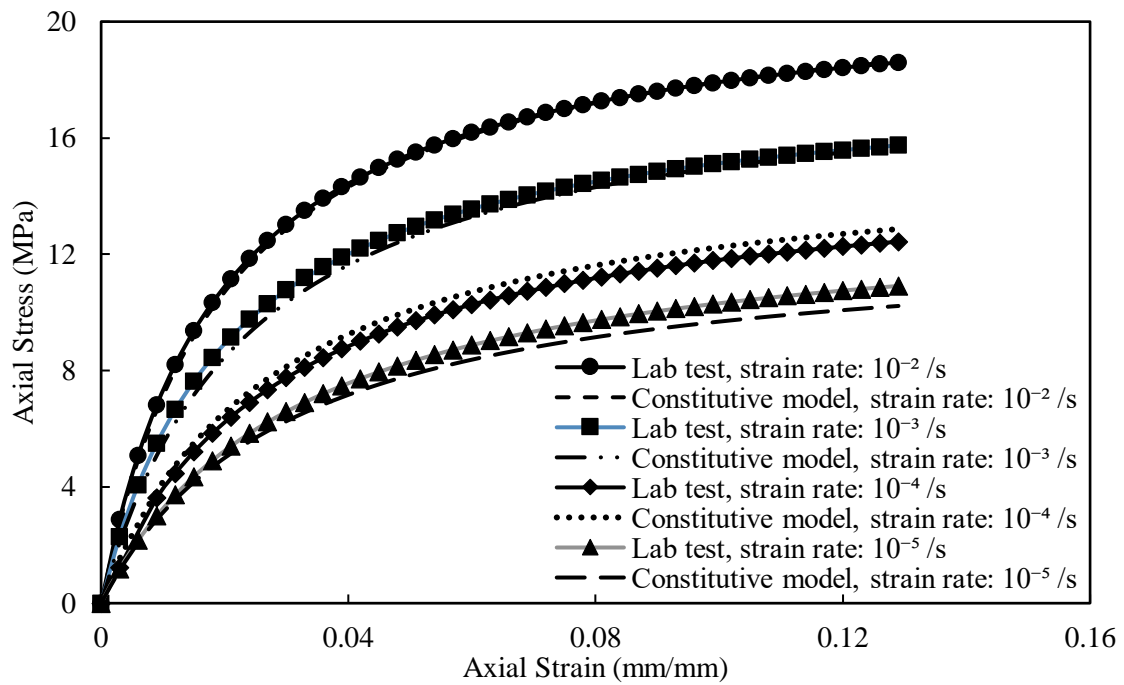


**Fig. 3.15.** Comparison of mean test results with hyperbolic model.

### 3.7 Implementation in Abaqus

In Abaqus, the elastic modulus,  $E$  (initial slope of the stress-strain curve), and nonlinear part of the stress-strain relation can be provided as separate inputs. The nonlinear part is obtained from the total stress-strain relation (e.g., Eq. 3.6) through subtracting the linear component of the strain calculated as  $\sigma/E$ . Each of the inputs can also be defined against field variables. In the current study, the strain-rate is employed as the variable so that the appropriate stress-strain relation can be used based on the magnitude of the strain-rate. The strain-rate is calculated and communicated with the main part of the analysis in Abaqus using the user subroutine, USDFLD (after Muntakim et al. 2018). The USDFLD allows defining field variables at a material point as a function of time or solution dependent parameters. It provides access to material point quantities at the start of a time-step increment and gives an explicit solution. In this process, the material properties are not influenced by the results obtained during the increment. Thus, the accuracy of the solution depends on the size of the time increment used, which can be controlled by the variable PNEWDT (Dassault Systemes 2015). At the start of the increment, a utility routine, GETVRM, is used to access the material point. By calling GETVRM with the appropriate output variable keys, the values of the material point quantities are obtained. The variables ARRAY, JARRAY, FLGRAY are used to recover the values of material point data (the floating-point, integer, and character data). At each increment, the field variables are restored to the values interpolated from the nodal values and introduced with user-defined state variables, STATEV, which can be re-called using variable key 'SDV' in the utility routine, GETVRM.

In this study, GETVRM is used to access all the strain components. The user-defined state variables are assigned to store current strain component, time increment, and the calculated strain rate for using in subsequent time steps. The strain rate is calculated based on the current strain

(accessed by the GETVRM), the previous strain (stored in user-defined variables), and time increment (accessed by USDFLD).

The variable, FIELD, which is an array containing field variables at the current material point, is used to assign the strain rate. Based on the information of the FIELD variables given in the input file, Abaqus calculate the material parameters from the given strain-rate dependent stress–strain models.

Along with USDFLD discussed above, the creep law features are included to account for the creep and relaxation effect. The creep law parameters obtained from creep tests are given in Abaqus input file.

### **3.7.1 Validation of the Modeling Approach**

Finite element analysis was performed to simulate the test results using the proposed method for validation. As discussed earlier, tension tests were conducted using coupon specimens of 13 mm width (width of the narrow section) and 50 mm gauge length. The tests were performed with the application of constant strain rates ranging from  $10^{-6}$  /s to  $10^{-2}$  /s. These strain-rate dependent stress–strain relations were simulated using FE modeling using Abaqus. Fig. 3.16 shows the FE mesh used in the analysis. The same size of the specimen was modeled. Smooth rigid boundaries were used at the bottom and the left side. The horizontal and vertical translations were restrained at the corner node to ensure stability. At the top of the mesh, a uniform deformation was applied at the same rates as those applied during the tests.

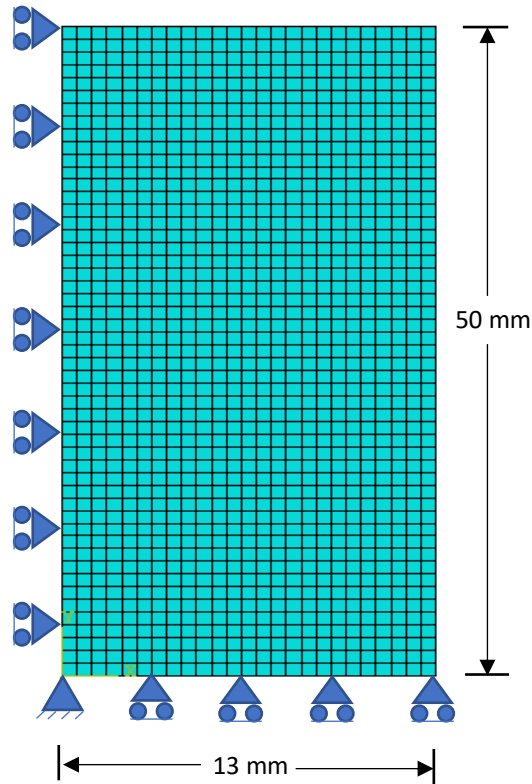
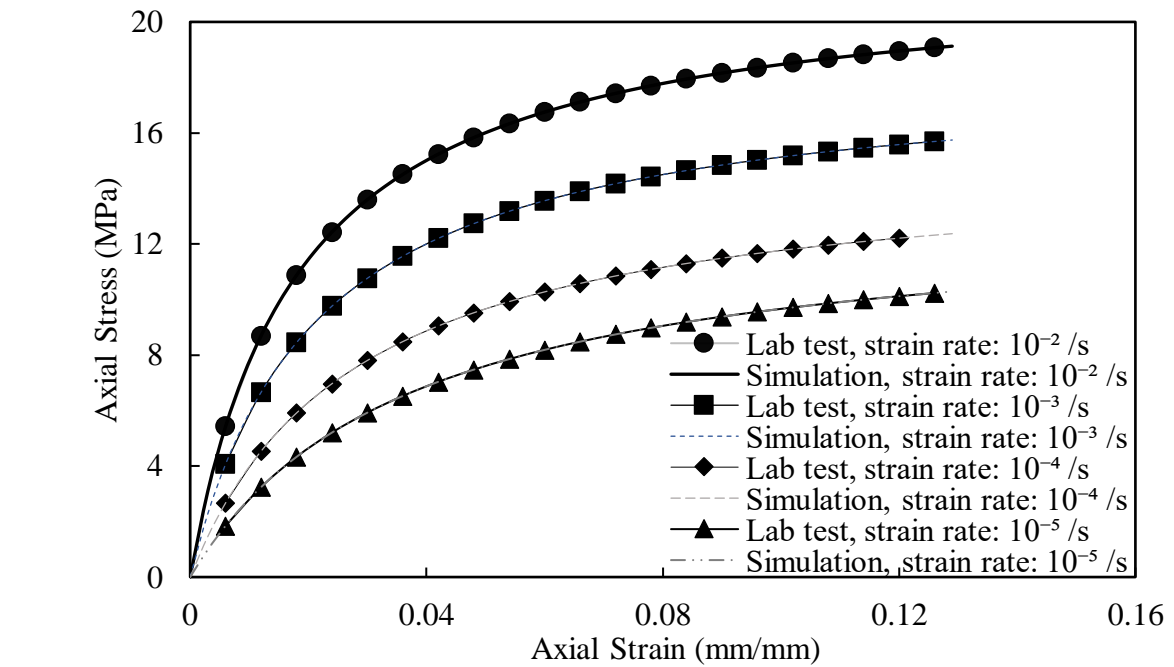


**Fig. 3.16.** FE model.

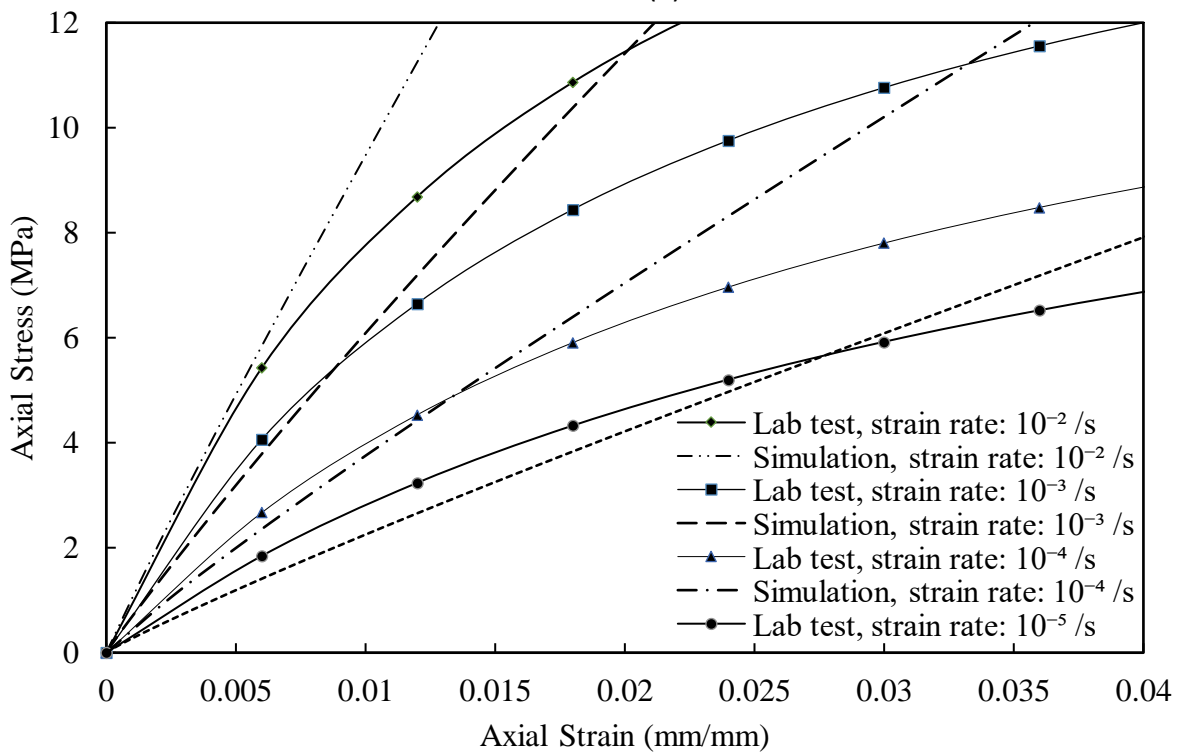
### 3.7.2 Simulation of Uniaxial Tension Tests

The results of FE simulation of the uniaxial tension tests are compared with test results in Fig. 17. The stress–strain relations obtained using the proposed method are compared in Fig. 3.17(a). A reasonable agreement between the simulated and experimental results is seen in the figure. Thus, the method employed is capable of predicting the rate-dependent stress–strain behavior of the MDPE material. Fig. 3.17(b) compares the test result with the results of the simulation using the conventional Prony series. It appears that the conventional Prony series is only applicable at very low strain (less than 1%) where the stress–strain response is linear. During the Prony series simulation, instantaneous elastic modulus and mean normalized relaxation modulus ( $g_t$ ) obtained from relaxation tests were used. As the Prony series approach cannot

account for the nonlinearity of material, the nonlinear stress–strain relations observed at higher strain cannot be successfully simulated.



(a)



(b)

**Fig. 3.17.** Finite element simulations of uniaxial tension tests: a) Proposed model; b) Prony series.

A strain rate change test performed during the experimental tests is also successfully simulated by the proposed method of analysis. During the experiment, the strain rate was changed from  $10^{-3}/s$  to  $10^{-2}/s$  at an axial strain of 0.065 (mm/mm) and then back to  $10^{-3}/s$  at an axial strain of 0.11 (mm/mm). Fig. 3.18 shows the comparison of simulated and experimental results of this test. It shows that the proposed technique has reasonably predicted the experimental behavior during the change in strain rate. There are some numerical noises in the results of simulation during the changes of strain rates. To minimize the noise, a control was applied to the strain increment using the USDFLD. The maximum strain increment of less than 15% was found to reduce the noise to a reasonable level.

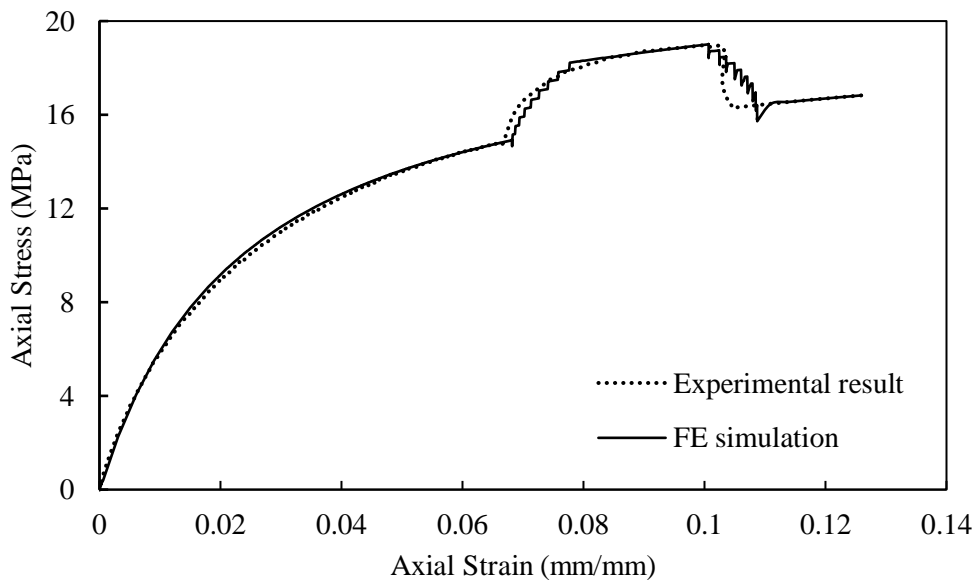


**Fig. 3.18.** Simulation of strain-rate-change test.

The proposed method also predicted reasonably the loading-unloading-reloading response observed in the tests. Fig. 3.19 compares the results of FE simulation and experimental results. This figure shows that the observed behavior of loading-unloading-reloading matches with the FE

simulation. However, the hysteresis loop during unloading-reloading cycle is not successfully simulated.

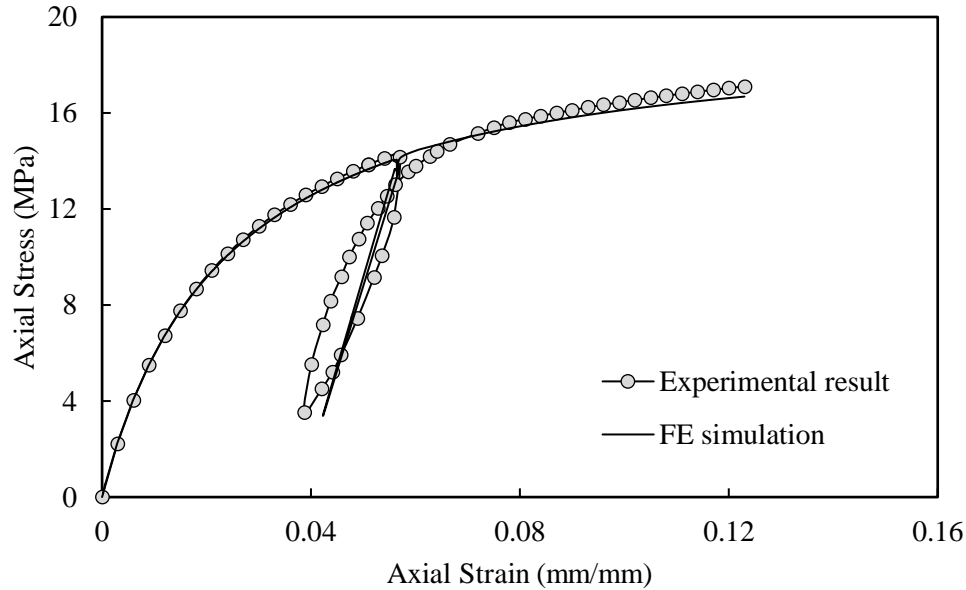
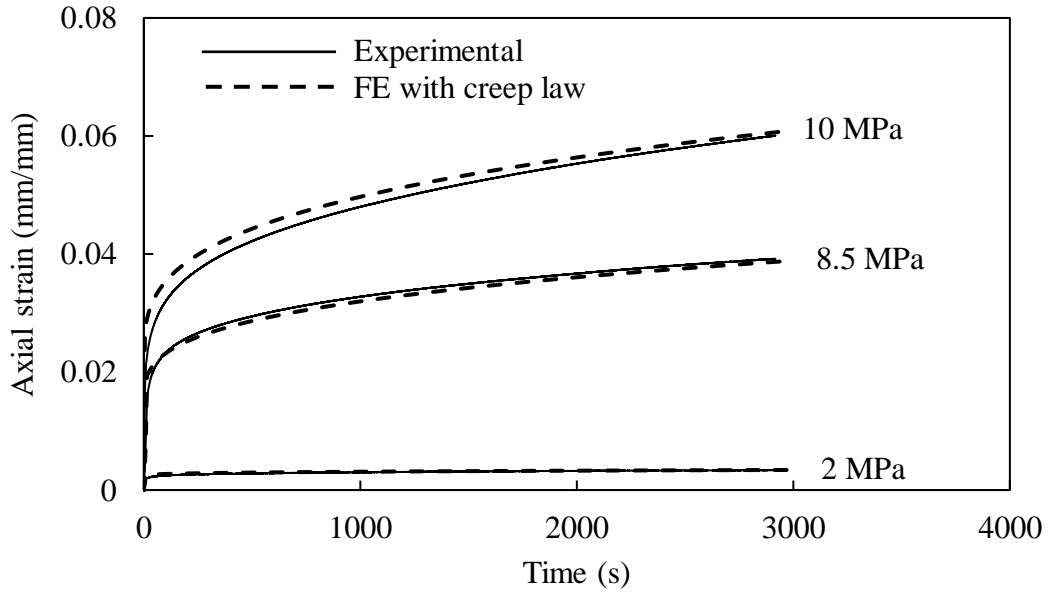


**Fig. 3.19.** Simulation of loading-unloading-reloading test.

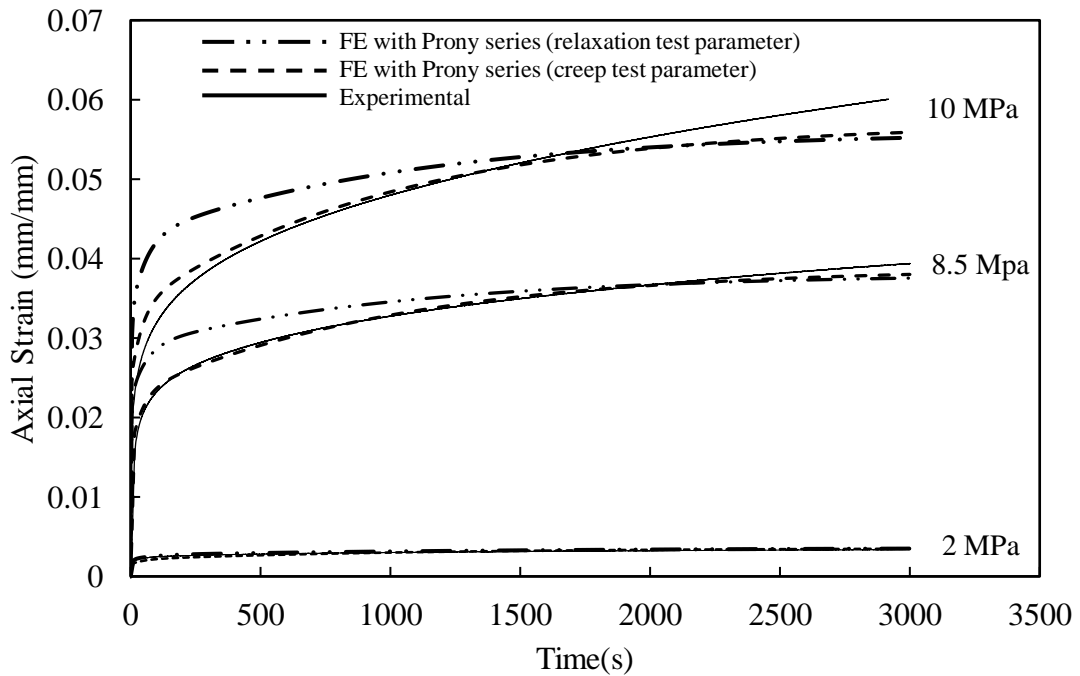
### 3.7.3 Simulation of Creep and Relaxation Tests

During the creep and relaxation tests, the specimen is first loaded with certain strain rates to the desired level of stress and strain, respectively. This loading path can be simulated using the proposed strain-rate dependent stress-strain model. The creep and the relaxation processes can then be simulated using the proposed creep law model. The Prony series can also be used to simulate the creep and relaxation behavior. In this case, secant modulus can be used to reach the desired level of stress and strain as the nonlinear loading path cannot be simulated using the conventional Prony series model. The creep and relaxation behaviors are simulated using the proposed modeling approach and using conventional Prony series. The simulation results of creep behavior are compared with test results in Fig. 3.20. It reveals that the proposed model can

reasonably predict the creep behavior observed during the tests (Fig. 3.20a). The Prony series with parameters obtained from both creep tests and relaxation tests were employed.



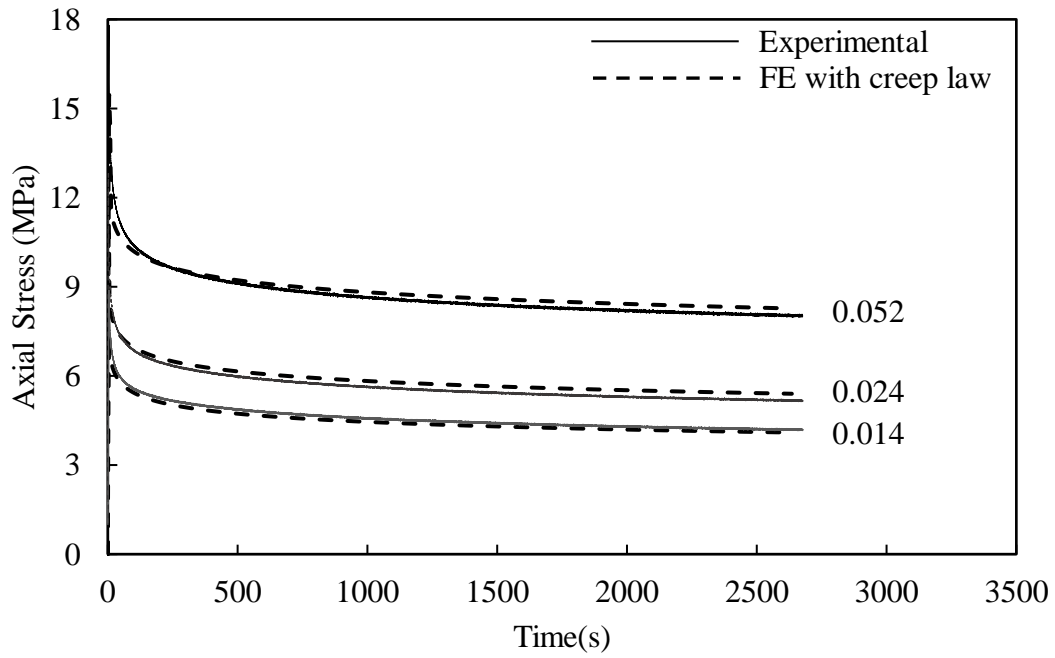
(a)



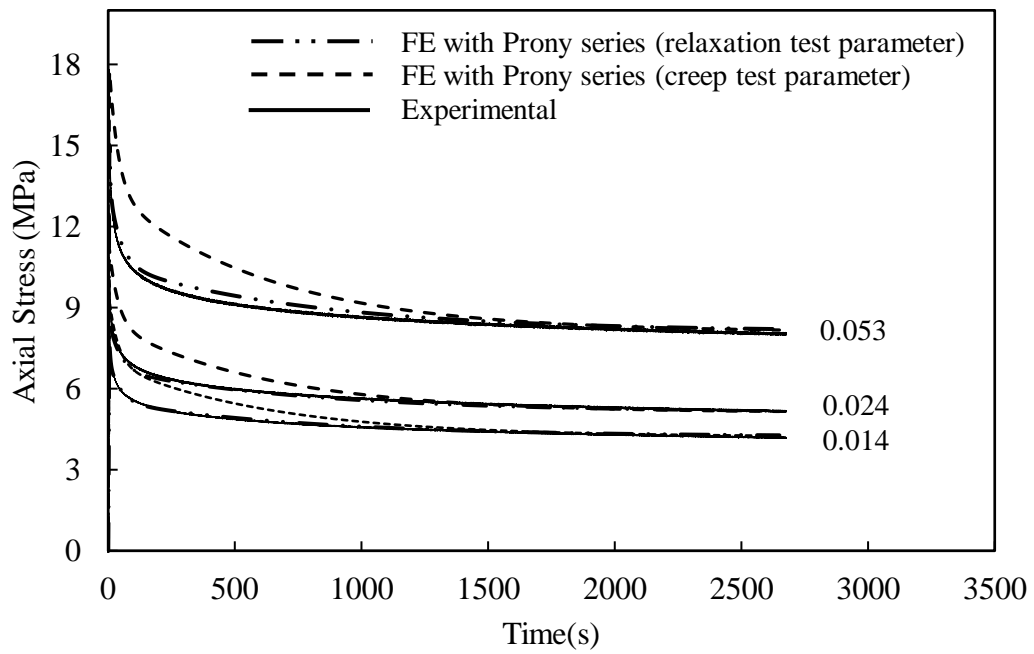
(b)

**Fig. 3.20.** Simulation for creep tests: a) Proposed model; b) Prony series.

Fig. 3.20(b) shows that both creep test-based parameters and relaxation test-based parameters can calculate the creep behavior to some extent. The creep test-based parameters provided a better prediction of the creep behavior, as expected. The discrepancies of the simulation from the tests results are observed in Fig. 3.20(b), which is attributed to the nonlinearity of the material behavior that could not be captured using the Prony series. However, the proposed modeling approach can be used to account for the nonlinearity. Similar results are obtained from the comparison for the relaxation test results (Fig. 3.21). The proposed modeling approach reasonably simulates the relaxation behavior (Fig. 3.21a), while the Prony series model overpredicts the stresses when creep-based parameters are used. However, the Prony series method reasonably simulated the relaxation test results (Fig. 3.21b) with parameters based on relaxation test data. The Prony series approach is applicable to simulate linear viscoelastic responses and, therefore, not suitable for large strain when the stress–strain responses are nonlinear. The proposed modeling technique can be applied to simulate the nonlinear viscous response of the MDPE pipe material. In this case, the creep law model can be used to simulate the creep and relaxation behavior.



(a)



(b)

**Fig. 3.21.** Simulation for relaxation tests: a) Proposed model; b) Prony series.

### 3.8 Conclusions

The time-dependent nonlinear behavior of an MDPE material is systematically investigated using laboratory tests and numerical methods. The major findings from this research are as follows:

- 1) The stress–strain responses of MDPE pipe material are highly nonlinear and strain-rate dependent. However, these can be approximated as linear at a very small strain.
- 2) The stress–strain response can be approximated to be independent of strain rate at the strain rate at or below  $10^{-6}/s$ . This strain rate of  $10^{-6}/s$  can be termed as 'reference strain rate' for isotach based modeling.
- 3) Initial values of the modulus of elasticity are strain-rate dependent. For a strain of  $10^{-6}/s$  to  $10^{-2}/s$ , the initial modulus ranged from 325 MPa to 1,054 MPa.
- 4) A hyperbolic constitutive model has been developed for MDPE pipe material at various strain rates that can simulate the nonlinear rate-dependent stress–strain behavior. This model is applicable at and above “Reference strain rate”
- 5) A new modeling technique is proposed for FE modeling of nonlinear strain-rate dependent material behavior of MDPE pipe material using Abaqus. The modeling approach can successfully simulate the strain rate dependent stress–strain response observed in laboratory tests. It also reasonably simulates the loading-unloading-reloading response and a change in the strain rate.
- 6) The Prony series approach is only applicable for a linear viscoelastic material. To account for the nonlinear responses, the creep law model is implemented in the proposed framework. The proposed creep law model simulates the observed creep and relaxation behavior successfully.

7) The creep law model involves three parameters (A, n, m). The magnitude of 'A' and 'm' are found to be independent of applied stress and strain levels, while parameter 'n' was found to increase with the increase of stress levels in creep tests and decrease with the increase of strain levels in relaxation tests. The temperature effect has not been considered in this study.

## References

- ASTM. (2003). "Standard test method for tensile properties of plastics." *2003 annual book of standards*, D638-14, Vol.08.01, West Conshohocken, Pa., 46-59.
- Hamouda, B. H., Laiarinandrasana L., Piques, R., (2007). "Viscoplastic behavior of a medium density polyethylene (MDPE): Constitutive equations based on double nonlinear deformation model." *International Journal of Plasticity.*, 23 (2007) 1307-1327.
- Bilgin, Ö, Stewart, H. E., and O'Rourke, T. D. (2007). "Thermal and mechanical properties of polyethylene pipes." *J. Mater. Civ. Eng.*, 10.1061/(ASCE)0899-1561(2007)19:12(1043), 1043-1052.
- Bilgin, Ö. (2014). "Modeling viscoelastic behavior of polyethylene pipe stresses." *ASCE Pipelines 2014.*, [10.1061/\(ASCE\)MT.1943-5533.0000863](https://doi.org/10.1061/(ASCE)MT.1943-5533.0000863).
- Brachman, R.W. I., Moore, I. D., and Rowe, R. K. (2000). "Local strain on a leachate collection pipe." *Can. J. Civ. Eng.*, 27(6), 1273-1285.
- Cholewa, J.A., Brachman, R.W.I. and Moore, I.D. (2011). "Axial stress–strain response of HDPE from whole pipes and coupons." *Journal of Materials in Civil Engineering.*, ASCE, Vol. 23, No. 10, pp. 1377-1386.
- Chehab, A.G., and Moore, I. D. (2006). "Constitutive Model for High Density Polyethylene to Capture Strain Reversal." *ASCE Pipelines 2006.*, 15419.

- Chehab, A.G. (2008) "Time Dependent Response of Pulled-In-Place HDPE Pipes", PhD Thesis, Queen's University, Kingston, Ontario, Canada.
- Chua, K. M., and Lytton, R. L. (1989). "Viscoelastic Approach to Modeling Performance of Buried Pipes." *Journal of Transportation Engineering.*, 115(3), 253–269.
- Colak, O. U. and Dusunceli, N. (2006) "Modeling viscoelastic and visoplastic behavior of high density polyethylene", *Journal of the Engineering Materials and Technology*, Vol. 128, pp. 572-578.
- Dassault Systemes (2013). *ABUQUS/CAE user's Guide*. Dassault Systemes Simulia Corp. Providence, RI, USA.
- Dassault Systemes (2015). *Abaqus User Subroutines Reference Guide*. Dassault Systemes Simulia Corp. Providence, RI, USA.
- Duncan, J. M., and Chang, C. Y. (1970). "Nonlinear analysis of stress and strain in soils." *J. Soil Mech. Found. Div.*, 96(5), 1629–1653.
- Hashash, N. M. A. (1991). "Design and analysis of deeply buried polyethylene drainage pipes." Ph.D. thesis, Department of Civil Engineering, University of Massachusetts at Amherst, Amherst, Mass.
- Kondner, R. L. (1963). "Hyperbolic stress–strain response: Cohesive soils." *J. Soil Mech. Found. Div.*, 89(1), 115–143.
- May, D.L., Gordon, A.P. and Segletes, D.S. (2013) "The application of the norton-bailey law for creep prediction through power law regression", *Proceedings of ASME Turbo Expo 2013: Turbine Technical Conference and Exposition*, June 3-7, 2013, San Antonio, Texas, USA

- Moore, I.D. (1994). "Three-dimensional time dependent model for buried HDPE pipe." *Computer methods and Advances in Geomechanics, Siriwardane & Zaman (eds)*, 8<sup>th</sup> International Conf. On Computer Methods and Advances in Geomechanics, pp. 1515-1520.
- Muntakim, A. H, Dhar, A. S. and Reza, A. (2018). "Modelling Time Dependent Behavior of Buried Polyethylene Pipes Using Abaqus", *Proc. of GeoEdmonton 2019*, 71st Canadian Geotechnical Conference, Edmonton, AB.
- Popelar, C. F., Popelar C. H. and Kenner, V. H. (1990). "Viscoelastic material characterization and modeling of polyethylene." *Polymer Engineering and Science.*, 30 (10): 577-586.
- Powel, P. C. (1983). *Engineering with polymers*, Chapman and Hall and Methuen, NY, pp. 14-19.
- Perzyna, P. (1966). "Fundamental problems in viscoplasticity." *Advances in Applied Mechanics*, Vol. 9, pp. 243-377.
- Pulungan, D., Yudhanto, A., Goutham, S., Lubineau, G., Yaldiz, R., Schijve, W. (2018) "Characterizing and modeling the pressure- and rate-dependent elastic-plastic-damage behaviors of polypropylene-based polymers", *Polymer Testing*, doi: 10.1016/j.polymertesting.2018.02.024.
- Siddiquee, M.S.A. and Dhar, A.S. (2015). "A Novel Elasto-Viscoplastic model of High-Density Polyethylene Material." *Geosynthetics International.*, Vol.22, No.2, pp: 173-182.
- Debnath S., and Dhar A. S. 2019. "Assessment of Stress Intensity Factor for buried cast iron pipeline using finite element analysis." 72nd Canadian Geotechnical Conference. St. John's.
- Suleiman, M.T., and Coree, B.J. (2004). "Constitutive model for high density polyethylene material: systematic approach." *Journal of Materials in Civil Engineering.*, 16(6), 511–515.

- Swain, A., and Ghosh, P. (2019). "Determination of viscoelastic properties of soil and prediction of static and dynamic response." *International Journal of Geomechanics.*, ASCE Vol. 19, No. 7: 0419072-1.
- Tobolsky, A. V. (1960). *Properties and structure of polymers*, Wiley, New York.
- Zhang, C. and Moore, I.D. (1997). "Nonlinear mechanical response of High-Density Polyethylene. Part II: uniaxial constitutive modeling." *Polymer Engineering and Science.*, Vol. 37, No.2, pp. 414-420.
- Weerasekara, L. and Rahman, M. (2019). "Framework for assessing integrity of natural gas distribution pipes in landslide areas." Geo St. John's 2019 – The 72nd Canadian Geotechnical Conference, September 30 – October 2, 2019, St. John's, NL, Canada.

## Chapter 4

### Modeling Time-Dependent Behavior of Medium Density Polyethylene Pipes

**Co-Authorship:** This chapter has been submitted for publication in the ASCE Journal as: Das, S. and Dhar, A.S. (2020), ‘Modeling time-dependent behavior of medium density polyethylene pipes.’ Most of the research presented in this chapter has been conducted by the first author. He also prepared the draft manuscript. The co-author mainly supervised the research and reviewed the manuscript.

#### 4.1 Introduction

Pipelines are the most efficient and common means of transporting natural gas, water, sewage, and other products from one location to another. Cast iron, ductile iron, steel, and polymers are the typical types of pipe materials used for liquid and gas transportation and distribution systems. The polyethylene/polymer pipe has become popular over the last few decades due to its various advantages, including low cost, lightweights, ease of installation, and corrosion resistance. Water supply, cold water distribution, sewer, gas distribution, and irrigation are the major areas of application of the polymer pipes. The use of medium density polyethylene (MDPE) pipe is rapidly increasing in recent years for various applications.

A major challenge in predicting the behavior of polymer pipe is its time-dependent material behavior. To account for the time-dependent behavior, the short-term and long-term values of the modulus of elasticity of pipe material is commonly employed for calculating the short-term and long-term responses, respectively (AASHTO 2010). Different approaches were proposed to express the modulus of elasticity for high-density polyethylene (HDPE) as a power-law function

with time. Chua (1986) expressed the time-dependent relaxation modulus for HDPE pipes material as below (Eq. 4.1),

$$E(t) = 52.6 + 460 t^{0.97786} \quad (4.1)$$

Hashash (1991) conducted tests on corrugated HDPE pipe material and proposed the following time-dependent modulus (Eq. 4.2).

$$E(t) = 329 t^{0.0859} \quad (4.2)$$

However, the time-dependent modulus of elasticity does not account for the strain-rate dependent behavior of the pipe material. Moore (1994) developed a linear viscoelastic model using nine-kelvin elements in series for describing the viscous effect of an HDPE pipe material. This model was found to successfully simulate the stress–strain behavior of HDPE at lower strain levels (less than 1%) (Moore 1994). A nonlinear viscoelastic and viscoplastic modeling approach was then employed to reasonably simulate the stress–strain behavior under various loading conditions (Zhang and Moore,1997; Chehab and Moore, 2006). Siddiquee and Dhar (2015) developed a strain-rate dependent nonlinear three-component elastic viscoplastic model for an HDPE pipe material. However, very limited information is currently available in the literature on the time-dependent behavior of MDPE pipe material. Das et al. (2019) and Das and Dhar (2020) conducted a comprehensive laboratory study to characterize the time-dependent behavior of MDPE pipe material commonly used in the gas distribution system. Based on the test results, Das and Dhar (2020) developed constitutive models adaptable to the framework of a widely used finite element (FE) model, Abaqus (Dassault System 15). The modeling framework for the MDPE pipe materials is employed in the current study to investigate the time-dependent behavior of buried MDPE pipes using FE analysis using Abaqus. Two examples of buried pipe problems are considered for the

investigation. The first problem is a conventional buried pipe subjected to ground and surface load. The time-dependent deflection of a buried pipe is examined. The second problem is a pipeline subjected to rate-dependent lateral ground movement. Pipelines are sometimes subjected to lateral ground movements at different rates due to landslide or fault movements due to earthquakes. The stresses develop in the pipe due to the ground movements at different rate are examined. Finally, a practical method of accounting for the time-dependent behavior of MDPE for the pipe-soil interaction problem is developed.

## 4.2 Time-Dependent Model

Das and Dhar (2020) conducted a detailed laboratory investigation to characterize the time-dependent behavior of MDPE pipe material. It was revealed that the stress–strain response of MDPE is nonlinear and strain-rate dependent. To account for the nonlinear strain rate dependent behavior, a hyperbolic model proposed in Suleiman and Coree (2004) was employed (Eq. 4.3):

$$\sigma = E_{ini} \left( \frac{\varepsilon}{1+\eta\varepsilon} \right) \quad (4.3)$$

where  $E_{ini}$  is the initial modulus and  $\eta$  is a hyperbolic constant. The parameters are strain-rate dependent and can be obtained using the following equations (Suleiman and Coree 2004),

$$E_{ini} = a(\dot{\varepsilon})^b \quad (4.4)$$

$$\eta = \frac{a(\dot{\varepsilon})^b}{c+d\ln(\dot{\varepsilon})} \quad (4.5)$$

Where  $\dot{\varepsilon}$  is the strain rate, and a, b, c, d are constants that can be determined by fitting with the stress-strain responses obtained from uniaxial tension or compression tests. Parameters for the

models are determined based on the strain-rate dependent stress-strain relations derived from the uniaxial tensile tests, shown in Table 4.1.

**Table 4.1.** Parameters for the hyperbolic model (Das and Dhar 2020).

Hyperbolic parameters	Values
a	2000
b	0.137
c	27.5
d	1.29

Das and Dhar (2020) also developed a framework for simulating the MDPE pipe material's creep and relaxation behavior using the features available in a commercially available FE software, Abaqus (Dassault systems 2015). In Abaqus, two features are available for modeling the viscous behavior of material such as the Prony series and 'creep law.' The Prony series is based on the linear viscoelastic theory, where the elastic and viscous components are modeled as combinations of springs and dashpots. Since the nonlinear behavior was observed for the MDPE pipe material during laboratory tests, the use of the 'creep law' was proposed. The equation of the time hardening form of the creep law is given in Eq. (4.6):

$$\dot{\epsilon}_c = A\tilde{q}^n t^m \quad (4.6)$$

Where,

$\dot{\epsilon}_c$  = Creep strain rate,

$\tilde{q}$  = Deviatoric stress (major principal stress – minor principal stress),

t = Total time,

A, n, m are the power-law constants determined from curve fitting with the creep and relaxation test data (Das and Dhar 2020). The strain-rate dependent nonlinear stress-strain model and the creep law are employed in the current study for rigorous time-dependent modeling of the behavior of buried MDPE pipes. Since viscoelasticity and viscoplasticity in polymer generally occur during the deviatoric deformations (Pulungan et al. 2018; Siddiquee and Dhar 2015), the von Mises equivalent strains and strain rates are employed for the rate-dependent modulus of elasticity and the creep law.

### 4.3 Deflections of Buried Pipes

In the design of flexible polyethylene pipes, the major consideration is to limit the deflection of the pipes under overburden and live loads. Excessive deflections of the pipes may affect the integrity of the joints and cause excessive ground settlements. A semiempirical equation, known as the “Iowa Equation” (Spangler 1941), has been widely used to calculate the deflection for flexible steel pipes. The Iowa equation was developed considering bending deflection (pipe cross-section ovalization) only. McGrath (1998) demonstrated for flexible polymer pipes that circumferential shortening also contributes to the deflection of the pipe and proposed a simplified equation for pipe deflection accounting for the circumferential shortening and flexural bending, as shown in Eq. (4.7), (Dhar et al., 2002).

$$\frac{\Delta_v}{D} = \frac{VAF \cdot q_v}{\frac{EA}{R} + 0.57 M_s} + \frac{D_l K_b q_v}{\frac{EI}{R^3} + 0.061 M_s} \quad (4.7)$$

Where,

$\Delta_v$  = Decrease in vertical pipe diameter (mm, in.)

$D$  = Pipe diameter (mm, in.)

$VAF$  = Vertical arching factor =  $0.76 - 0.71 \times \frac{S_h - 1.17}{S_h + 2.92}$

$$S_h = \text{Hoop stiffness} = \frac{M_s R}{E A_p}$$

$q_v$  = Overburden pressure at the springline (MPa)

$E$  = Pipe material modulus (MPa)

$A$  = Effective area of pipe wall per unit length of pipe (mm<sup>2</sup>/mm)

$R$  = Radius of the centroid of the pipe section (mm)

$M_s$  = One-dimensional soil modulus (MPa)

$D_l$  = Deflection leg factor

$K_b$  = Bedding coefficient

The first term in Eq. (4.7) represents the average circumferential shortening. The second term represents the bending deflection, which depends on the hoop stiffness and flexural stiffness, respectively, of the pipe wall.

For the polymer pipes with time-dependent material property, Eq. (4.7) is used to calculate and short-term and long-term (50 years) deflection using the short-term and long-term values of the moduli of elasticity (secant moduli), AASHTO (2010). One of the major limitations in applying this approach for calculating long-term deflection is the unavailability of long-term data for estimating the long-term modulus or the pipe's behavior. Secondly, since a constant modulus of elasticity is used, the strain-rate dependent effects on the pipe responses cannot be calculated using this method. Suitability of using the method of secant modulus and the strain-rate independent responses of MDPE pipes are examined in this study through a rigorous soil-pipe interaction analysis using the time-dependent constitutive model developed in Das and Dhar (2020).

A 320 mm diameter (internal) pipe with a wall thickness of 15 mm buried at a depth of 1.2 m is investigated. A uniform pressure of 200 kPa is applied on the ground surface to simulate the earth and live load. The 200 kPa of earth pressure corresponds to a load from approximately a 10 m high

embankment. A relatively high overburden pressure is chosen to cause high deflections of the pipe for convenience in comparison.

### 4.3.1 Finite Element Model

A Finite element model is developed to represent a deeply buried pipe. Two-dimensional plane strain analysis is performed. The geometry of the model is chosen to avoid the influence of the boundaries on the pipe responses, based on previous studies (Dhar and Moore 2000 and Dhar et al. 2004). Fig. 4.1 shows the FE mesh employed.

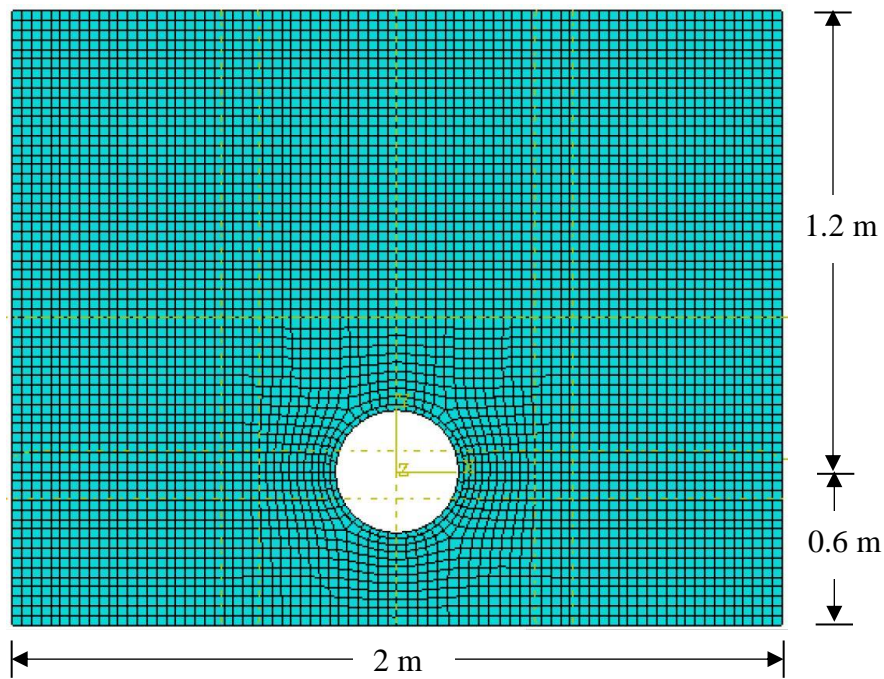


**Fig. 4.1.** FE model of buried pipe.

Four noded plane strain elements (Abaqus element type CPE4R) are used for both the pipe and the surrounding backfill soil. The nodal points along the vertical boundaries are only restrained in the horizontal direction to allow vertical movement. The nodal points along the bottom boundary have been fixed in both horizontal and vertical directions.

Since the focus of the current study is to examine the effect of the time-dependent behavior of pipe material, a simple linear elastic perfectly plastic model for the soil is used. The soil parameters are selected as the typical values for medium to dense sand. The modulus of elasticity and the Poisson's ratio of the soil is chosen as 35 MPa and of 0.25, respectively.

For MDPE pipe material, the time-dependent material model developed in Das and Dhar (2020) is used. Poisson's ratio of the MDPE is assumed to be 0.46. Nonlinear strain-rate dependent stress-strain relations (Eq. 4.3) are used to calculate the pipe deflection during loading. For the time-dependent material, creep and relaxation occur at constant stress and strain, respectively. As a result, the pipe's deflection can change with time after application of the load. The pipe deflection during creep/relaxation is calculated using the "creep law" (Eq. 4.6). Das and Dhar (2020) used creep tests and relaxation tests to determine the parameters for the "creep law" model. Since the creep behavior would govern rather than the relaxation for the buried pipe, parameters obtained from the creep tests are considered. Table 4.2 shows the parameters obtained through the fitting with creep test data (Das and Dhar, 2020). It shows that 'A' and 'm' are the same for each stress level, while 'n' increases with the increment of stress level. Using the magnitudes in Table 4.2, a value corresponding to the maximum stress level experienced by the pipe is obtained for 'n' (i.e.,  $n = 1.82$ ) through interpolation.

**Table 4.2.** Creep law parameters for creep tests (Das and Dhar 2020).

Maximum stress (MPa)	A	n	m
2	$3 \times 10^{-11}$	1.825	-0.7
8.5	$3 \times 10^{-11}$	1.87	-0.7
10	$3 \times 10^{-11}$	1.89	-0.7

As the conventional practice of pipe deflection assessment uses a linear time-dependent modulus (short-term and long-term moduli), a linear FE analysis is also performed for comparison with the results from the rigorous analysis discussed above. The elastic moduli for linear elastic analysis are obtained at the secant value corresponding to the time, discussed later in the paper.

### **4.3.2 Time-Dependent Responses**

To calculate the responses of the pipe under the surface load of 200 kPa, the load is first applied at various rates. Then, the analyses are continued under the constant load to calculate the time-dependent responses. Note that even though the applied load is constant with time, the pipe stresses can change due to the time-dependent behavior of the material. Thus, pipe behavior can be governed by the combined effect of creep and relaxation. To account for the effects, a creep law is used where the parameters for the models are selected based on creep or relaxation test data as discussed above in chapter 3.

Fig. 4.2 shows the calculated deflections with time during the increase of load (short-term response) and during creep and relaxation (time-dependent response). The analysis was stopped at around 30,000 sec to limit the computational time. Fig. 4.2 shows that the deflections are loading rate dependent. The vertical deflection increases (Fig. 4.2a), and the horizontal deflection decreases (Fig. 4.2b) with the decrease of the loading rate. Beyond the loading step (short-term responses), the vertical deflections continue to increase while the horizontal deflections decrease with time (long-term responses). Note that the magnitudes of the long-term deflection are higher when the short-term deflections are higher. The constant short-term and long-term moduli of elasticity (recommended in the design codes) cannot be used to calculate these deflections. In Fig. 4.2(a), the 'time' is presented in logarithmic scale to show the rate of increase of vertical

deflections with time since the calculated increase of deflection is small (and not well visible in normal scale) within the time considered (i.e., 30,000 sec  $\approx$  8.5 hrs).

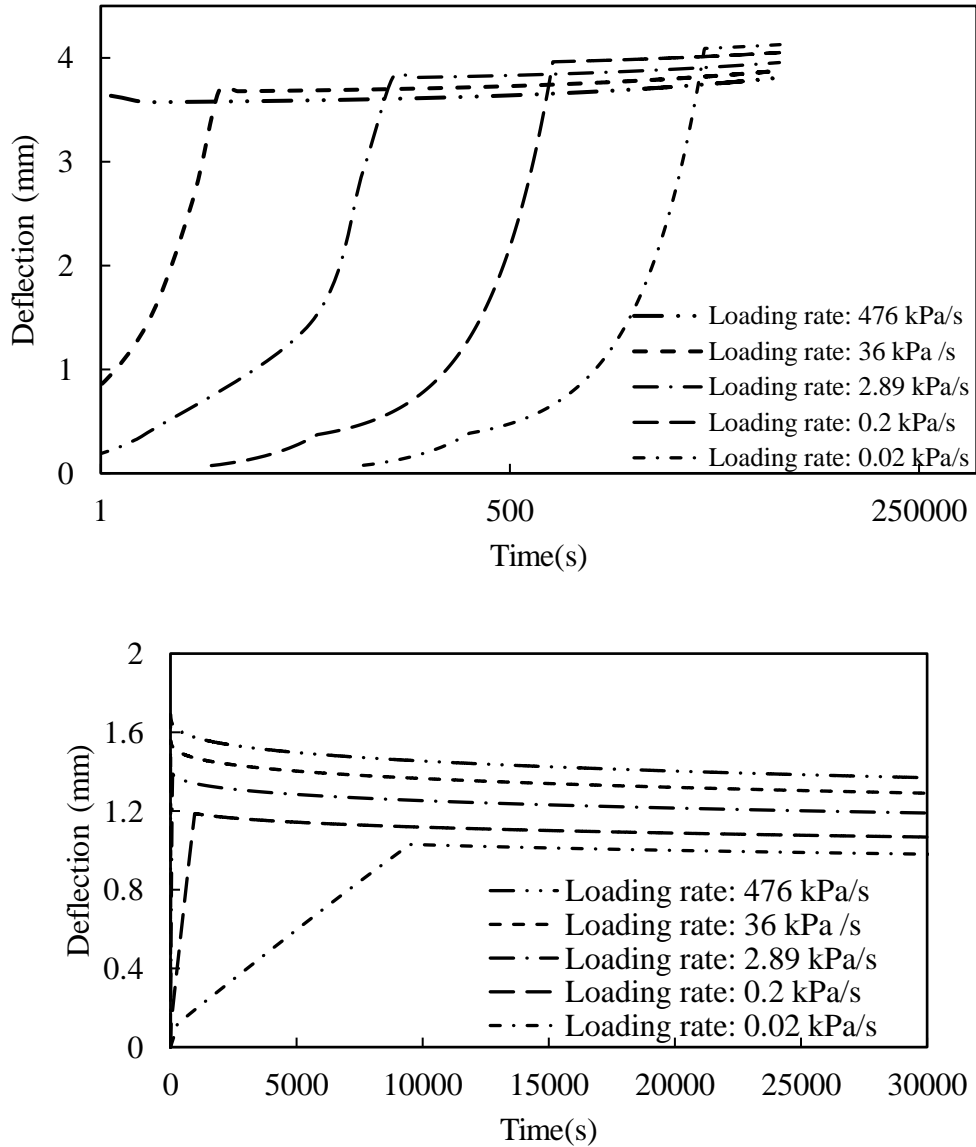


**Fig. 4.2.** Time-dependent deflections of buried MDPE pipe: (a) Vertical deflection; (b) Horizontal deflection.

The von Mises stresses in the pipe wall at the crown, and the springline are investigated to examine the stress relaxation due to the time-dependent effects. Fig. 4.3 plots the calculated von Mises stresses with time. It reveals that even though the vertical deflections are higher and horizontal deflections are lower at lower loading rates (Fig. 4.2), the stresses both at the crown and

the springline decrease with the decrease of loading rate. The stresses are reduced further with time under the constant applied pressure, indicating stress relaxation behavior. Thus, the long-term performance of the pipes appears favorable in terms of pipe wall stresses (and hence strain). Long-term deflection is the major concern for the performance of the pipe. The time-dependent deflection of the pipes is, therefore, further examined below.

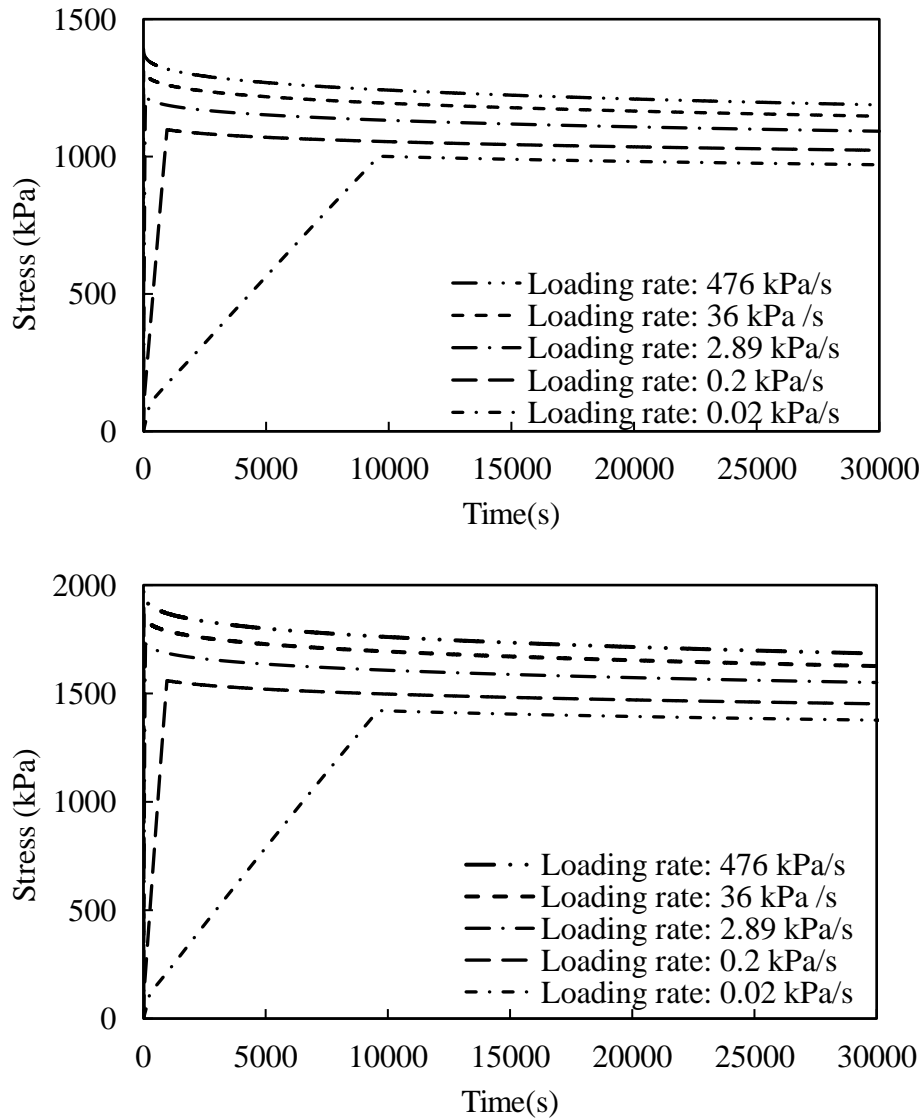


**Fig. 4.3.** Von Mises stresses in the pipes with time: (a) Crown stresses; (b) Springline stresses.

The present study presents a rigorous time-dependent soil-pipe interaction analysis to calculate the responses of buried pipe, including deflections. However, the rigorous FE analysis is often prohibitive for engineering design. A simplified analysis using a constant time-dependent modulus of elasticity is examined below to calculate time-dependent deflections.

### **4.3.3 Short-Term Deflections**

Current design code (i.e., AASHTO 2010) recommends using a short-term modulus to estimate the short-term deflection (immediately after application of the loads). However, as discussed above (Fig. 4.2), the short-term deflection significantly depends on the rate of loading. The suitability of using a rate-dependent modulus in calculating the rate-dependent deflections is examined here. The rate-dependent initial modulus is estimated using Eq. (4) based on the strain rates calculated from the FE analysis. Although the strain-rate dependent stress–strain response is nonlinear, a linear stress-strain relation (i.e., a constant modulus of elasticity) can be assumed at low strain levels ( $< 0.01$ ) for MDPE (Das and Dhar 2020, Bilgin et al. 2007). In the current study, the maximum strain in the pipe is calculated to be less than 0.0045. Therefore, a constant strain-rate dependent modulus of elasticity (initial tangent modulus) can be used. Using the constant modulus, the deflections of the pipe are calculated using a linear FE analysis. The calculated deflections are compared with those obtained using the time-dependent analysis (discussed above) in Table 4.3. It reveals that both horizontal and vertical deflections calculated using the strain-rate dependent constant modulus matches well (within around 2%) with those calculated using the rigorous time-dependent analysis. Thus, the rate-dependent constant modulus can reasonably be used to calculate the short-term deflections if the strain rate within the pipe can reasonably be estimated. For the MDPE material, the following equation is proposed to calculate the strain-rate dependent short-term modulus.

$$E_0 = 2000(\dot{\epsilon})^{0.137} \quad (4.8)$$

where,  $E_0$  is the short-term modulus in MPa and  $\dot{\epsilon}$  is the strain-rate per second.

**Table 4.3.** Comparison of Initial deflections

Loading rate	Calculated strain rate	Initial modulus (MPa)	Deflection using time-dependent analysis, mm		Deflection using constant initial modulus, mm	
			Vertical	Horizontal	Vertical	Horizontal
476 kPa/s	0.01 /s	1064	3.57	1.69	3.62	1.70
36 kPa/s	0.0016 /s	828	3.68	1.55	3.70	1.58
2.89 kPa/s	0.00012 /s	580	3.80	1.38	3.84	1.40
0.2 kPa/s	0.000008/s	400	3.96	1.18	4.02	1.19
0.02 kPa/s	0.000001/s	325	4.09	1.03	4.12	1.06

### 4.3.4 Time-Dependent Deflections

For the time-dependent deflections, the use of a time-dependent constant modulus is examined against the results from the rigorous time-dependent analysis. The time-dependent deflections under the constant applied pressure are governed by the creep and relaxation behavior of the material. As reported in Das and Dhar (2020), the creep behavior and relaxation behavior of the MDPE material significantly depends on the stress levels and deformation levels. Thus, the stress-specific creep or strain-specific relaxation parameters would be required to simulate the time-dependent deflection. Since the calculated stresses and strains are less (as discussed above), the test data corresponding to the lowest stress and the lowest strain is used to estimate the modulus of elasticity of the material for calculating time-dependent deflections.

With the creep data, the applied stress is divided by the time-dependent strains, and with the stress relaxation data, the time-dependent stresses are divided by the applied strain to calculate the time-dependent elastic secant modulus ( $E_t$ ). The calculated elastic moduli are normalized by the corresponding initial value ( $E_0$ ) and plotted in Fig. 4.4. The figure shows that the normalized

elastic moduli obtained from the creep and relaxation test data for the particular stress and strain levels are close to each other. The normalized modulus can be represented using a power-law model, as in Eq. (4.9)

$$\frac{E_t}{E_0} = 0.9582t^{-0.07} \quad (4.9)$$

The normalized modulus (Eq. 4.9) can be used to estimate the elastic modulus at any time through multiplying by the initial modulus (strain-rate dependent) of the material. Thus, the long-term modulus is dependent on the initial modulus, accounting for the effect of short-term deflections on the long-term deflections. Deflections calculating using FE analysis with constant time-dependent modulus are compared with those from the rigorous time-dependent analysis in Table 4.4. The deflections calculated using the simplified FE analysis using a constant elastic modulus are within 3% of the deflections calculated using rigorous time-dependent FE analysis. Thus, the simplified approach of FE analysis (based on a constant elastic modulus) can reasonably be applied to calculate the time-dependent or long-term deflections. Considering that the stress levels expected for buried pipe are typically less (Bilgin et al. 2007), Eq. (4.8) can be used to calculate the time-dependent elastic modulus for estimating the long-term deflections using the power law equation (Eq. 4.9).

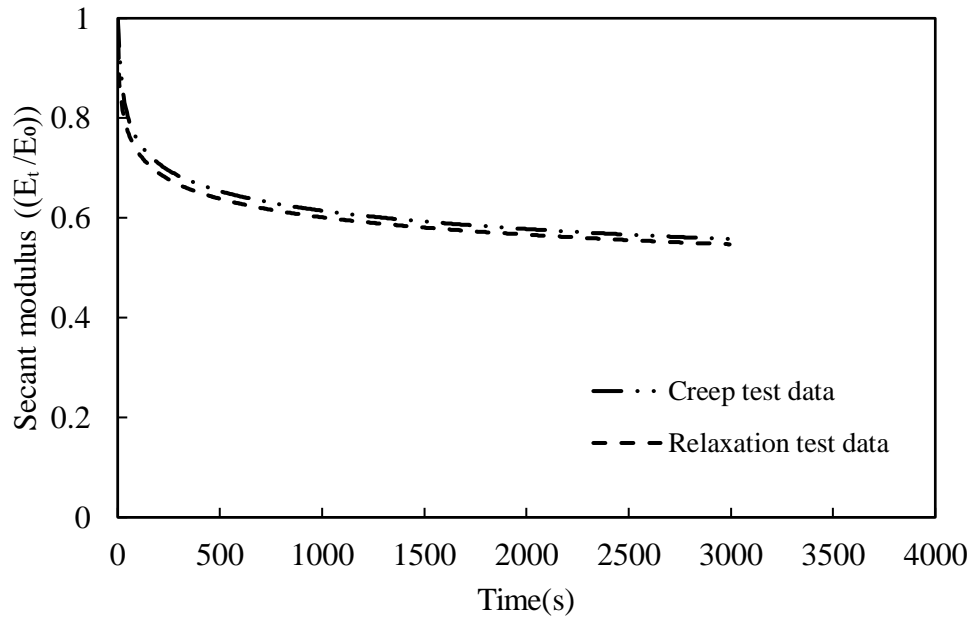


**Fig. 4.4.** Normalized time-dependent elastic moduli.

**Table 4.4:** Comparison of time dependent deflections

Time	Vertical Deflection (mm)		Horizontal Deflection (mm)	
	Using time-dependent elastic modulus	Rigorous time dependent analysis	Using time-dependent elastic modulus	Rigorous time dependent analysis
0	3.62	3.57	1.7	1.69
5000	3.85	3.71	1.4	1.50
10000	3.87	3.75	1.36	1.45
15000	3.88	3.77	1.34	1.43
20000	3.898	3.78	1.33	1.4
25000	3.9	3.79	1.32	1.38
30000	3.91	3.8	1.31	1.37

### 4.3.5 The Proposed Method of Deflection Calculation

The above study reveals that the short-term and long-term pipe deflections calculated using the rigorous time-dependent models can reasonably be obtained using an equivalent linear model (with a constant modulus of elasticity). However, the short-term modulus of elasticity is strain-rate dependent. The long-term modulus of elasticity also depends on the initial stress/strain levels. The following methods are proposed for calculating the deflections of buried MDPE pipes, accounting for the strain-rate dependent short-term modulus and stress-dependent long-term modulus.

- For short-term deflection, Eq. (4.8) can be used to calculate the strain-rate dependent modulus of elasticity of the pipe material. To estimate the strain rates during design, the maximum strain corresponding to an applied load can be first calculated using a constant modulus. Then, the rate of strain can be calculated through dividing the maximum strain by the duration for the application of the load (i.e., construction period).
- For long-term deflection, Eq. (4.9) can be used to calculate the time-dependent modulus, where the initial modulus ( $E_0$ ) is the short-term modulus calculated in the above step.

### 4.3.6 Evaluation of the Simplified Design Equation:

The deflections obtained from the FE analysis are compared with those calculated using the simplified design equation (Eq.4.7) for evaluation. The deflection lag factor  $D_i$  and the constant  $k_b$  in Eq. (4.7) are assumed as 1 and 0.1, respectively, as suggested in Zhou et al. (2017). All other parameters are as those used in the FE analysis. Fig. 4.5 compares the calculated short-term deflections with the various rates of loading. It shows that the simplified design equation overestimates the vertical deflections with respect to the FE calculations. The maximum overestimation was around ~16.4% at the lowest loading rate.

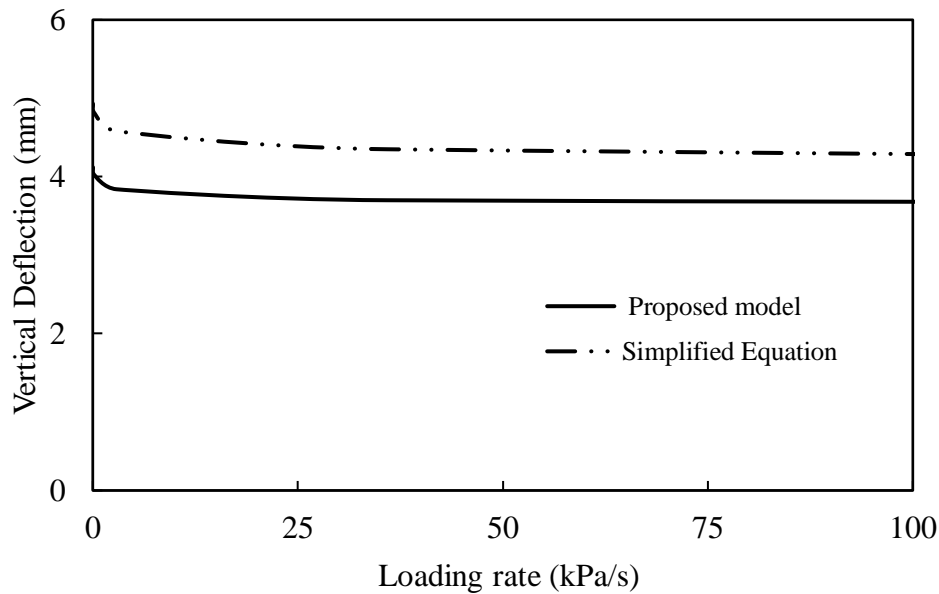


**Fig. 4.5.** Comparison of deflections from FE analysis and simplified design equation.

#### 4.4 Pipelines Subjected to Lateral Ground Movement

Pipelines buried underground are often exposed to various hazards, including differential ground movement resulting from natural disasters (e.g., landslide, earthquake, etc.) and human activities (e.g., construction, mining, tunneling, etc.). The ground movements have been identified as one of the significant causes of pipeline failure (CEPA 2017). The pipelines can be subjected to longitudinal, lateral and/or oblique ground movements depending upon ground movement orientation. A problem of pipelines subjected to lateral ground movement is investigated here.

Early research on pipelines subjected to a lateral ground movement focused on identifying the loads on the pipe. Audibert and Nyman (1978) conducted tests with steel pipes of different diameters (25 mm, 60 mm and 114 mm) and observed the soil load against the pipe’s lateral displacements in sand. Trautman and O’Rourke (1983) also conducted full-scale experiments and proposed lateral forces resulting from relative movement between the pipe and the surrounding

soil under plane strain conditions. Based on these studies, load-displacement relations were developed, which are used as the basis of calculating spring constants to represent soil-pipe interaction for the analysis of pipelines. The current industry practice for pipe stress/strain assessment is to idealize the pipeline as a series of beams and model the soil-pipe interaction using Winkler springs. ALA (2001) recommends the spring parameters to represent soil resistance in lateral, axial, and vertical directions. Almahakeri et al. (2012 & 2014) conducted large scale tests with steel pipes and Glass Fiber Reinforced Polymer (GFRP) pipes to experimentally examine the bending behavior of the buried pipes. They employed three-dimensional finite element analysis to simulate the pipe responses numerically, where the soil was idealized as an elastoplastic continuum. However, the continuum-based three-dimensional FE analysis is impractically time-consuming (Ni et al., 2018). In this regard, a simplified FE modeling idealizing the pipes as beam-type structures surrounded by a Winkler spring is more suitable for engineering analysis and design. Beam-spring type of analysis is, therefore, performed here for the stress/strain assessment of MDPE pipes considering the rate-dependent material properties.

#### **4.4.1 Pipe-Soil Interaction Element**

The pipe-soil interaction (PSI) element available in Abaqus, the finite element analysis software, is used to idealize the soil as a Winkler media. The PSI element is a special type of element that interacts with the structural beam element, as shown in Fig. 4.6. One side of the PSI element shares nodes with the nodes of the pipe element, which is a beam-type element. The other side of the PSI element represents a far-field surface, where the boundary condition (i.e., ground movement) can be applied. The number of nodes on the side sharing the pipeline matches the number of pipe/beam element's nodes. Thus, there are two nodes per side (total four nodes) for a linear pipe element and three nodes per side (total six nodes) for the quadratic pipe element (Fig.

4.6). Abaqus/Standard provides 4-noded and 6-noded two-dimensional elements (PSI24 and PSI26) and three-dimensional elements (PSI34 and PSI36) for modeling soil-pipe interaction. Each node of the element has only one displacement degree of freedom.

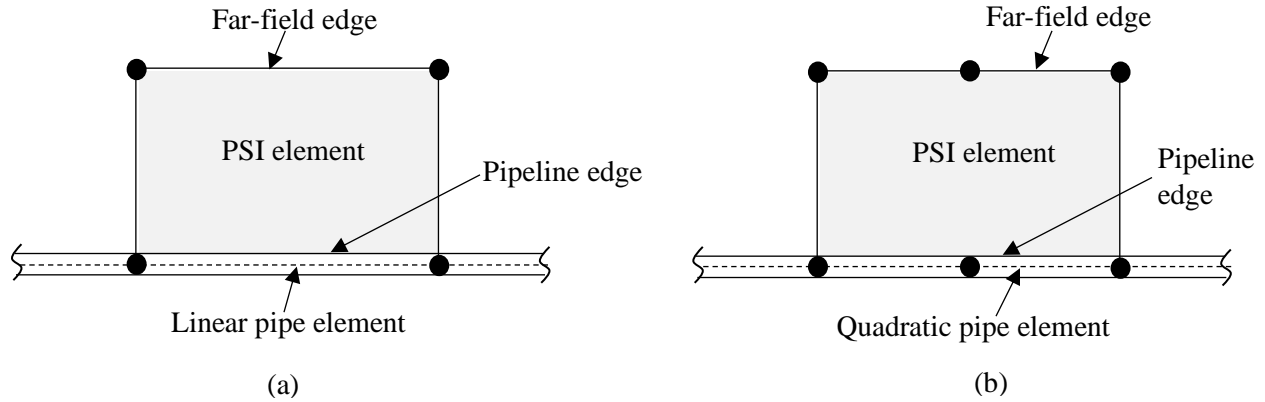


**Fig. 4.6.** Pipe-soil interaction model: (a) 4 noded PSI element; (b) 6 noded PSI element.

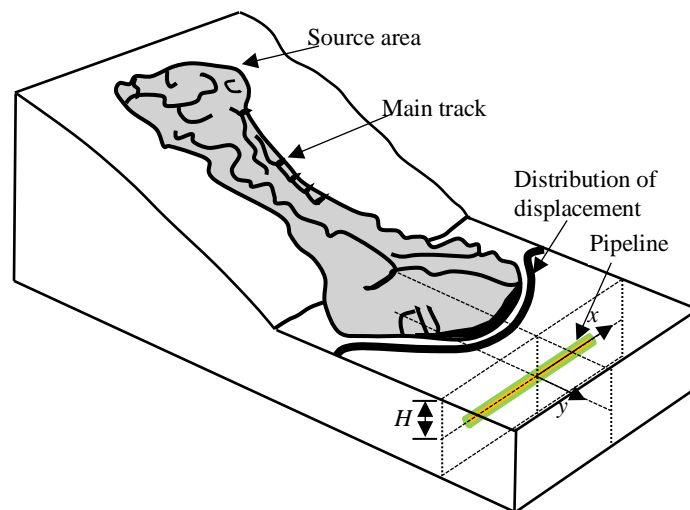
The deformation in the PSI element is defined as the relative displacements between the two edges of the element. If the relative displacement is greater than zero, forces are applied to the pipeline nodes. The applied forces can be a linear (elastic) or nonlinear (elastic-plastic) function of the “strains,” defined by

$$\varepsilon_{ii} = \Delta u \cdot e_i \quad (4.10)$$

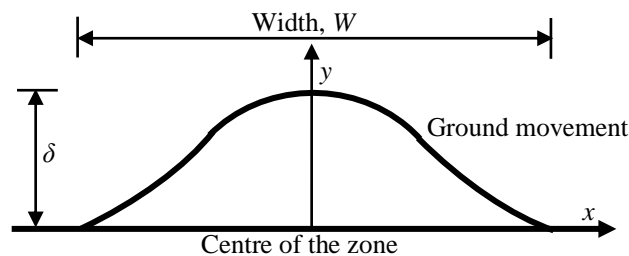
Where,  $\Delta u = u^f - u^p$ , is the relative displacement between two edges ( $u^f$  is the far-field displacement and  $u^p$  is the pipeline displacement);  $e_i$  is the local direction vector. A suitable constitutive model is required to calculate the nodal forces from the strains. The constitutive relation of PSI elements is usually determined based on experimental results, which is expressed as a force per unit length along each of the orthogonal directions. Data for a linear or a multilinear model can be provided as tabular input in Abaqus.

#### 4.4.2 FE Modeling

Ground movement due to landslide can impact the pipelines in many different ways (Argyrou et al. 2018). A pipeline crossing a landslide perpendicular to the general direction of soil movement (Fig. 4.7) is considered in the present study. Distribution of the ground movement over the length of the pipe affected by the landslide is shown in Fig. 4.7b. The ground deformation is the maximum at the center of the affected zone and the minimum near the margins. The length of the affected zone can vary from several meters to over kilometers. A landslide length of 8 m is considered in the present study to demonstrate the effect of time-dependent pipe material's behavior.



(a) Direction of ground movement



(b) Distribution of ground movement

**Fig. 4.7.** Pipeline perpendicular to ground movement.

Two-dimensional FE analysis is performed for investigation of the pipe subjected to the lateral ground movement. A type of beam element (PIPE21 in Abaqus) is used to idealizing the pipe, and the element PSI24 is used to model the soil-pipe interaction. The displacements corresponding to the ground movement are applied to the pipe. Researchers employed cosine functions to approximate the type of ground movement shown in Fig. 4.7b (O'Rourke 1989, Suzuk et al. 1988, Ni et al. 2018b). The deflections given by the cosine function shown in Eq. (4.11) are applied in the perpendicular direction of the pipeline.

$$y(x) = \delta \left[ \cos \frac{\pi x}{W} \right]^2 \quad (4.11)$$

In Eq. (11),  $y(x)$  is the ground displacement at a distance  $x$  measured from the center of the ground movement zone,  $W$  is the width of the zone, and  $\delta$  is the peak ground displacement (at the center). The power of the cosine term (i.e., 2) in the equation accounts for the spread of the area with a smaller power corresponding to a greater spreading.

Fig. 4.8 shows the finite element mesh used in the analysis. A pipe length of 10 m is modeled, which is 2 m greater than the width of the ground displacement zone. The pipe is discretized with a uniform element size of 0.01 m. Hinge support is applied at the two ends of the pipeline.

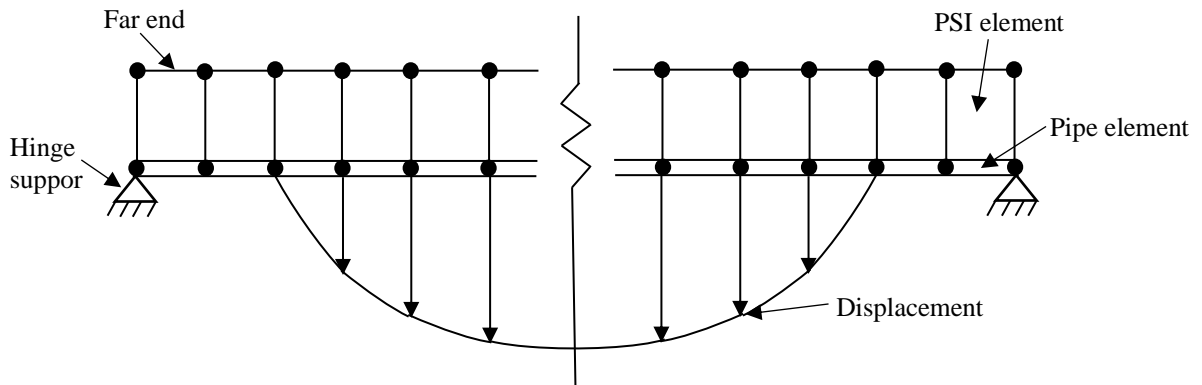


**Fig. 4.8.** Finite element mesh for the analysis of ground movement (schematic).

For the MDPE pipe material, the rate-dependent material model developed in chapter 3, is used here. Poisson’s ratio of the MDPE is assumed to be 0.46. A bilinear (elastic-perfectly plastic) constitutive model is used for the PSI elements to model the nonlinear soil pipe interaction. The parameters for the constitutive model are selected based on a previous study (Luo et al., 2014). Table 4.5 shows the detailed parameters considered in this study.

**Table 4.5:** Parameters considered for the analysis of pipe subjected to ground movement.

Item	Parameter	Numerical model
Pipe	Diameter, D(mm)	110
	Wall thickness, t (mm)	6.3
	Material	Time-dependent model (Das and Dhar 2020)
Ground displacement	Peak ground displacement, (m)	0.6
	Width of ground movement zone (m)	8.1
Springs	Axial resistance, (kN/m)	12.38
	Axial elastic displacement, (mm)	8
	Lateral resistance, (kN/m)	31.21
	Lateral elastic displacement, (mm)	8

#### 4.4.3 Time-Dependent Responses

To investigate the effects of the rate of ground movement on the pipe responses, the deformation is applied at five different rates, such as 1.5 m/s, 0.15 m/s,  $1 \times 10^{-2}$  m/s,  $1 \times 10^{-3}$  m/s, and  $1.5 \times 10^{-5}$  m/s, respectively. The maximum pipe stresses calculated due to rate-dependent ground movement is illustrated in Fig. 4.9. This figure shows that the pipe stress increases with the increase of ground displacement. The rate of increase of the stress is higher for higher rates of ground displacement. At the peak displacement of 0.6 m, the maximum pipe stress increased from 6.9 MPa to 14.3 MPa (more than double) for an increase of the ground movement rate from  $1.5 \times 10^{-5}$  m/s to 1.5 m/s. Thus, the buried MDPE pipe can experience stress as high as its allowable limit, depending on the size of the landslide and the rate of the ground movement. However, the strain

on the pipe wall during the ground movement process may not be significant. Fig. 4.10 shows the maximum pipe wall strains against ground displacement for different movements rates. As in pipe wall stress, the maximum strains occur at the mid-length of the pipe. For the range of ground movement rate considered, the maximum pipe wall strain ranges from 3.9% to 4.7% at the peak displacement of 0.6 m. The smallest strain is for the highest rate of ground movement, unlike the stress. The stress was the maximum for the highest rate of ground movement. Note that the effect of the ground movement rate on the pipe wall strain is less significant (the difference is ~17%) than the pipe wall stress.

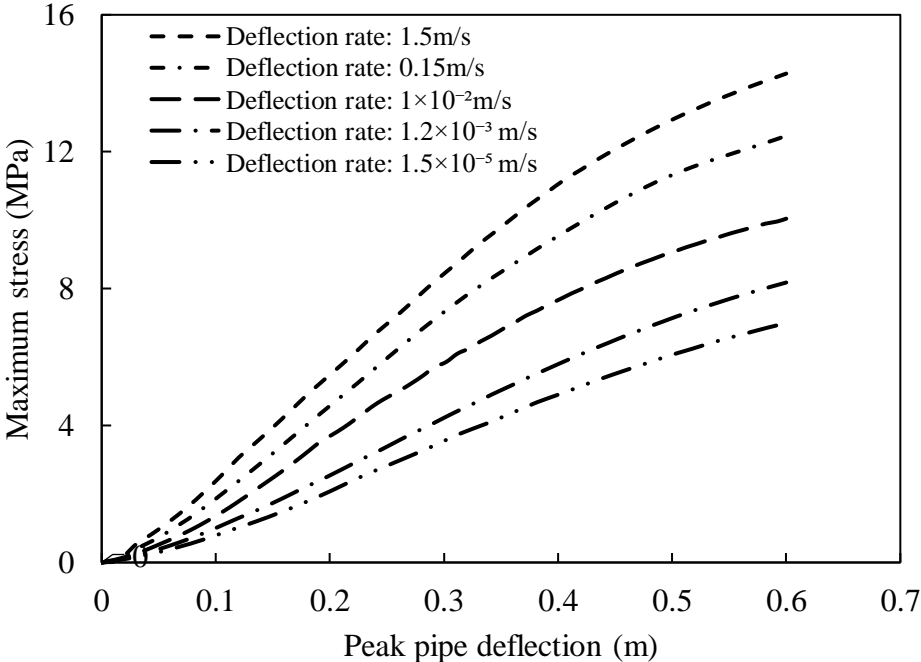


**Fig. 4.9.** Maximum stress at different rates of ground movement.

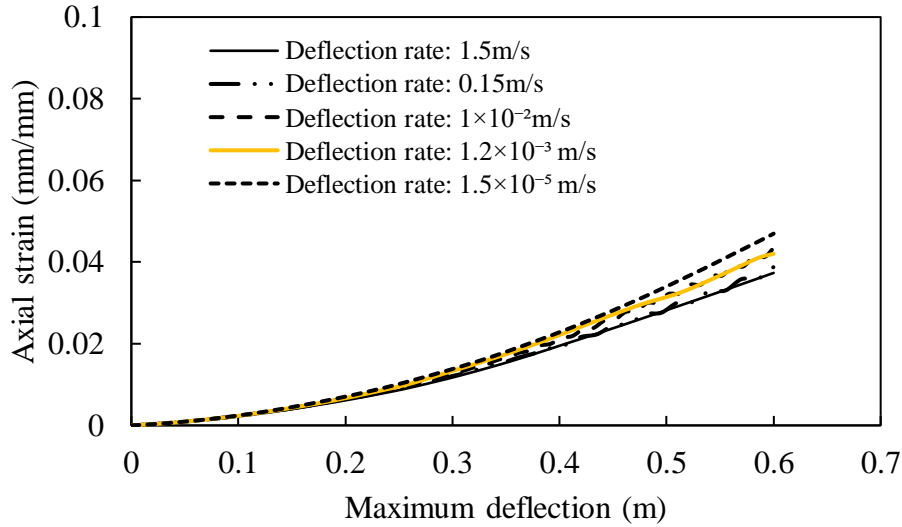


**Fig. 4.10.** Maximum strain at different rates of ground movement.

The pipe stress and strain experienced by MDPE pipe after the incident of ground movement will change with time due to the time-dependent property of the material. The changes in the maximum stress and strain corresponding to the highest ground movement rate are calculated using the proposed power-law model for MDPE pipe shown in Eq. (4.9). Fig. 4.11 shows the changes in stress and strain over a period of 50 years. The stress is found to reduce by about 35% in 50 years since the incident of ground movement (i.e., reaching the maximum displacement of 0.6 m). However, the pipe wall strain continues to increase with time. In 50 years, the strain was increased by 5.66%.

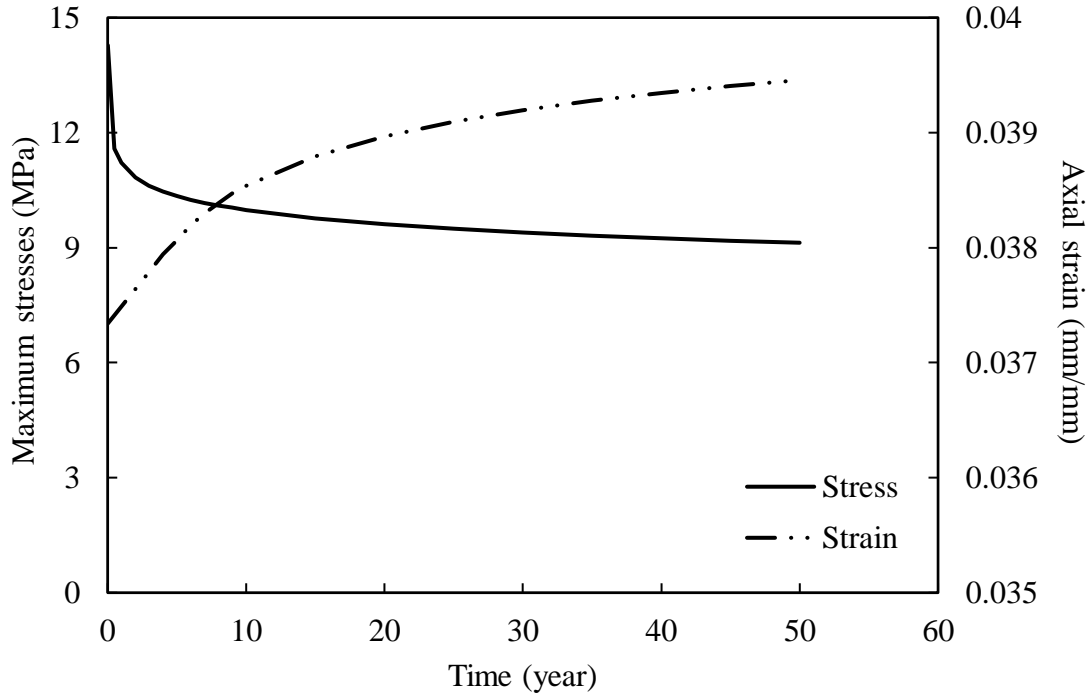


**Fig. 4.11.** Time-dependent responses of the deflected pipe.

## 4.5 Conclusions

In this paper, the time-dependent behavior of buried MDPE pipe is investigated considering a conventional buried pipe problem under vertical load and a pipeline subjected to rate-dependent lateral ground movement. A rigorous modeling technique and an equivalent simplified method (using secant modulus) were employed to recommend a practical approach to account for the time-dependent effects during analysis. The major findings of this study are as follows:

- 1) The rigorous time-dependent modeling technique can be used to investigate the responses of buried pipes having time-dependent material properties.
- 2) For the pipe under the vertical load, the pipe's vertical deflection is higher, and the horizontal deflection is less for a slower loading rate. Beyond the loading stage, the vertical deflection increases and the horizontal deflection decreases with time under a fixed applied pressure. However, the pipe wall stress is less for the slower loading rate that reduces further with time

under the constant load. Thus, long-term vertical deflection is the primary consideration for the design of the pipe.

- 3) The rate-dependent constant modulus proposed by the authors can reasonably be used to calculate the short-term deflections during the application of loads. For calculation of the long-term deflection (under a fixed applied pressure), a time-dependent secant modulus can be used. However, the time-dependent soil modulus depends on the initial stress level in the pipe. An equation for time-dependent normalized modulus is proposed for calculating the secant modulus at a given time ( $t$ ). Based on these observations, simplified methods are proposed for calculating the short-term and long-term deflections of buried MDPE pipes using a constant elastic modulus.
- 4) The existing simplified design equation is found to overestimate the deflections of MDPE pipes.
- 5) For the pipes subjected to lateral ground movement, stresses experienced by the pipe are higher for a higher rate of ground movement. However, the pipe strain is less for the higher ground movement rates. The effect of the ground movement rate on the increase of the stress is also significantly higher than the effect on the decrease of pipe wall strain.
- 6) The pipe wall stresses reduce and the pipe wall strain increase with time since the incident of ground movement.

## References

- AASHTO (2010). “LRFD Bridge Design Specifications”. 2<sup>nd</sup> ed., AASHTO, Washington, D.C., 1997.
- ALA, 2001. Guidelines for the design of buried steel pipe. G&E Engineering Systems Inc. A report by public-private partnership between American Society of Civil Engineers (ASCE) & Federal Emergency Management Agency (FEMA), American Lifeline Alliance (ALA).
- Almahakeri, M., Moore, I. D., and Fam, A. (2012). “The Flexural Behavior of Buried Steel and Composite Pipes Pulled Relative to Dense Sand: Experimental and Numerical Investigation”. *Volume 1: Upstream Pipelines; Project Management; Design and Construction; Environment; Facilities Integrity Management; Operations and Maintenance; Pipeline Automation and Measurement*.
- Almahakeri, M., Fam, A., and Moore, I. D. (2014). “Experimental Investigation of Longitudinal Bending of Buried Steel Pipes Pulled through Dense Sand”. *Journal of Pipeline Systems Engineering and Practice*, vol. 5, no. 2, p. 04013014.
- Argyrou, C., Bouziou, D., O’Rourke, T.D. and Stewart, H.E. (2018) “Retrofitting pipelines with cured-in-place linings for earthquake-induced ground deformations”, *Soil Dynamics and Earthquake Engineering*, Vol. 115 (2018), 156-168.
- Audibert, J., and Nyman, K. (1978). “Soil restraint against horizontal motion of pipes”. *International Journal of Rock Mechanics and Mining Sciences & Geomechanics Abstracts*, vol. 15, no. 2, 1978.

- Bilgin, Ö, Stewart, H. E., and O'Rourke, T. D. (2007). "Thermal and mechanical properties of polyethylene pipes." *J. Mater. Civ. Eng.*, 10.1061/(ASCE)0899-1561(2007)19:12(1043), 1043-1052.
- CEPA (2017). "2017 Performance data." Canadian Energy Pipelines Association, Calgary, AB, Canada.
- Chehab, A.G., & Moore, I. D. (2006). "Constitutive Model for High-Density Polyethylene to Capture Strain Reversal." *ASCE Pipelines 2006.*, 15419.
- Chua, K. M. (1986). Time-dependent interaction of soil and flexible pipe. Ph.D. thesis, Texas A & M University, College station, Texas.
- Dassault Systemes (2015). *ABUQUS/CAE user's Guide*. Dassault Systemes Simulia Corp. Providence, RI, USA.
- Das, S., Dhar, A.S., Muntakim, A.H., (2019). "Nonlinear Behavior of a Medium Density Polyethylene Pipe Material". *CSCE Annual Conference 2019*, Greater Montreal, Laval, Canada.
- Das, S., Dhar, A.S., (2020). "Nonlinear Time-dependent Mechanical Behavior of a Medium Density Polyethylene Pipe Material". Submitted, *Journal of Materials in Civil Engineering.*, ASCE.
- Dhar, A.S. and Moore, I.D. (2000). "Non-linear analysis of buried hdpe pipe by the finite element method: comparison with laboratory test". Proceedings of the international conference of Geotechnical and Geological Engineering (GEOENG2000), Melbourne, Australia, November 19-24, 2000.

- Dhar, A.S. and Moore, I.D. (2002). "Corrugated High-Density Polyethylene Pipe: Laboratory Testing and Two-dimensional Analyses to Develop Limit States Design" Transportation Research Record, Journal of the Transportation Research Board, No. 1814, pp: 157-163.
- Dhar, A.S. and Moore, I.D. (2004). "Laboratory Investigation of Local Bending in Profiled Thermoplastic Pipes", Advances in Structural Engineering-An International Journal, Vol. 7, No. 3, pp: 201-215.
- Hashash, N. M. A. (1991). "Design and analysis of deeply buried polyethylene drainage pipes." Ph.D. thesis, Department of Civil Engineering, University of Massachusetts at Amherst, Amherst, Mass.
- Luo, X.P., Ma, J.J., Zheng, J.Y., Shi, J.F. (2014). "Finite element analysis of buried polyethylene pipe subjected to seismic landslide". J. Pressure Vessel Technol. 136 (3) 031801.
- McGrath, T.J. (1998). "Design method for flexible pipe". A report to the AASHTO Flexible Culvert Liaison Committee, Simpson Gumpertz and Heger Inc., Arlington, MA.
- Moore, I.D (1994). "Three-dimensional time dependent model for buried HDPE pipe." *Computer methods and Advances in Geomechanics, Siriwardane & Zaman (eds)*, 8<sup>th</sup> International Conf. On Computer Methods and Advances in Geomechanics, pp. 1515-1520.
- Ni, P., Mangalathu, S. (2018). "Fragility analysis of gray iron pipelines subjected to tunneling induced ground settlement". Tunn. Undergr. Space Technol. 76, 133-144.
- Ni, P., Mangalathu, S. and Yi, Y. (2018b) "Fragility analysis of continuous pipelines subjected to transverse permanent ground deformation", Soils and Foundations, 58(2018), 1400-1413.

- Pulungan, D., Yudhanto, A., Goutham, S., Lubineau, G., Yaldiz, R., Schijve, W. (2018) “Characterizing and modeling the pressure- and rate-dependent elastic-plastic-damage behaviors of polypropylene-based polymers”, *Polymer Testing*, doi: 10.1016/j.polymertesting.2018.02.024.
- O’Rourke, M.J., 1989. Approximate analysis procedures for permanent ground deformation effects on buried pipelines. In: *Second U.S.-Japan Workshops on Liquefaction, Large Ground Deformation and Their Effects on Lifelines*, Buffalo, New York, pp. 336-347.
- Siddique, M.S.A. and Dhar, A.S. (2015). “A Novel Elasto-Viscoplastic model of High-Density Polyethylene Material.” *Geosynthetics International.*, Vol.22, No.2, pp: 173-182.
- Spangler, M.G (1941). “The structural design of flexible pipe culverts.” Bulletin 153, Iowa Engineering Experiment Station, Ames, Iowa.
- Suleiman, M.T., and Coree, B.J. (2004). “Constitutive model for high density polyethylene material: systematic approach.” *Journal of Materials in Civil Engineering.*, 16(6), 511–515.
- Suzuki, N., Arata, O., Suzuki, I. (1988). “Parametric study of deformation analysis of welded pipeline subjected to liquefaction-induced permanent ground displacement”. In: *First Japan-U.S. Workshop on Liquefaction, Large Ground Deformation and Their Effects on Lifeline Facilities*, Tokoyo, Japan, pp.155-162.
- Trautmann, C. H., and O’Rourke, T. D. (1983). “Behavior of pipe in dry sand under lateral and uplift loading”. *Geotechnical Engineering Rep.*, Cornell Univ., Ithaca, NY, 83–87. © ASCE 04013014-10 J. Pipeline Syst. Eng. Pract. J. Pipeline Syst. Eng. Pract., 2014, 5(2).

Zhang, C. and Moore, I.D. (1997). “Nonlinear mechanical response of High-Density Polyethylene. Part II: uniaxial constitutive modeling.” *Polymer Engineering and Science.*, Vol. 37, No.2, pp. 414-420.

Zhou, M., Wang, F., Du, Y.J. & Liu, M.D. (2017). “Performance of buried HDPE pipes. Part II: total deflection of the pipe. *Geosynthetics International*, 24, No. 4, 396-407.

## **CHAPTER 5**

### **Conclusions and Recommendations for Future Research**

#### **5.1 Conclusions**

Buried MDPE pipes are widely used for liquid/gas distribution systems. As MDPE possesses viscous properties, understanding and modeling the time-dependent behavior are required for performance assessment of the pipes. The objective of the present study is to systematically investigate the nonlinear time-dependent behavior of an MDPE pipe material using laboratory tests and numerical methods. A literature review is conducted first (presented in Chapter 2), which provides a theoretical background and the concerns for the experimental investigation and the theoretical development of the constitutive models.

This thesis work has incorporated the following tasks: 1) systematic experimental investigation to characterize the nonlinear time-dependent behavior of MDPE pipe material under various loading conditions; 2) development of rate-dependent constitutive relations based on the experimental investigations; 3) development of a FE modeling technique to simulate the nonlinear time-dependent behavior; 4) Application of developed modelling framework to a conventional buried pipe subjected to ground and surface load and a pipeline subjected to rate-dependent lateral ground movement. A summary of each of these tasks is given in this chapter, followed by recommendations for future research.

##### **5.1.1 Experimental Investigation Under Uniaxial Tension Test**

Tests are conducted with samples (coupons) cut from the wall of a 60 mm diameter MDPE pipe and a sample of a full cross-section of the pipe. The test program includes uniaxial testing at

various strain rates to capture the effects of loading rates, creep testing, and relaxation testing. The followings are the major conclusions from the test program:

- Under both loading and unloading conditions, the stress-strain responses are found to be highly nonlinear and strain rate dependent. However, these can be approximated as linear at a very small strain. During the experimental investigation, no strain rate history dependence and cyclic hardening were observed.
- The stress-strain response can be approximated to be independent of the strain rate at or below  $10^{-6}/s$ . This strain rate of  $10^{-6}/s$  can be termed as ‘reference strain rate’ for isotach based modeling.
- Initial values of the modulus of elasticity of MDPE are strain-rate dependent. For a strain of  $10^{-6}/s$  to  $10^{-2}/s$ , the initial moduli ranged from 325 MPa to 1,054 MPa.

The conclusions are valid for the strain rates contained in the range of experiments.

### **5.1.2 Development of Rate Dependent Constitutive Relations**

The hyperbolic model, as one of the simplest approaches to model nonlinearity, was used to develop nonlinear strain-rate dependent constitutive relations for MDPE. The model proposed in Suleiman and Coree (2004) is employed. The model parameters are determined based on the strain-rate dependent stress-strain relations obtained from the uniaxial tensile tests. As the stress-strain response corresponding to the reference strain rate is independent of strain rate, the strain rate-independent initial modulus and hyperbolic constant are used to model the stress-strain response at and below the reference strain rate.

### **5.1.3 Development of FE Modeling Technique**

A new modeling technique is proposed for FE modeling of nonlinear strain-rate dependent material behavior of MDPE pipe material using Abaqus. The modeling approach can successfully simulate the strain rate dependent stress-strain response observed in laboratory tests. It also reasonably simulates the loading-unloading-reloading response and a change in the strain rate. To account for the nonlinear time dependent responses, the creep law model is implemented in the proposed framework. The proposed creep law model successfully simulates the observed creep and relaxation behavior. The creep law model involves three parameters ( $A$ ,  $n$ ,  $m$ ). The magnitude of ' $A$ ' and ' $m$ ' are found to be independent of applied stress and strain levels, while parameter ' $n$ ' was found to increase with the increase of stress levels in creep tests and decrease with the increase of strain levels in relaxation tests.

### **5.1.4 A Conventional Buried Pipe Subjected to Ground and Surface Load**

The developed time-dependent modelling framework was employed to investigate a conventional buried pipe subjected to ground and surface load. The major findings of this study are as follows:

- The time-dependent responses of buried pipes can be investigated using the developed time-dependent modeling technique.
- For a slower loading rate, the vertical deflection of pipe is higher, and the horizontal deflection is lower. After the loading stage, the vertical deflection is found to be increased, and the horizontal deflection to be decreased with the increase of time. Hence, the long-term vertical deflection is the primary consideration for the design of pipe.

- In this study, the author has proposed rate-dependent constant moduli which can be used to calculate the short-term deflections during the application of loads. A time dependent secant modulus can be used for calculation of long-term deflection (under a fixed applied pressure).
- Existing simplified design equation overestimates the deflections of MDPE pipes.

### **5.1.5 A Conventional Buried Pipe Subjected to Lateral Ground Movement**

A pipeline subjected to the rate-dependent lateral ground movement was investigated using the developed time-dependent modeling framework. The major findings of this study are as follows:

- The rate of ground movement highly influences the responses of buried pipes. The stresses developed on the pipe are found to be higher and the pipe wall strain is found to be lower for a higher rate of ground movement. Also, the influence of increasing the ground movement rate on the increase of the stress is significantly higher than the effect on the decrease of the pipe wall strain.
- After the incident of ground movement, the pipe wall stresses decrease, and the pipe wall strain increases with time.

## **5.2 Recommendations for Future Study**

The study presented here investigates the mechanical properties of MDPE pipes commonly used in the Canadian gas distribution system (CSA B 137.4 certified). The study reveals that the mechanical properties of MDPE are highly nonlinear, rate-dependent, and time-dependent. Although the study is mainly focused on the research findings on the MDPE pipe, the theoretical derivations/approach is equally applicable to other flexible pipes employed in different applications. Some specific recommendation for future research in this area included below:

- 1) In the present study, the stress-strain behavior of MDPE was examined for a range of strain-rates of  $10^{-6}/s$  to  $10^{-2}/s$ . It is recommended to explore the stress-strain relation at a much slower strain-rate to confirm the reference strain-rate found from this study. Tests could also be performed at a much faster rate to examine the behavior.
- 2) The relaxation and creep behaviors are examined here for limited strain and stress levels, respectively. It is recommended to conduct tests for wider ranges of stresses and strains. The relaxation and creep also need to be investigated over a longer duration.
- 3) The primary, secondary and tertiary levels of creep are not investigated in this research. It is the opinion of the author that these creeps would be stress or strain-rate dependent and have a correlation with the material responses at the reference strain-rate, which require further exploration.
- 4) The models developed in the present study are specifically for analyzing MDPE pipe structures. It also has the potential for application to other polymer materials with the appropriate calibration of the material parameters.
- 5) Temperature dependency has not been considered in the present study, which can be a scope for future study.
- 6) The time-dependent modelling framework developed in this research for MDPE pipe can be used for investigating other practical problems like pipelines subjected to oblique loading (lateral-axial, axial-vertical, lateral-vertical).

## References:

- AASHTO (2010). "LRFD Bridge Design Specifications." 2<sup>nd</sup> ed., AASHTO, Washington, D.C., 1997.
- AZOM-2001. "Medium Density Polyethylene – MDPE." Available from <https://www.azom.com/article.aspx?ArticleID=422> .
- Bilgin, Ö, Stewart, H. E., and O'Rourke, T. D. (2007). "Thermal and mechanical properties of polyethylene pipes." *J. Mater. Civ. Eng.*, 10.1061/(ASCE)0899-1561(2007)19:12(1043), 1043-1052.
- Broutman, L. J. and Krishnakumar M. K. (1976). "Impact strength of polymers: 1. The effect of thermal treatment and residual stress." *Polymer Engineering and Science*. Vol. 16, NO. 2, pp. 74-81.
- Bilgin, Ö. (2014). "Modeling viscoelastic behavior of polyethylene pipe stresses." *ASCE Pipelines 2014.*, 10.1061/(ASCE)MT.1943-5533.0000863.
- Bhatnager, A. and Broutman, L. J. (1985). SPE ANTEC TECH. Papers, Vol. 43, 545.
- Beech, S. K., Burley, C. and BUM, H. C. (1 988). "Residual stress in large diameter MDPE water pipe." The Plastics and Rubber Institute, International Conference on Plastics Pipes VII, University of Bath, England, 20-22.
- Chua, K. M. (1986). "Time-dependent interaction of soil and flexible pipe." Ph.D. thesis, Texas A & M University, College station, Texas.
- Chua, K. M., & Lytton, R. L. (1989). "Viscoelastic Approach to Modeling Performance of Buried Pipes." *Journal of Transportation Engineering.*, 115(3), 253–269.

- Chehab, A.G., & Moore, I. D. (2006). "Constitutive Model for High Density Polyethylene to Capture Strain Reversal." *ASCE Pipelines 2006.*, 15419.
- Dassault Systemes (2015). *ABUQUS/CAE user's Guide*. Dassault Systemes Simulia Corp. Providence, RI, USA.
- DiFrancesco, L.C. (1993). "Laboratory testing of high-density polyethylene drainage pipes." M. S. thesis. Department of Civil Engineering, the University of Massachusetts at Amherst. U.S.A.
- Doshi S. R. (1989). "Prediction of residual stress distribution in plastic pipe and profile extrusion." Proceedings of ANTEC, pp. 546-549.
- Duncan, J. M., and Chang, C. Y. (1970). "Nonlinear analysis of stress and strain in soils." *J. Soil Mech. Found. Div.*, 96(5), 1629–1653.
- Ebbott, T. G. (1987). "Fracture Characteristics of a Viscoelastic Polymer under Constant Load: Experiments and Analysis." Ph.D. thesis, The University of Wisconsin-Madison.
- Findley, W. N. and Tracy, I. F. (1974). "16-year, creep of polyethylene and PVC." *Polymer Engineering and Science*. Vol. 14, No. 8, PP 577-580.
- Findley, W. N. (1987). "26-Year creep and recovery of poly (vinyl chloride) and polyethylene." *Polymer Engineering and Science*. Vol. 27, No. 8, pp 582-585.
- Hashash, N. M. A. (1991). "Design and analysis of deeply buried polyethylene drainage pipes." Ph.D. thesis, Department of Civil Engineering, University of Massachusetts at Amherst, Amherst, Mass.
- Hjelmquist, E. and Storakers, B. (1987). "Long-term deformation and failure of buried plastic pipes." *Journal of Engineering Mechanics*. Vol. 7, 1033- 1049.

- Husted, J. L., and Thompson, D. M. (1985). "Pull-out forces on joints in polyethylene pipe systems." A guideline for gas distribution engineering, E.I. Du Pont de Nemours.
- Janson, L.-E. (1985). "Investigation of the long-term creep modulus for buried polyethylene pipes subjected to constant deflection." Proc., Advances in Underground Pipeline Engineering, J. K. Jeyapalan, ed., *Pipeline Division of the ASCE*, Univ. of Wisconsin-Madison, Madison, WI, 253-262.
- Katona, M. G. (1988). "Allowable fill heights for corrugated polyethylene pipe." Transportation research record, 1191: 30-38.
- Katona M.G. (1990). "Minimum cover height for corrugated plastic pipe under vehicle loading." Transportation Research Record 1288, 127-135.
- Kondner, R. L. (1963). "Hyperbolic stress-strain response: Cohesive soils." *J. Soil Mech. Found. Div.*, 89(1), 115-143.
- Loven, A. and Janson, J.-F. (1972). "Material technical investigations of PVC and HDPE pipes for use as buried sewage pipes." Department of Polymer Technology, Royal Institute of Technology.
- MC, (1999). Metallurgical Consultants (MC). Available from [Materialsengineer.com/CA-Creep-Stress-Rupture.htm](http://Materialsengineer.com/CA-Creep-Stress-Rupture.htm).
- Moser, A.P. (1997). "Analytical methods for predicting performance of buried flexible pipes." Pre-print (CD-ROM), Transportation Research Board, Washington, D.C.

- Moore, I.D (1994). “Three-dimensional time dependent model for buried HDPE pipe.” *Computer methods and Advances in Geomechanics, Siriwardane & Zaman (eds)*, 8<sup>th</sup> International Conf. On Computer Methods and Advances in Geomechanics, pp. 1515-1520.
- Muntakim, A. H., Dhar, A. S., and Reza, A. (2018). “MODELLING TIME DEPENDENT BEHAVIOR OF BURIED POLYETHYLENE PIPES USING ABAQUS.” in *Proc. of Geo Edmonton, the 71st Canadian Geotechnical Conference and the 13th Joint CGS/IAH-CNC Groundwater Conference*.
- PPI-1993. “Engineering Properties of Polyethylene.” Plastics Pipe Institute (PPI), The Society for the Plastics Industry, Inc.
- PIPA-2001. “*Polyolefins technical information*.” Plastics Industry Pipe Association of Australia Limited (PIPA), Chatswood, NSW, Australia. Available from [www.pipa.com.au](http://www.pipa.com.au) .
- Powel, P. C. (1983). *Engineering with polymers*, Chapman and Hall and Methuen, NY, pp. 14-19.
- Stewart, H. E., Bilgin, O., O’Rourke, TD and Keeney, T. M. (1999). “Technical reference for improved design and construction to account for thermal loads in plastic gas pipelines.” Technical report, Cornell University, Ithaca, NY.
- Suleiman, M.T., Lohnes, R., Wipf, T., and Klaiber. W. (2003). “Analysis of deeply buried flexible pipes.” Transportation Research Record 1849, pp.
- Suleiman, M.T., and Coree, B.J. (2004). “Constitutive model for high density polyethylene material: systematic approach.” *Journal of Materials in Civil Engineering.*, 16(6), 511–515.
- Siddique, M.S.A. and Dhar, A.S. (2015). “A Novel Elasto-Viscoplastic model of High-Density Polyethylene Material.” *Geosynthetics International.*, Vol.22, No.2, pp: 173-182.

- Weerasekara, L. (2011). "Pipe-soil interaction aspects in buried extensible pipes." Ph.D. thesis, Department of Civil Engineering, University of British Columbia, Vancouver, B.C.
- Williams, J. G., Hodgkinson, J. M. and Gray. A. (1981). "The determination of residual stresses in plastic pipe and their role in fracture." *Polymer Engineering and Science*. Vol. 21, NO. 13, pp. 822-828.
- Zhang, C. and Moore, I.D. (1997). "Nonlinear mechanical response of High-Density Polyethylene. Part II: uniaxial constitutive modeling." *Polymer Engineering and Science*., Vol. 37, No.2, pp. 414-420.
- Zhang, C. (1996). "Non-linear mechanical response of high-density polyethylene in gravity flow pipes." Ph.D. thesis, Department of Civil Engineering, University of Western Ontario, London, Ontario.

## **APPENDIX A**

### **Nonlinear Behavior of a Medium Density Polyethylene Pipe Material**

This research work has been published as Das, S., Dhar, A.S., Muntakim, A.H., 2019. “Nonlinear Behavior of a Medium Density Polyethylene Pipe Material” in the CSCE Annual Conference 2019, Greater Montreal, Laval, Canada, June 12–15, 2019.



## Nonlinear Behavior of a Medium Density Polyethylene Pipe Material

Das, S.<sup>1,2</sup>, Dhar, A. S.<sup>1,3</sup>, Muntakim, A. H.<sup>1,4</sup>

<sup>1</sup> Memorial University of Newfoundland, Canada

<sup>2</sup> [sdas@mun.ca](mailto:sdas@mun.ca)

<sup>3</sup> [asdhar@mun.ca](mailto:asdhar@mun.ca)

<sup>4</sup> [ahm505@mun.ca](mailto:ahm505@mun.ca)

**Abstract:** Medium density polyethylene (MDPE) pipes are extensively used for gas distribution system in Canada and worldwide. MDPE pipe material possesses time-dependent behavior that governs the performance of the pipes in air or buried in the soil. However, very limited information is currently available in the literature on the time-dependent behavior of MDPE pipe materials. In this research, an extensive laboratory investigation is carried out to investigate the time-dependent behavior of MDPE pipe material. Uniaxial tensile tests are conducted with samples (coupons) cut from the wall of a 60 mm diameter MDPE pipe using waterjet. A surface planer has been used to remove the curvature. The coupon samples cut from the pipe might experience residual stresses during sample preparation, which might affect the test results. To investigate the effect of the residual stresses, tensile tests with samples of full cross-section of the pipe are also conducted. Tests are conducted at various strain rates to capture the effects of loading rates. The experimental results are used to develop numerical modelling approach for time-dependent material behaviour using a commercially available software, Abaqus. The strain-rate dependent material behavior of MDPE is incorporated in Abaqus through development of USDFLD subroutine. The proposed modeling approach successfully simulates the test results of the MDPE pipe. Temperature effects on the mechanical behavior of MDPE pipe were not considered.

### 1 INTRODUCTION

Many of today's plastics were developed during and just before World War II. Since then plastic pipe usage has increased at a significantly high rate due to its various advantages over metal pipes including low cost, light-weights, ease of installation and corrosion resistance. Water supply, cold water distribution, sewer, gas distribution and irrigation are the major areas of application of plastic pipes. Plastic pipes are divided into two groups: thermoset and thermoplastic. Usage of medium density polyethylene (MDPE) pipe, a thermoplastic material, is rapidly increasing due to its good shock and drop resistance properties.

The buried distribution pipes are subjected to loads from the weight of the soil column above the pipe, the surcharge loads including live traffic and dead load, internal pressure and loads from ground movement resulting from seismic activities. Generally, soil-pipe interaction analysis is performed to understand the behaviour of pipes under aforementioned loads. However, modelling of soil-pipe interaction for polyethylene pipes is complex as the behaviour of polymer material is time, temperature and strain rate dependent. Numerous attempts have been made for investigating the nonlinear time-dependent behaviour of polyethylene pipe materials with particular attention to High Density Polyethylene (HDPE) pipes. Earlier work focused on developing relaxation modulus used for calculating the time-dependent responses under a fixed stress. The modulus of elasticity of pipe material at a particular stress level is expressed using a power law relation of time (Chua and Lytton 1989). Moore (1994) developed a linear viscoelastic model

GEN155-1

using nine kelvin elements in series for describing the viscous effects of a HDPE pipe material. Although the linear viscoelastic model successfully simulated stress–strain responses at lower strains, the model was unsuccessful at the higher strains. A non-linear viscoelastic and viscoplastic modelling approaches are then employed to reasonably simulate the stress–strain behaviour under various loading conditions (Zhang and Moore 1997, Chehab and Moore 2006). Siddquee and Dhar (2015) developed a strain-rate dependent nonlinear three-component elastic viscoplastic model for a HDPE pipe material. However, very limited information is currently available on the study of MDPE pipe materials. Ben-Hadz-Hamouda et al. (2007) conducted an experimental investigation of a type of MDPE and demonstrated extensive strain rate effects on the material behaviour. The objective of the current study is to investigate the time-dependent behaviour of MDPE pipe material for pipe-soil interaction analysis. Muntakim et al (2018) have simulated the time dependent behavior of buried HDPE pipe using a commercially available finite element (FE) software, Abaqus (Dassault Systems 2015). This approach is employed here to simulate the time dependent behaviour of MDPE pipe material.

This study includes two components: 1) experimental investigation for identifying the nonlinear strain rate dependent behavior of MDPE in tension; 2) Development of a numerical modelling approach to simulate the strain rate dependent behaviour of MDPE pipe. The experimental results and the corresponding model predictions are reported in this paper. The capability of the modelling approach is evaluated through the simulation of rate-dependent stress–strain response.

## 2 SPECIMEN PREPARATION AND EXPERIMENTAL SETUP

To examine the strength and deformation behaviour of a MDPE material, several tensile tests were conducted in the structure lab at Memorial University of Newfoundland, Canada. All the tensile tests in this paper were performed on coupons, cut from the wall of a 60.3 mm diameter and 5.5 mm thick MDPE pipe. The samples were prepared according to ASTM D638-14 specifications. Water jet was used for cutting the tensile coupons and a surface planer was used to remove the curvature. The length of the test specimens was parallel to the length of the MDPE pipe. The INSTRON (5585H) machine was used to apply loads to the test specimens through moving the crosshead of the machine. The upward movement of the crosshead causes a tensile load and downward movement causes a compressive load on the specimens. A load transducer which is mounted in series with the specimen measures the applied load and converts the load into an electrical signal that a control system measures and displays. A strain transducer (extensometer) was also used on this system to measure strain. The testing system was controlled using an Instron proprietary software. Figure 1 shows the experimental set up of the tensile coupon tests.

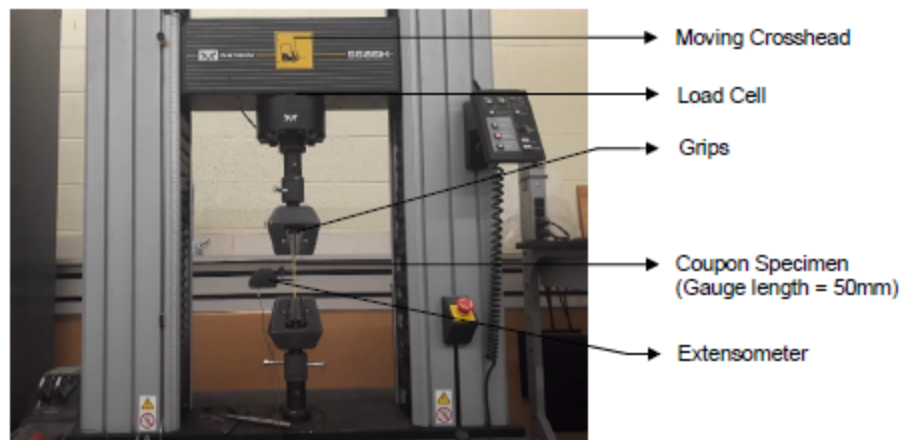


Figure 1: Test set up and loading apparatus for coupon test.

GEN155-2

The change of the height of the specimen was measured by recording the ram position through the displacement transducer of the Instron machine and the corresponding loads were measured by the load cell. A computer controlled system was used to monitor and record the outputs of the displacement transducer and the load cell. A tensile test with full pipe cross-section of MDPE pipe was also conducted to see whether the cutting of samples might affect the test result or not. Figure 2 shows the experimental set up of full pipe tensile test.

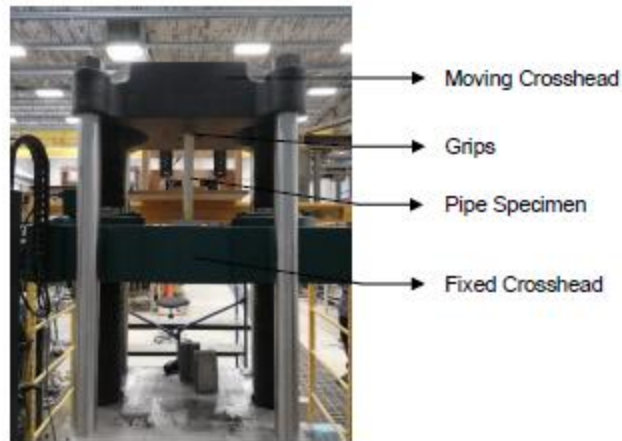


Figure 2: Test set up and loading apparatus for full pipe test.

## 2.1 Test Results

To understand the effect of the rate of loading, four uniaxial tension tests were conducted at constant strain rates ranging from  $10^{-5}$  /s to  $10^{-2}$  /s. A test range was selected for each test to avoid necking. The highest range for measuring the strain was 0.14 (mm/mm). The results are shown in Figure 3. From Figure 3, it is evident that the stress-strain relationship of the MDPE pipe is highly strain rate dependent.

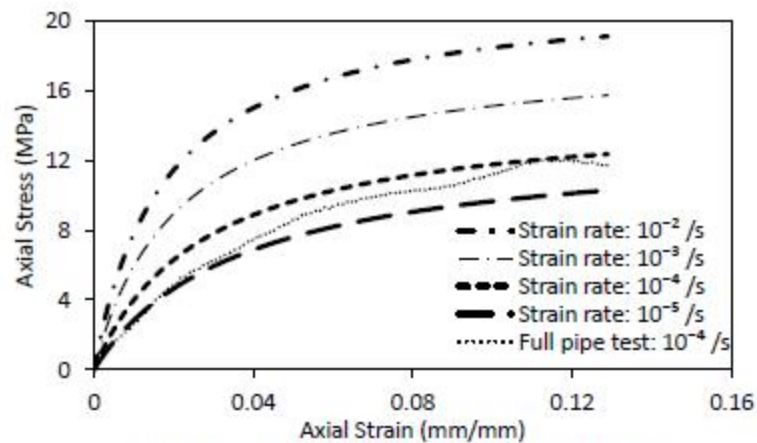


Figure 3: Experimental results for constant strain rate.

GEN155-3

Initially, the stress increases almost linearly with the strain, but the relationship quickly becomes nonlinear. Within the test range, there are no peak stresses found on the stress–strain curve. This figure also shows the result of stress–strain response conducted for the full pipe test. A strain rate of  $10^{-4}/s$  was used for this test. It initially underestimates the coupon test results because slipping at the grips occurred initially, however, at higher load it matches with the coupon test results conducted at the same strain rate ( $10^{-4}/s$ ). Thus, the coupon test results reasonably represent the mechanical behaviour of the pipe.

To see the strain-rate history dependency of MDPE pipe material, a strain rate jump test was implemented. Initially, a strain rate  $10^{-3}/s$  was applied up to a strain of 0.065. After that the rate was changed from  $10^{-3}/s$  to  $10^{-2}/s$  and then back to the previous rate at axial strain 0.11 (mm/mm). The results are shown in Figure 4 along with the stress–strain responses corresponding to the strain rates of  $10^{-3}/s$  and  $10^{-2}/s$ , respectively. As seen in the figure, at the change of the strain rate to  $10^{-2}/s$  from  $10^{-3}/s$ , a gradual increase of stress occurred. After increasing of rapid stress within a short period, the stress reached to the level it would have held if the new strain rate, i.e.  $10^{-2}/s$ , had been used from the beginning of the test (matches with the stress–strain response for the strain rate of  $10^{-2}/s$ ). Similarly, with the change of the strain back to  $10^{-3}/s$ , the response follows the stress–strain response corresponding to  $10^{-3}/s$  strain rate with a sudden drop. Similar responses were reported earlier for High Density Polyethylene (HDPE) in Zhang and Moore (1997). Therefore, the stress–strain responses of the MDPE do not have strain-rate history dependency, but follow the strain-rate dependent stress–strain relations.

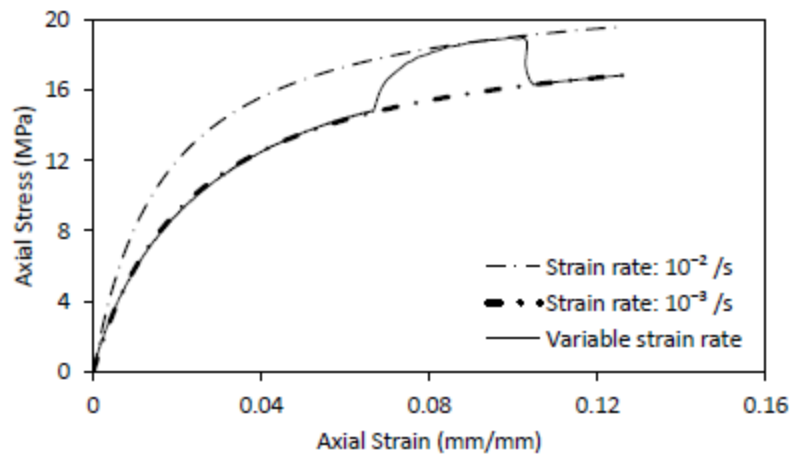


Figure 4: Experimental result for strain rate jump test.

A cyclic loading test was also performed to see the loading-unloading-reloading behavior of the MDPE pipe. Figure 5 shows the results of the cyclic loading test. The test was conducted at the same magnitude of strain rate  $10^{-3}/s$  during the load-unload-reload cycle. The stress–strain curve for reloading gradually approached the monotonic loading curve.

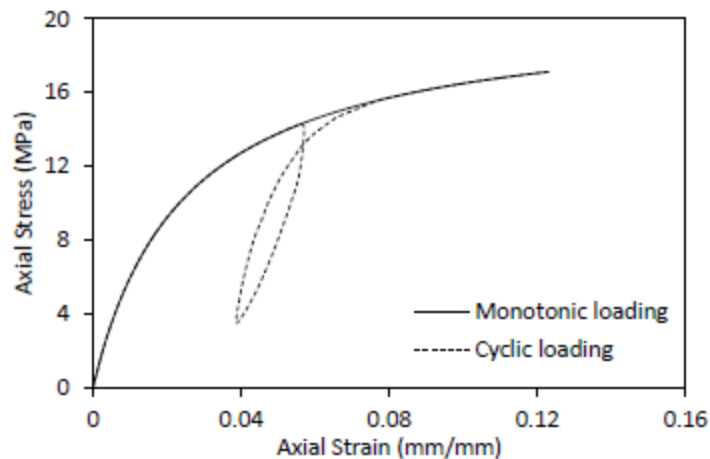


Figure 5: Experimental result for cyclic loading test (Strain rate:  $10^{-3}$ /s)

### 3 MODELLING OF TIME-DEPENDENT RESPONSES

A number of different constitutive models were developed to capture the nonlinear time-dependent behavior of HDPE materials (Chua and Lytton 1989, Zhang and Moore 1997, Chehab and Moore 2006, Suleiman and Coree 2004, Siddiquee and Dhar 2015). However, none of these models are implemented in commercially available finite element (FE) software. As a result, the models are not widely used for analysing engineering problems. Muntakim et al (2018) employed the features available in a commercially available FE software, Abaqus (Dassult system 2015) to simulate the time-dependent behaviour of a HDPE pipe material. The technique used in Muntakim et al (2018) is employed here for modelling the time-dependent behaviour of MDPE pipe material. Tensile and/ or compression tests are generally performed with the application of different rates of loading to investigate the time dependent response of material. Strain rate dependent stress-strain relationships are used to simulate the time-dependent response. These data are implemented using user subroutine, USDFLD, in Abaqus. USDFLD allows defining field variables at a material point as a function of time or solution dependent material properties. It provides access to material point quantities at the start of the increment and gives explicit solution. In this process, the material properties are not influenced by the results obtained during the increment. So, the accuracy depends on the size of the time increment and this time increment can be controlled by the variable PNEWDT (Dassult Systems 2015). At the start of the increment, a utility routine, GETVRM, is used to access the material point. By calling GETVRM with the appropriate output variable keys, the values of the material point quantities are obtained. ARRAY, JARRAY, FLGRAY are used to recover the values of material point data (the floating point, integer and character data). At each increment, the field variables are restored to the values interpolated from the nodal values and introduced with user defined state variables, STATEV, which can be recalled using variable key 'SDV' in the utility routine, GETVRM.

In this study, GETVRM is used to access all the strain components. User-defined state variables are assigned to store current strain component, time increment and the calculated strain rate for using in subsequent time steps. The strain rate is calculated based on the current strain (accessed by the GETVRM), the previous strain (stored in user defined variables) and time increment (accessed by USDFLD).

FIELD variable, which is an array containing field variables at the current material point, is used to assign the strain rate. On the basis of the information of these FIELD variables given in the input file, Abaqus

GEN155-5

interpolates the material parameters. In this interpolation, an average value is used for linear elements and an approximate linear variation is used for quadratic elements.

The strain rate dependent stress–strain responses of MDPE pipe were found in experimental investigation. These test data were given in Abaqus input file for modelling of time-dependent behaviour of MDPE pipe using the feature in Abaqus. On the basis of these test data and FIELD variable from USDFLD, Abaqus uses its default constitutive model to calculate Jacobian matrix and stress and other parameters.

### 3.1 FE Simulation of Test Results

Finite element analysis was performed for numerical simulations of the uniaxial tension tests carried out. As discussed earlier, tension tests were conducted using coupon specimens of 13 mm width (width of the narrow section) and 50 mm gauge length. The tests were performed with the application of constant strain rates ranging from  $10^{-5}/s$  to  $10^{-2}/s$ . These strain-rate dependent stress–strain data were given in the input file and simulated using FE modelling using Abaqus. In the FE analysis, the same size of the specimen was used. Smooth rigid boundaries were used at the bottom and the left side. Figure 6 shows the FE mesh. The horizontal and vertical translations were restrained at the corner node. At the top of the mesh, a uniform strain was applied at the same rates as those applied during the tension tests.

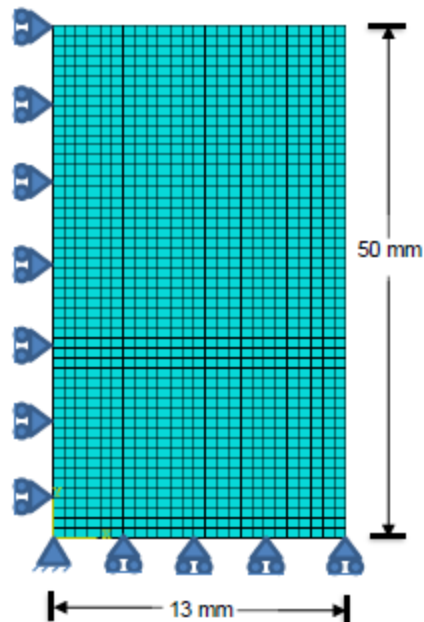


Figure 6: FE model

### 3.2 Comparison of Results

The stress–strain relationships obtained from the finite element analysis and experimental investigation are shown in Figure 7. A reasonable agreement appears between the simulated and experimental curves in the figure. Thus, the method employed is capable of predicting the time dependent stress–strain behaviour of the MDPE material.

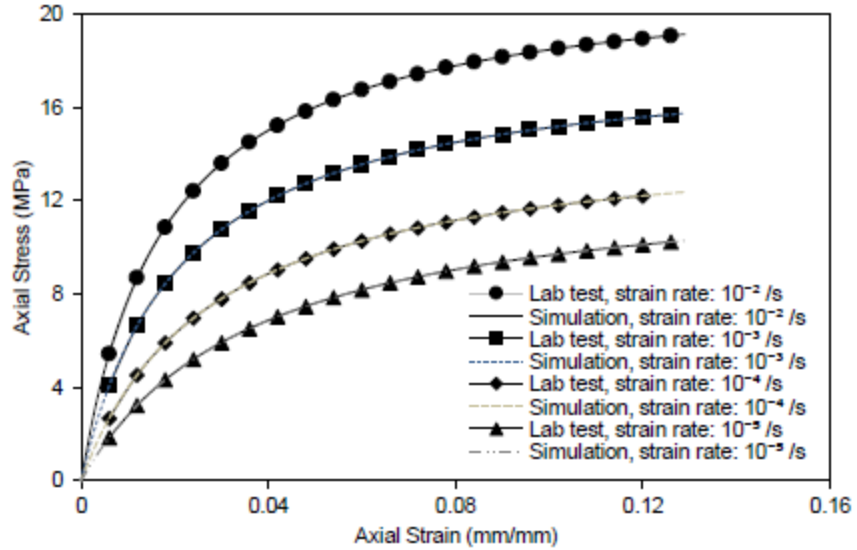


Figure 7: Comparison of test results with finite element analysis.

A strain rate jump test performed during the experimental tests is also successfully simulated by this method of analysis. During the experimental test, the strain rate was changed from  $10^{-3}$  /s to  $10^{-2}$  /s at axial strain 0.065 (mm/mm) and then back to  $10^{-3}$  /s at axial strain 0.11 (mm/mm). This jump in the strain rate is simulated using the proposed method. Figure 8 shows the comparison of simulated and experimental results. From this comparison, we can see that the applied technique reasonably predicted the experimental behaviour during the change in strain rate. There is little numerical noise in the results of simulation during the change of strain rate. Initially, the noise was large. To minimize it, a control was applied on the strain increment using the code of USDFLD. The maximum strain increment of less than 15% was found to reduce the noise to a reasonable value.

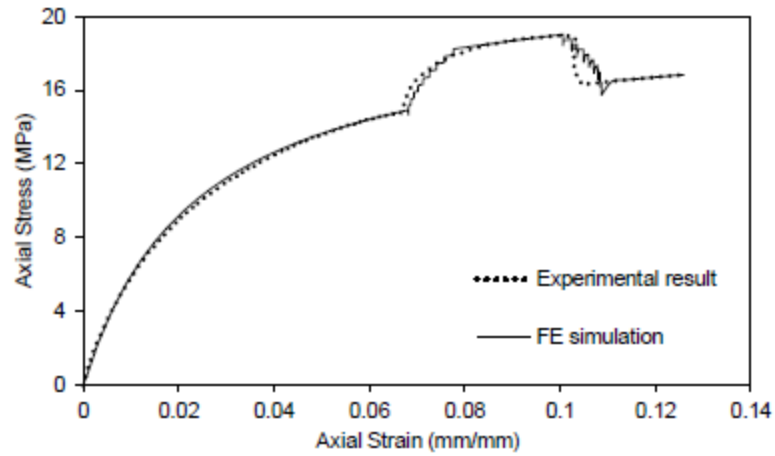


Figure 8: Simulation of a jump in the strain rate

The proposed method also reasonably predicted the loading-unloading-reloading response found from the experimental tests. During experimental investigation, a cyclic test was conducted with the same strain rate of  $10^{-3}$ /s for loading-unloading-reloading. Figure 9 compares the results of FE simulation and experimental investigation. This figure shows that the observed behaviour of cyclic loading can be reasonably predicted by the proposed method.

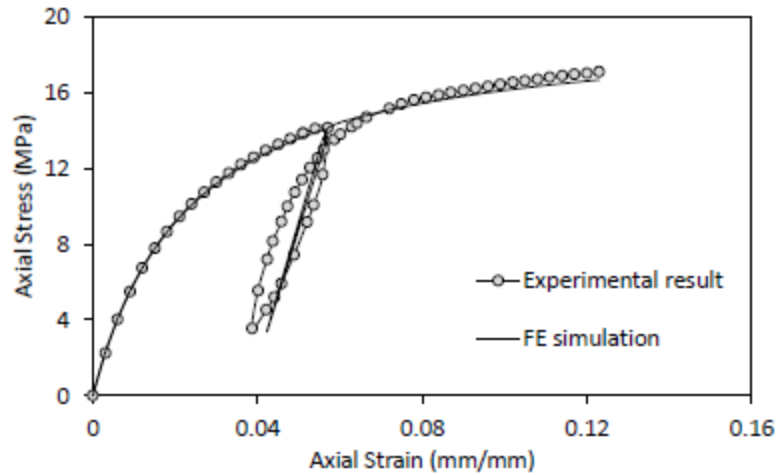


Figure 9: Simulation of cyclic loading test.

GEN155-8

#### 4 CONCLUSION

The time dependent nonlinear behavior of a MDPE material is systematically investigated using a series of uniaxial tension tests. The stress-strain responses are found to be highly nonlinear and strain rate dependent. During the experimental investigation, no strain rate history dependence was observed. A modelling technique is developed for simulating the behavior of MDPE pipe material using a commercially available FE software, Abaqus. It is found that, the modelling approach can successfully simulate the strain rate dependent stress-strain response observed in laboratory tests. It can also reasonably simulate the loading-unloading-reloading response and a jump in the strain rate.

#### 5 ACKNOWLEDGEMENTS

The funding of this research project was provided by the Natural Sciences and Engineering Research Council of Canada (NSERC) through its Collaborative Research and Development Grants, InnovateNL in the province of Newfoundland and Labrador and FortisBC Energy Inc. The financial supports are gratefully acknowledged.

#### 6 REFERENCES

- ASTM. (2003c). Standard test method for tensile properties of plastics. *2003 annual book of standards*, D638-14, Vol.08.01, West Conshohocken, Pa., 46-59.
- Ben Hadj Hamouda, H., Laiarinandrasana L., Piques, R., 2007. Viscoplastic behavior of a medium density polyethylene (MDPE): Constitutive equations based on double nonlinear deformation model. *International Journal of Plasticity*, 23 (2007) 1307-1327.
- Chehab, A.G., & Moore, I. D. (2006). Constitutive Model for High Density Polyethylene to Capture Strain Reversal. *ASCE Pipelines 2006*, 15419.
- Chua, K. M., & Lytton, R. L. (1989). Viscoelastic Approach to Modeling Performance of Buried Pipes. *Journal of Transportation Engineering*, 115(3), 253-269.
- Dassault Systemes (2015). *Abaqus User Subroutines Reference Guide*. Dassault Systemes Simulia Corp. Providence, RI, USA.
- Moore, I.D (1996). Three-dimensional time dependent model for buried HDPE pipe. *Computer methods and Advances in Geomechanics, Siriwardane & Zaman (eds)*, 8<sup>th</sup> International Conf. On Computer Methods and Advances in Geomechanics, pp. 1515-1520.
- Muntakim, A.H., Dhar, A.S., Reza, A. (2018). Modelling time dependent behavior of buried polyethylene pipes using Abaqus. *Geo Edmonton 2018*, Edmonton, Alberta.
- Siddique, M.S.A. and Dhar, A.S. (2015). A Novel Elasto-Viscoplastic model of High-Density Polyethylene Material. *Geosynthetics International*, Vol.22, No.2, pp: 173-182.
- Suleiman, M., Lohnes, R., Wipf, T., & Klaiber, F. (2003). Analysis of Deeply Buried Flexible Pipes. *Journal of the Transportation Research Board*, 1849, 124-134.
- Zhang, C. and Moore, I.D. (1997). Nonlinear mechanical response of High-Density Polyethylene. Part II: uniaxial constitutive modeling. *Polymer Engineering and Science*, Vol. 37, No.2, pp. 414-420.

GEN155-9

A sample of inp file used in Chapter 3 for modeling purpose have been attached below

```
*Heading
** Job name: Job-1 Model name: Model-1
** Generated by: Abaqus/CAE 6.14-1
*Preprint, echo=NO, model=NO, history=NO, contact=NO
**
** PARTS
**
*Part, name=Part-1
*Node
    1,          0.,          0.
    2, 0.000508000026,          0.
    3, 0.001016000005,          0.
    4, 0.001523999996,          0.
    5, 0.00203200011,          0.
    6, 0.00254000002,          0.
    7, 0.003047999993,          0.
    8, 0.003556000007,          0.
    9, 0.00406400021,          0.
   10, 0.00457199989,          0.
   11, 0.00508000003,          0.
   12, 0.00558800017,          0.
   13, 0.00609599985,          0.
   14, 0.00660399999,          0.
   15, 0.00711200014,          0.
   16, 0.00761999981,          0.
   17, 0.00812800042,          0.
   18, 0.00863599963,          0.
   19, 0.00914399978,          0.
   20, 0.00965199992,          0.
   21, 0.0101600001,          0.
   22, 0.0106680002,          0.
   23, 0.0111760003,          0.
   24, 0.0116839996,          0.
   25, 0.0121919997,          0.
```

---

1344, 0.00863599963, 0.0253999997  
1345, 0.00914399978, 0.0253999997  
1346, 0.00965199992, 0.0253999997  
1347, 0.0101600001, 0.0253999997  
1348, 0.0106680002, 0.0253999997  
1349, 0.0111760003, 0.0253999997  
1350, 0.0116839996, 0.0253999997  
1351, 0.0121919997, 0.0253999997  
1352, 0.0126999998, 0.0253999997

\*Element, type=CPS4R

1,	1,	2,	28,	27
2,	2,	3,	29,	28
3,	3,	4,	30,	29
4,	4,	5,	31,	30
5,	5,	6,	32,	31
6,	6,	7,	33,	32
7,	7,	8,	34,	33
8,	8,	9,	35,	34
9,	9,	10,	36,	35
10,	10,	11,	37,	36
11,	11,	12,	38,	37
12,	12,	13,	39,	38
13,	13,	14,	40,	39
14,	14,	15,	41,	40
15,	15,	16,	42,	41
16,	16,	17,	43,	42
17,	17,	18,	44,	43
18,	18,	19,	45,	44
19,	19,	20,	46,	45
20,	20,	21,	47,	46
21,	21,	22,	48,	47
22,	22,	23,	49,	48
23,	23,	24,	50,	49
24,	24,	25,	51,	50

```

1273, 1323, 1324, 1350, 1349
1274, 1324, 1325, 1351, 1350
1275, 1325, 1326, 1352, 1351
*Nset, nset=_PickedSet2, internal, generate
    1, 1352,    1
*Elset, elset=_PickedSet2, internal, generate
    1, 1275,    1
*Elset, elset=_Surf-1_S3, internal, generate
    1251, 1275,    1
*Surface, type=ELEMENT, name=Surf-1
_Surf-1_S3, S3
** Section: Section-1
*Solid Section, elset=_PickedSet2, material=Material-1
,
*End Part
**
**
** ASSEMBLY
**
*Assembly, name=Assembly
**
*Instance, name=Part-1-1, part=Part-1
*End Instance
**
*Nset, nset=Set-1, instance=Part-1-1, generate
    1327, 1352,    1
*Elset, elset=Set-1, instance=Part-1-1, generate
    1251, 1275,    1
*Nset, nset=_PickedSet4, internal, instance=Part-1-1, generate
    1, 1327,    26
*Elset, elset=_PickedSet4, internal, instance=Part-1-1, generate
    1, 1251,    25
*Nset, nset=_PickedSet5, internal, instance=Part-1-1, generate
    1, 26,    1

```

```

1251, 1275, 1
*Nset, nset=_PickedSet4, internal, instance=Part-1-1, generate
1, 1327, 26
*Elset, elset=_PickedSet4, internal, instance=Part-1-1, generate
1, 1251, 25
*Nset, nset=_PickedSet5, internal, instance=Part-1-1, generate
1, 26, 1
*Elset, elset=_PickedSet5, internal, instance=Part-1-1, generate
1, 25, 1
*Nset, nset=_PickedSet6, internal, instance=Part-1-1, generate
1327, 1352, 1
*Elset, elset=_PickedSet6, internal, instance=Part-1-1, generate
1251, 1275, 1
*End Assembly
*Amplitude, name=Amp-1, time=TOTAL TIME
0., 0., 14., 1
**
** MATERIALS
**
*Material, name=Material-1
*Density
0.94,
*Depvar
5,
*Elastic, dependencies=1
325000., 0.46, , 1e-06
413000., 0.46, , 1e-05
566000., 0.46, , 0.0001
902000., 0.46, , 0.001
1.064e+06, 0.46, , 0.01
*Plastic, dependencies=1
975., 0., , 1e-06
2600.18, 0.000999449, , 1e-06
3773.11, 0.00339043, , 1e-06

```

```

*User Defined Field
**
** BOUNDARY CONDITIONS
**
** Name: BC-1 Type: Displacement/Rotation
*Boundary
_PickedSet4, 1, 1
** Name: BC-2 Type: Displacement/Rotation
*Boundary
_PickedSet5, 2, 2
** -----
**
** STEP: Step-1
**
*Step, name=Step-1, nlgeom=YES, inc=1000000
*Dynamic,application=QUASI-STATIC,initial=NO
0.01,14.,1e-05,0.1
**
** BOUNDARY CONDITIONS
**
** Name: BC-3 Type: Displacement/Rotation
*Boundary, amplitude=Amp-1
_PickedSet6, 2, 2, 0.003556
**
** OUTPUT REQUESTS
**
*Restart, write, frequency=0
**
** FIELD OUTPUT: F-Output-1
**
*Output, field, frequency=50
*Node Output

```

```
** Name: BC-2 Type: Displacement/Rotation
*Boundary
_PickedSet5, 2, 2
** -----
**
** STEP: Step-1
**
*Step, name=Step-1, nlgeom=YES, inc=1000000
*Dynamic,application=QUASI-STATIC,initial=NO
0.01,14.,1e-05,0.1
**
** BOUNDARY CONDITIONS
**
** Name: BC-3 Type: Displacement/Rotation
*Boundary, amplitude=Amp-1
_PickedSet6, 2, 2, 0.003556
**
** OUTPUT REQUESTS
**
*Restart, write, frequency=0
**
** FIELD OUTPUT: F-Output-1
**
*Output, field, frequency=50
*Node Output
RF,
*Element Output, directions=YES
E, FV, LE, PE, PEEQ, S, SDV
**
** HISTORY OUTPUT: H-Output-1
**
*Output, history, variable=PRESELECT
*End Step
```